Heavy-fermion systems studied by μSR technique

A. Amato

Paul Scherrer Institute, CH-5232 Villigen PSI, Switzerland

The author attempts to give a comprehensive discussion of studies performed with the positive-muon spin rotation and relaxation technique (also known as the μSR technique) on heavy-fermion compounds. The subtle competition between the demagnetizing Kondo interaction and the intersite Ruderman-Kittel-Kasuya-Yosida exchange interaction is believed to be the primary ingredient for the wealth of different ground states observed for this class of rare-earth– and actinide-containing intermetallic compounds. Due to its microscopic character, its sensitivity to extremely small internal fields, and its capacity to detect spatially inhomogeneous magnetic features, the μSR technique has been extensively utilized to investigate the peculiar magnetic properties of these ground states and improve our knowledge of heavy-fermion phenomena. In addition to providing a short introduction to μSR, where the intrinsic difficulties of the method are clearly stated, this article reviews the main results obtained by this technique on the best-known heavy-fermion compounds (superconductors, band magnets, local-moment magnets, non-Fermi-liquid systems, and Kondo insulators). Special emphasis is placed on the particular information obtainable by monitoring the implanted muon. [S0034-6861(97)00104-9]

CONTENTS

I. INTRODUCTION

A. Puzzle of heavy-fermion physics

A main development in condensed-matter physics in the last 20 years has been the discovery and investigation of the class of intermetallic compounds known as heavy-fermion (or, alternatively, heavy-electron) compounds.[1] For this class of systems, based on some

---

[1] For a broad spectrum of experimental results and theoretical concepts, the reader is referred, for example, to the review article of Grewe and Steglich (1991).

rare-earth and actinide elements (i.e., elements with a partially filled 4f or 5f electron shell), the attribute "heavy" is connected to the observation of a characteristic energy much smaller than in ordinary metals that reflects a thermal effective mass m^* of the conduction electrons orders of magnitude larger than the bare electron mass. These heavy masses manifest themselves, for example, by a large electronic coefficient γ of the specific heat C ($\gamma = C/T$ for $T \rightarrow 0$), an enhanced Pauli susceptibility, a huge T^2 term in the electrical resistivity, and highly temperature-dependent de Haas–van Alphen oscillation amplitudes at very low temperature.

The large m^* value (of the order of the muon mass) is usually believed to derive from the strong correlation between the localized f moments and the conduction electrons. While at high temperature the f electrons and conduction electrons interact weakly, at low temperature these two subsets of electrons become strongly coupled, resulting in the formation of a narrow resonance in the density of states near the Fermi energy. Thus, at a sufficiently low temperature, the heavy-fermion compounds behave like a system of heavy itinerant electrons, the properties of which can be described in the framework of a Landau Fermi-liquid formalism.

A fascinating aspect of this class of compounds is the observation that, within the heavy-fermion regime, a wealth of ground states can occur.

Superconductivity is observed in few systems and usually coexists and couples with static magnetism. This latter property seems to indicate that the attractive effective interaction between the electrons in the superconducting heavy-fermion systems is not provided by the electron-phonon interaction as in ordinary BCS superconductors, but rather is mediated by electronic spin fluctuations. In consequence, it is believed that heavy-fermion superconductivity exhibits an unconventional configuration, which may involve anisotropic, nonzero-angular-momentum states.

Among the heavy-fermion compounds, the magnetically ordered states appear rather anomalous and are often characterized by random, incommensurate, or extremely short-range orders, sometimes associated with extremely small static moments (10^{-2}–10^{-3} μ_B). Moreover, heavy-fermion compounds can display paramagnetic and, more surprisingly, even semiconducting ground states.

Although a myriad of experiments have been devoted to the characterization of these ground states, a comprehensive understanding of heavy-fermion properties at low temperature is still lacking. The heavy-fermion ground-state properties are highly sensitive to impurities, chemical composition, and slight changes of external parameters. This sensitivity indicates that a subtle interplay between different interactions produces a richness of experimental phenomena. It is widely believed that the competition between the Kondo effect (reflecting the interaction between the localized f moments and the conduction electrons) and the magnetic correlations between the periodically arranged f moments consti-

tutes the key factor as far as the magnetic properties of heavy-fermion compounds are concerned.

More generally, an understanding of heavy-fermion physics requires a compilation of collective results obtained by both macroscopic and microscopic techniques. Among the latter positive-muon spin rotation and relaxation (μSR) spectroscopy has in recent years found a wide application in the study of the microscopic magnetic and ground-state properties of heavy-fermion compounds.

The purpose of this review is to provide a broad, albeit incomplete, account of the application of the μSR technique to the study of heavy-fermion systems.[2]

B. Tentative classification of heavy-fermion systems

A first classification of the rare-earth and actinide-based metals can be obtained in the framework of the Doniach (1977) "Kondo-necklace" model, developed more than 15 years ago for Kondo-lattice systems.

Before discussing the properties of Kondo lattices, it is suitable to describe briefly the behavior of a localized magnetic impurity in a host lattice. The most widely utilized theoretical model was initially developed by Anderson (1961) to study the occurrence of a localized moment in a nondegenerate orbital. The Anderson Hamiltonian can be expressed by

$$\mathcal{H} = \sum_{\mathbf{k}\sigma} \varepsilon(\mathbf{k}) c_{\mathbf{k}\sigma}^+ c_{\mathbf{k}\sigma} + E_f \sum_m n_m^f + \frac{U}{2} \sum_{m \neq m'} n_m^f n_{m'}^f$$
$$+ \sum_{km} (V_{k,f} f_m^+ c_{\mathbf{k}\sigma} + V_{k,f}^* c_{\mathbf{k}\sigma}^+ f_m), \quad (1)$$

where $c_{\mathbf{k}\sigma}^+$ and $c_{\mathbf{k}\sigma}$ are the creation and annihilation operators of a conduction electron of energy $\varepsilon(\mathbf{k})$ and spin σ. The operators f_m^+ and f_m are the creation and annihilation operators of a localized electron (say an f electron of energy E_f, with m being the z component of the total angular momentum $\mathbf{J}$) and $n_m^f = f_m^+ f_m$ is the corresponding number operator. Finally, U represents the Coulomb repulsion that corresponds to the energy required to add a second electron to the localized f state, and $V_{k,f}$ is the hybridization matrix.

The paramount advantage of the Anderson Hamiltonian is that it describes several limiting cases, such as the intermediate valence regime or the Kondo regime. This latter regime is achieved when the Coulomb repulsion is very large, and consequently the f electron may exchange its spin component with that of a conduction electron, without an actual charge transfer from the f shell to the conduction band. It has been shown that the Kondo problem can be solved starting from a simple exchange Hamiltonian

$$\mathcal{H} = \sum_{\mathbf{k}\sigma} \varepsilon(\mathbf{k}) c_{\mathbf{k}\sigma}^+ c_{\mathbf{k}\sigma} - 2\mathcal{J}\mathbf{s}(0) \cdot \mathbf{S}, \quad (2)$$

---

where **S** is the spin of the localized magnetic moment placed at the origin 0 and $\mathbf{s}(0)$ is the spin of the conduction electrons. The coupling constant $\mathcal{J}$ is related to the hybridization matrix between the f state and the conduction electrons, as well as to the position of the f level with respect to the Fermi level E_F (Schrieffer and Wolff, 1966)

$$\mathcal{J} \simeq \frac{V_{k,f}^2}{E_F - E_f}. \qquad (3)$$

Below a characteristic temperature T_K (Kondo temperature) the spin of a magnetic impurity embedded in a nonmagnetic host is screened by a spin polarization of the surrounding conduction electrons, leading to the formation of a local singlet ground state (Kondo effect). The binding energy of the singlet can be identified with $k_B T_K$, which can be expressed as

$$k_B T_K \propto \exp\left(-\frac{1}{g}\right), \quad \text{with} \quad g = N(E_F)\mathcal{J}, \qquad (4)$$

where $N(E_F)$ is the conduction-band density of states at the Fermi level.

The magnetic Kondo screening involves low-lying particle-hole excitations which lead, below T_K, to a narrow scattering resonance in the one-particle spectrum near E_F (Abrikosov-Suhl or Kondo resonance). For $T \to 0$ this many-body effect can be described within the Fermi-liquid theory (Nozières, 1974), involving strongly renormalized quasiparticles.

The so-called Kondo-lattice systems, for which the local moments have the lattice periodicity, present a close similarity with the single-impurity model. The characteristic energy scale of the Kondo effect $k_B T^*$, for example, usually appears comparable to the value of $k_B T_K$ of the single-impurity problem. A paramount difference occurs at low temperature, where coherence effects arise in the lattice-periodic system, resulting in the formation of a real band of heavy quasiparticles with a width of the order of $k_B T^*$. The presence of such heavy quasiparticles is thought to be at the origin of the peculiar properties of the heavy-fermion compounds at low temperature.

Furthermore, apart from Kondo processes, intersite Ruderman-Kittel-Kasuya-Yosida (RKKY) interactions may appear in these systems, owing to the large concentrations of localized magnetic moments. The strength of the RKKY interactions is characterized by an energy $k_B T_{RKKY}$, which, within the simple exchange Hamiltonian, can be expressed as

$$k_B T_{RKKY} \propto g^2. \qquad (5)$$

Therefore the competition between the demagnetizing on-site Kondo interaction and the intersite RKKY exchange interaction in Kondo-lattice systems is usually believed to be the key factor in the occurrence of the heavy-fermion ground state (see Fig. 1). One should nevertheless keep in mind that other effects can contribute to the complexity of the problem. For example, crystalline electric-field effects will, depending on the crystal
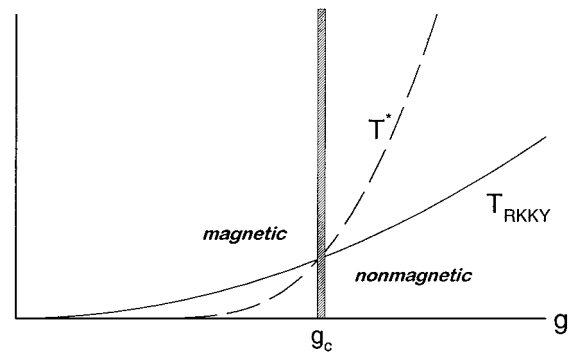

FIG. 1. Schematic behavior of the characteristic temperatures of the Kondo and RKKY interactions as a function of the parameter $g = N(E_F)\mathcal{J}$. The heavy-fermion regime is located around g_c (see text and Fig. 2).

symmetry, split the degenerate spin-orbit ground state of the f ion and therefore deeply affect the Kondo and the RKKY interactions. A further complication, compared to the simple Doniach model, where the influence of the reduced dimensionality is not specifically treated, is provided by the extreme diversity of the crystal structures adopted by the heavy-fermion compounds.

In the simple Doniach model, systems with stable f moments are characterized by $T_{RKKY} \gg T^*$ (i.e., $g \ll g_c$, see Fig. 2), which corresponds to a regime where the energy gained by the screening of the local moments is negligible. For these systems, magnetic ground states with large static moments are usually observed. On the other hand, if the hybridization between the f state and the conduction electrons is large (i.e., $T^* \gg T_{RKKY}$, or $g \gg g_c$), paramagnetic ground states will be the rule. Furthermore, in that case a picture of localized moments will eventually be unworkable, owing to the occurrence of real charge fluctuations between f-shell and conduction-band electrons (intermediate valence regime).

The heavy-fermion regime is found between the two limiting cases described above, i.e., in a region where T_{RKKY} and T^* have roughly equivalent strength (see Fig. 2).
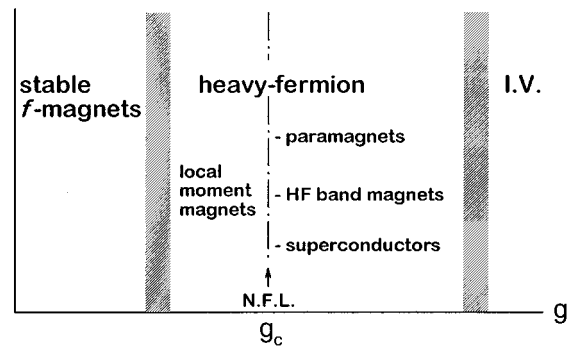

FIG. 2. Tentative classification of the Kondo lattices with respect to their parameter g (NFL: non-Fermi-liquid compounds, IV: intermediate-valence compounds; adapted from Steglich *et al.*, 1994).

The majority of the heavy-fermion systems are located in the region where $T_{\mathrm{RKKY}} \gtrsim T^*$ (or $g \lesssim g_c$) and are characterized by a moderate effective mass of the quasiparticles, well-localized f moments (though somewhat renormalized by the Kondo effect, $\mu_s \simeq 0.1 - 1\ \mu_B$), and usually rather complex magnetic structure. The systems belonging to this particular class are usually referenced as local-moment magnetic (LMM) heavy-fermion compounds.

If the energy gained by forming local Kondo singlets is larger than the condensation energy due to the coupling of neighboring f moments via RKKY interactions ($T^* \gtrsim T_{\mathrm{RKKY}}$ or $g \gtrsim g_c$), local-moment magnetism is lost. For this region a paramagnetic ground state, interpreted in the framework of the Landau Fermi-liquid theory, where the properties of the strongly interacting electron system are described by those of noninteracting, strongly renormalized quasiparticles, was once thought to be predominant. In fact, as we will see in the following sections, this ground state appears rather unstable against heavy-fermion band magnetism (HFBM). The occurrence of a HFBM state can be ascribed to the exchange splitting of the heavy quasiparticles' band (i.e., to the low-energy excitations of the interacting system) and is usually characterized by complex magnetic structure and extremely small static moments ($\mu_s \simeq 10^{-2} - 10^{-3}$ μ_B). As discussed in Sec. IV, μSR has played a key role in the phenomenological classification of heavy-fermion compounds by detecting HFBM features in systems that were long believed to behave like Fermi-liquid paramagnets.

An additional instability of the Fermi-liquid paramagnetic ground state is the occurrence of superconductivity with $T_c \ll T^*$, which has been proven to be a cooperative phenomenon in the system of renormalized heavy quasiparticles. The situation appears further confused by the observation of coexistence between superconductivity and magnetism of usually HFBM type.

The situation where $g \simeq g_c$, i.e., corresponding to the situation where the Kondo effect and RKKY interaction have the same magnitude, has recently attracted considerable interest. Compounds of this class exhibit unusual behavior in their specific heat, magnetic susceptibility, and electrical resistivity at low temperature, which are ascribed to non-Fermi-liquid (NFL) effects possibly arising from a quantum phase transition between magnetic and nonmagnetic ground states at zero temperature.

Aside from the above classification of the heavy-fermion compounds, based on the relative strength of the Kondo and RKKY interactions, two additional classes of systems exhibiting heavy-fermion behaviors have been discovered.

The Kondo insulators constitute one of the oldest known forms of heavy-fermion behavior. These systems display local-moment properties at high temperatures (similar to what is observed for usual heavy-fermion compounds) and relatively large characteristic temperatures T^*. Below T^* these materials show a semiconducting ground state that is attributed to the hybridization between the f-level and conduction electrons. If the electron count including the f and conduction electrons is exactly two, the material is a band-gap insulator to satisfy the Luttinger sum rule.

Finally, the so-called low-carrier-density (LCD) heavy-fermion systems exhibit semiconducting behaviors at high temperature, as well as a large linear term in the specific heat C at low temperature. The origin of the gigantic ratio C/T for $T \to 0$ remains unclear and has led to speculations about the presence of either a Kondo resonance *within* the band gap, local Kondo states, or magnetic transitions at very low temperature.

C. Advantages of the μSR technique in studying heavy-fermion compounds

There are several advantages in using μSR for investigating the magnetic and ground-state properties of the heavy-fermion compounds.

The μSR technique is sensitive to extremely small internal fields (down to about ~ 0.1 G) and therefore can probe local magnetic fields that may be nuclear or electronic in origin. Since no applied field is necessary to polarize the spin of the implanted muons, such measurements can be made in the absence of a perturbative external field. As we will see in the following sections, the detection of magnetism characterized by extremely small values of the static moments in heavy-fermion compounds has been one of the main contributions of μSR to the investigation of heavy-fermion phenomenon. In addition, μSR has the capability to detect temporal as well as spatial changes of the internal fields.

Another primary advantage of μSR, compared, for example, to NMR experiments, lies in the fact that the muon is a spin-$\frac{1}{2}$ particle and consequently is free of quadrupolar interactions. This simplifies the analysis of μSR, with a reduced set of adjustable parameters.

As we will see in Sec. IV, the local-probe character of the muon makes μSR very sensitive to spatially inhomogeneous magnetic properties. Hence the occurrence of different phases in a sample will be reflected by different components in the μSR signal, and a careful analysis of these components furnishes a direct measure of the fraction of the sample volume involved in a particular phase. For many heavy-fermion compounds, the μSR technique can therefore be utilized to check the coexistence of different types of ground states at the microscopic level that is only assumed by traditional macroscopic techniques. In this respect, the study of the coexistence between heavy-fermion superconductivity and magnetism constitutes a clear demonstration of the unrivalled information furnished by μSR.

Finally, μSR is one of the very few methods that provides information on both the magnitude and temperature dependence of the London magnetic penetration depth in a type-II superconductor. In favorable situations, valuable information about the temperature dependence of the spin susceptibility below the superconducting critical temperature can be extracted from the

μ^+ Knight shift, and may possibly allow one to probe for the unconventional character of heavy-fermion superconductivity.

Despite the above described advantages, different problems inherent to the technique have to be carefully analyzed. The implanted muons will stop at an interstitial site, the knowledge of which is required for a quantitative interpretation of the μSR data. μSR studies on single crystals, notably the study of the angular dependence of the different parameters of the μSR signal, are usually necessary for the μ^+ site determination. In view of the difficult metallurgy of many heavy-fermion compounds, such studies can prove to be impossible, therefore restricting the interpretation of the μSR data.

Another potential problem is the presence of μ^+ diffusion. Fortunately, observations show that diffusion is usually restricted to high temperatures ($T \gg T^*$). Since most of the novel aspects of the heavy-fermion physics occur at low temperatures ($T \ll T^*$), μ^+ diffusion will usually be of no concern.

Finally, the most problematic characteristic of μSR is the addition of an extra positive charge in the lattice. This leads to a modified local charge distribution, due to the screening of the muon's positive charge, and to a slight lattice relaxation, reflected by a small shift in the position of the nearest-neighbor ions. This latter effect can be exactly quantified by a careful comparison between the data and simple theoretical calculations. For the heavy-fermion systems, it is plausible that the changed distances between f moments in the vicinity of the μ^+ stopping site could alter the local magnetic properties. However, to date no compelling evidence for such a modification has been found. On the other hand, it is expected that the variation of the local charge distribution will deeply modify the spin-density distribution at the μ^+ site and therefore the contact hyperfine field. Such a modification is not easily determined and will, for example, alter the value of the μ^+ Knight shift. Nevertheless, since the μ^+ Knight shift also contains a large dipole-field contribution (which is the opposite of the NMR technique), its quantitative analysis will still remain possible and will furnish, for example, valuable information about the μ^+ stopping site.

Another, more disturbing, effect of the implantation of a positive charge in the lattice is that the modification of the local charge density can possibly affect the crystal electric field (CEF) of the neighboring f ions and therefore lead to a slight change of the atomic magnetic susceptibility for these ions. It has been shown (Feyerherm, Amato, Gygax, Schenck, Zimmerman et al., 1994) that such a modification is particularly important for singlet ground-state systems where the splitting between the excited states and the singlet ground state is very low ($\lesssim 1$ meV). Although a clear instance of muon-induced modification of the CEF splitting has so far only been observed in the non-heavy-fermion compound $PrNi_5$, it is conceivable that such effects could also be present in some uranium-based heavy-fermion compounds. It is therefore of primary importance to systematically compare, in each particular case, the atomic susceptibility sensed by the interstitial muon to the bulk susceptibility, to detect the potential presence of such muon-induced effects.

In any case, μSR has, so far, always detected magnetic and superconducting transitions at temperatures in agreement with the determinations by bulk measurements. Furthermore, the phase transitions discovered by μSR studies have subsequently been confirmed by other techniques at coinciding temperatures. A μSR experimentalist would therefore be strongly tempted to consider the μSR technique to be fairly innocent for the investigated systems, with rare exceptions of interest. The open question will be to determine whether a system follows the rule or, rather, the exception.

D. Organization of the review

Section II of this review gives a brief introduction to μSR, beginning with a short description of how muon beams are obtained. The remainder of the section describes the different variants of μSR and addresses the question of how to interpret the parameters furnished by the data analysis.

Section III is a review of the μSR studies on different heavy-fermion superconductors. Special emphasis is placed on the particular information revealed by the implanted muons, such as the question of the microscopic coexistence between magnetism and superconductivity and the indication of the nonconventional nature of the superconductivity.

μSR investigations of the magnetic properties of heavy-fermion systems are presented in Sec. IV. In addition to a schematic classification, in view of the μSR results, between local-moment magnets and heavy-fermion band magnets, the occurrence of unusual features characterized by inhomogeneous form of magnetism, spin-glass type of order, and/or short-range order will be discussed for particular systems.

A review of the μSR results obtained on the few remaining heavy-fermion compounds with Fermi-liquid paramagnetic ground state is the subject of Sec. V.

Section VI gives a review of the μSR data available for systems belonging to the "exotic" heavy-fermion classes. Non-Fermi-liquid paramagnets are treated in the first subsection. The following subsection addresses the problem of the real nature of the ground state of low-carrier-density heavy-fermion compounds. The last subsection presents the few μSR results obtained on Kondo insulators.

The final section offers a brief discussion and my conclusion.

II. OVERVIEW OF THE μSR TECHNIQUE

This section furnishes a brief introduction to the μSR technique. For more details, the interested reader is referred to several specialized reviews (see, for example, Schenck, 1985; S. F. J. Cox, 1987; Brewer, 1994; Schenck and Gygax, 1995).

A. Muon production

The collision of an accelerated proton beam (typical energy 600 MeV) with the nuclei of a production target produces positive pions (π^+) via the possible reactions

$$p+p\rightarrow p+n+\pi^+,$$
$$p+n\rightarrow n+n+\pi^+. \tag{6}$$

From the subsequent decay of the pions ($\tau_{\pi^+}=26.03$ ns), positive muons (μ^+) are formed via the two-body decay

$$\pi^+\rightarrow\mu^++\nu_\mu, \tag{7}$$

where both the neutrino and the μ^+ have their spin antiparallel to their momentum in the pion rest frame. According to the value of the pion momentum at the decay time, two types of μ^+ beams are available for μSR measurements.

The first type of muon beam is formed by the π^+ decaying in flight (usually in a long superconducting solenoid). Due to the relativistic transformation to the laboratory frame, and after momentum selection by bending magnets, typical muon beams are produced with a polarization of ~80% and energies of ~40–50 MeV. Although such a high-energy beam requires the use of suitable moderators and samples with sufficient thickness, it guarantees a homogeneous implantation of the muons in the sample volume.

The second type of muon beam is often called the "surface" or "Arizona" beam (after the pioneering work of Pfifer et al., 1976, from the University of Arizona). Here, muons are used that arise from π^+ decaying at rest near the surface of the production target. Such muons, which are 100% polarized and have a very low momentum, have a range width in matter of the order of 180 mg/cm^2. Hence the paramount advantage of this type of beam is the possibility to use thin samples. Moreover, novel low-background apparati, with special detector arrangements (see, for example, Kiefl et al., 1994), were recently developed to drastically reduce the lateral dimensions of the sample. This has opened the fascinating possibility of investigating tiny single crystals (~1 mm^3). However, a possible drawback is that the implanted μ^+ are stopped on the surface layer of the sample, which could present different properties than the bulk. Therefore special care should be taken with the preparation of the specimens and reproducibility of the observed μSR results.

B. Principle of μSR

After the implantation in the solid sample, the muon is decelerated within 100 ps, which is too rapid to allow any significant loss of polarization and sufficiently rapid for the μSR time window. The μ^+ implanted in the sample decays after an average time of $\tau_\mu=2.197$ μs, according to

$$\mu^+\rightarrow e^++\nu_e+\bar{\nu}_\mu, \tag{8}$$

where e^+ is a positron and ν_e and $\bar{\nu}_\mu$ are neutrinos. The parity violation in the weak interaction leads to an anisotropic distribution of the positron emission with respect to the spin direction of the μ^+ at the decay time. The positron emission probability is given by

$$W(\theta)d\theta\propto(1+\mathcal{A}\cos\theta)d\theta, \tag{9}$$

where θ is the angle between the positron trajectory and the μ^+ spin. This anisotropic emission constitutes the basics for the μSR technique. Hence, by measuring the positron distribution, it is possible to determine the original μ^+ spin direction. The asymmetry of $W(\theta)$ is given by $\mathcal{A}=aP_\mu(0)$, where $P_\mu(0)=|\mathbf{P}_\mu(0)|$ is the beam polarization (of the order of ~1) and a is an intrinsic asymmetry parameter determined by the weak-decay mechanism. Theoretically, an average of $\langle a\rangle=\frac{1}{3}$ is obtained if all emitted positrons are detected with the same efficiency irrespective of their energy. Practically, values of $\mathcal{A}\approx0.25$ are routinely obtained.

If the implanted μ^+ are subject to magnetic interactions, their polarization becomes time dependent [$\mathbf{P}_\mu(t)$]. The time evolution of $\mathbf{P}_\mu(t)$ can be deduced by measuring the positron distribution as a function of time. In the time-differential μSR technique (hereafter only called the μSR technique), repeated measurements (~10^7!) are made of the time interval between the μ^+ implantation into the sample and the detection of the emitted positron in a particular direction [say, in the direction of the initial polarization $\mathbf{P}_\mu(0)$; the extension of the following discussion for other arbitrary directions of detection is straightforward]. The time histogram of the collected intervals has the form

$$N_{e^+}(t)=B+N_0e^{-t/\tau_\mu}\left[1+\mathcal{A}\frac{P_\mu(t)}{P_\mu(0)}\right], \tag{10}$$

where B is a time-independent background, N_0 is a normalization constant, and the exponential accounts for the decay of the μ^+. $P_\mu(t)$ is defined as the projection of $\mathbf{P}_\mu(t)$ along the direction of the initial polarization, i.e., $P_\mu(t)=\mathbf{P}_\mu(t)\cdot\mathbf{P}_\mu(0)/P_\mu(0)=G(t)P_\mu(0)$, where $G(t)$ reflects the normalized μ^+-spin autocorrelation function

$$G(t)=\frac{\langle\mathbf{S}(t)\cdot\mathbf{S}(0)\rangle}{S(0)^2}, \tag{11}$$

which depends on the average value, distribution, and time evolution of the internal fields and therefore contains all the physics of the magnetic interactions of the μ^+ inside the sample. Equation (10) can therefore be written as

$$N_{e^+}(t)=B+N_0e^{-t/\tau_\mu}[1+\mathcal{A}G(t)], \tag{12}$$

where $\mathcal{A}G(t)$ is often called the μSR signal and the envelope of $G(t)$ is known as the μ^+ depolarization function. In the case of static local magnetic fields ($\mathbf{B}_\mu$) at the μ^+ site, $G(t)$ is given by

$$G(t)=\int f(\mathbf{B}_\mu)[\cos^2\theta+\sin^2\theta\cos(\gamma_\mu B_\mu t)]d\mathbf{B}_\mu, \tag{13}$$

TABLE I. Properties of the positive muon (from Schenck, 1985; and Feyerherm, 1995). m_e is the mass of the electron and m_p the mass of the proton; μ_N is the nuclear magneton.

Mass m_μ	206.76826(11) $m_e = 0.112609513(17)$ m_p
Charge	$+e$
Spin	1/2
Magnetic moment μ_μ	3.18334547(47) $\mu_p = 8.8905981(13)$ μ_N
Gyromagnetic ratio γ_μ	$\gamma_\mu/(2\pi) = 13.553879(\pm 0.7$ ppm) kHz/G
Average lifetime τ_μ	2.19703(4) μs

where $f(\mathbf{B}_\mu)$ is the magnetic-field distribution function, θ is the angle between the local field and $\mathbf{P}_\mu(0)$, $B_\mu = |\mathbf{B}_\mu|$, and $\gamma_\mu/(2\pi) = 13.553\,879(\pm 0.7$ ppm) kHz/G is the gyromagnetic ratio of the muon (see Table I).

In a particular structure, the possible presence of different μ^+ stopping sites with different magnetic environments will be identified by a μSR signal with different components, i.e., with different spin autocorrelation functions $G_i(t)$. Moreover, since the μ^+ are uniformly implanted, the coexistence in the sample of different domains, characterized by different types of ground states, will also be detected by the presence of different components with distinct functions $G_i(t)$, even if only one μ^+ stopping site is present. For this last case, the amplitude ($\mathcal{A}_i$) of the different components will readily be a measure of the volume fractions associated with different domains, with the condition

$$\sum_i \mathcal{A}_i = \mathcal{A}. \tag{14}$$

As we will see in the following sections, this unique possibility to investigate at the microscopic level, the coexistence of different phases in a sample has played a major role in the growing use of μSR to study the heavy-fermion ground state.

C. The μSR transverse-field (TF) technique

1. μ^+ Knight shift

For this technique, an external field $\mathbf{H}_{\text{ext}}$ is applied perpendicular to the initial μ^+ polarization $\mathbf{P}_\mu(0)$. $\mathbf{P}_\mu(t)$ precesses around the total field $\mathbf{B}_\mu$ at the μ^+ site, the value of which can be extracted from the oscillatory component of $G(t)$, recalling that the μ^+ frequency $\nu_\mu = \omega_\mu/(2\pi) = \gamma_\mu B_\mu/(2\pi)$. For a system that is not magnetically ordered, the total field at the μ^+ site is given by

$$\mathbf{B}_\mu = \mathbf{H}_{\text{ext}} + \mathbf{B}_{\text{hf}} + (\mathbf{B}_{\text{DF}} + \mathbf{B}_{\text{LF}}). \tag{15}$$

The last two terms are the demagnetization and Lorentz fields, which can be calculated from the bulk magnetization and demagnetization tensor (see, for example, Schenck, 1985). $\mathbf{B}_{\text{hf}}$ are the internal fields induced by $\mathbf{H}_{\text{ext}}$.

The μ^+ frequency shift

$$K_\mu^* = \frac{|\mathbf{B}_\mu| - |\mathbf{H}_{\text{ext}}|}{|\mathbf{H}_{\text{ext}}|} = \frac{\omega_\mu}{\omega_{\text{ext}}} - 1 \tag{16}$$

(where $\omega_{\text{ext}} = \gamma_\mu |\mathbf{H}_{\text{ext}}| \equiv \gamma_\mu H_{\text{ext}}$) can be corrected for the contributions of $\mathbf{B}_{\text{DF}}$ and $\mathbf{B}_{\text{LF}}$ to furnish the μ^+ Knight shift K_μ, which contains the relevant information about the hyperfine fields. For the rare-earth and actinide compounds, the μ^+ Knight shift can be written as

$$K_\mu = K_0 + K_f, \tag{17}$$

where K_0 and K_f correspond, respectively, to the contributions to $\mathbf{B}_{\text{hf}}$ arising from the polarization of conduction electrons and localized f moments induced by $\mathbf{H}_{\text{ext}}$.

As in s- or p-electron metals, K_0 is a result of the Pauli paramagnetism of the conduction electrons and their Fermi contact interaction with the μ^+. K_f at low temperature is usually much larger than K_0 and contains two contributions of the localized f moments: (i) the dipole-dipole interaction between the f moments and the μ^+, and (ii) an indirect RKKY interaction producing an additional spin polarization of the conduction electrons at the μ^+ site, which results in an increased hyperfine contact field. Since both contributions are proportional to the susceptibility component due to the f moments ($\overleftrightarrow{\chi}_f$), K_f is given by

$$K_f = \frac{1}{H_{\text{ext}}^2} (\mathbf{H}_{\text{ext}} \cdot \overleftrightarrow{A}_f \cdot \overleftrightarrow{\chi}_f \cdot \mathbf{H}_{\text{ext}})$$

$$= \frac{1}{H_{\text{ext}}^2} (\mathbf{H}_{\text{ext}} \cdot \overleftrightarrow{A}_{\text{dip}} \cdot \overleftrightarrow{\chi}_f \cdot \mathbf{H}_{\text{ext}})$$

$$+ \frac{1}{H_{\text{ext}}^2} (\mathbf{H}_{\text{ext}} \cdot \overleftrightarrow{A}_c \cdot \overleftrightarrow{\chi}_f \cdot \mathbf{H}_{\text{ext}}), \tag{18}$$

where $\overleftrightarrow{\chi}_f \cdot \mathbf{H}_{\text{ext}}$ is the localized moment induced by the external field, $\overleftrightarrow{A}_{\text{dip}}$ is the dipolar coupling tensor, and $\overleftrightarrow{A}_c$ is the hyperfine contact coupling tensor. $\overleftrightarrow{A}_{\text{dip}}$ is traceless, symmetric, and depends on the given crystallographic structure and the assumed μ^+ site,

$$A_{\text{dip}}^{ij} = \sum_f \frac{1}{r^3} \left(3 \frac{r_i r_j}{r^2} - \delta_{ij} \right), \tag{19}$$

where the sum is done over the localized f moments inside the Lorentz sphere and $\mathbf{r} = (r_1, r_2, r_3)$ is the vector connecting the μ^+ site and the considered f moment.

Since the hyperfine contact coupling is normally independent of the direction of $\mathbf{H}_{\text{ext}}$, one can write $\overleftrightarrow{A}_c = A_c \cdot \mathbb{1}$. Therefore, and keeping in mind that $\text{Tr}(\overleftrightarrow{A}_{\text{dip}}) = 0$, the experimental determination of K_f along the principal crystallographic directions of the crystal allows one to extract A_c and A_{dip}^{ii}, the latter yielding direct

information about the μ^+ stopping site via Eq. (19). A_c also contains valuable information about the effective exchange interaction between the f moment and the conduction electrons. However, A_c also depends on the spin-density enhancement factor, reflecting the μ^+-induced changes in the local electronic structure. The difficulty to estimate such a factor has, so far, hampered detailed analysis of A_c.

2. Inhomogeneous line broadening

If an inhomogeneous field distribution described by $f(\mathbf{B}_{\text{int}})$ and caused by static nuclear or electronic dipole fields is present at the μ^+ site, the muons located at different sites will feel slightly different fields. Such a field inhomogeneity will result in a loss of polarization by dephasing of the muon ensemble. In transverse-field experiments, H_{ext} is usually much larger than any internal fields, and only the field inhomogeneity along the direction of $\mathbf{H}_{\text{ext}}$ (say, the z direction) has to be considered. Noting that $\theta = 90°$, Eq. (13) can be written as

$$G(t) = \int f(B_{\text{int}}^z) \cos[\gamma_\mu(\langle B_\mu^z \rangle + B_{\text{int}}^z)t] dB_{\text{int}}^z$$
$$= g_{\text{TF}}(t) \cos(\gamma_\mu \langle B_\mu^z \rangle t). \qquad (20)$$

If $f(B_{\text{int}}^z)$ is a Gaussian distribution, the depolarization function $g_{\text{TF}}(t)$ will be given by

$$g_{\text{TF}}(t) = \exp(-\tfrac{1}{2}\sigma^2 t^2), \qquad (21)$$

where $\sigma^2 = \gamma_\mu^2 M_2$, with M_2 the second moment of the field distribution along the direction of $\mathbf{H}_{\text{ext}}$. If the field distribution is caused by nuclear dipole fields, M_2 can be easily calculated and will usually depend on the orientation of $\mathbf{H}_{\text{ext}}$. Hence the comparison of the angular dependence of the observed depolarization rate σ with the calculated M_2 will provide an additional test for the determination of the μ^+ site (see, for example, Fig. 25 in Sec. III.C).

3. Homogeneous line broadening: $1/T_2$ processes

Fluctuating internal fields will also cause an exponential loss of polarization of the precessing spins. The depolarization function will be given by

$$G(t) = e^{-\lambda_2 t}\cos(\omega_\mu t) \equiv e^{-t/T_2}\cos(\omega_\mu t), \qquad (22)$$

where $\omega_\mu = \gamma_\mu \langle B_\mu \rangle$. This type of depolarization, which arises from the dephasing of the μ^+ spins and is often called the spin-spin or transverse depolarization, does not involve any energy transfer between the μ^+ spin ensemble and the lattice. Note that in a transverse-field μSR experiment, $1/T_2$ processes may not be easily distinguished from dephasing due to inhomogeneous line broadening.

D. Zero-field (ZF) μSR technique

A fascinating aspect of the μSR technique compared to other microscopic techniques, is the possibility of measuring properties in zero external field. With this technique one monitors the time evolution of the muon ensemble under the action of internal magnetic fields. The very large magnetic moment of the muon ($\mu_\mu = 8.9\,\mu_{\text{N}}$) makes μSR sensitive to extremely small internal magnetic fields, down to the order of 0.1 G, which corresponds to the magnitude of fields originating from nuclear dipole fields.

This zero-field technique has been widely utilized to measure the spontaneous μ^+ Larmor frequencies in magnetically ordered phases, providing valuable information about the values of the static moment and the magnetic structures. The observation of spontaneous μ^+ frequencies is, however, limited to systems where the presence of static electronic moments produces well-defined local fields at the μ^+ stopping site. Hence the μ^+-spin autocorrelation function $G(t)$ depends sensitively on details of the magnetic structure and of course on the μ^+ stopping site. In the simplest case, the magnetic structure produces a hyperfine field of well-defined magnitude B_μ and direction (with respect to the crystal structure) at the μ^+ sites. In this case in a single-domain monocrystalline sample, $f(\mathbf{B}_\mu)$ is represented by a δ function, and Eq. (13) simplifies to

$$G(t) = \cos^2\theta + \sin^2\theta\,\cos(\omega_\mu t), \qquad (23)$$

with $\omega_\mu = \gamma_\mu B_\mu$. The polycrystalline average over the angular dependence yields

$$G(t) = \tfrac{1}{3} + \tfrac{2}{3}\cos(\omega_\mu t). \qquad (24)$$

The second term in both latter equations represents the spontaneous μ^+ Larmor precession in the internal field. The above discussion is easily generalized, on one hand, to the presence of a distribution of fields around a well-defined nonzero value of B_μ (which will introduce an additional depolarization, see below) and, on the other hand, to the occurrence of several well-defined internal-field values.

1. Inhomogeneous line broadening

A static distribution of internal fields (for example, arising from static nuclear or electronic dipole fields) will produce, as in the transverse-field case, a depolarization. Assuming that the internal fields are Gaussian distributed in their values and randomly oriented (which is realized if the field distribution is due to nuclear magnetic moments, which are usually static in the μSR time window, or to randomly frozen electronic spins), i.e.,

$$f(B_i) = \frac{1}{\sqrt{2\pi}}\frac{\gamma_\mu}{\Delta}\exp\left(-\frac{\gamma_\mu^2 B_i^2}{2\Delta^2}\right) \quad (i=x,y,z), \qquad (25)$$

the field distribution has zero average value, and no spontaneous frequency is observed. $G(t)$ assumes the form

$$G_{\text{KT}} = \tfrac{1}{3} + \tfrac{2}{3}(1-\Delta^2 t^2)\exp(-\tfrac{1}{2}\Delta^2 t^2), \qquad (26)$$

where Δ^2/γ_μ^2 represents the second moment of the field distribution along one cartesian axis perpendicular to the initial μ^+ polarization, i.e.,

$$\Delta^2/\gamma_\mu^2 = \langle B_x^2 \rangle = \langle B_y^2 \rangle = \langle B_z^2 \rangle. \tag{27}$$

Equation (26) represents the well-known Kubo-Toyabe (KT) function, first derived by Kubo and Toyabe (1967). For early times ($t \ll \Delta^{-1}$) the KT function approaches a Gaussian function with $G(t) \simeq \exp(-\Delta^2 t^2)$.

In some cases, each cartesian component of the internal fields is believed to be Lorentzian distributed, and $G(t)$ has the form

$$G_{KT}^L(t) = \tfrac{1}{3} + \tfrac{2}{3}(1 - \lambda t)\exp(-\lambda t), \tag{28}$$

where λ/γ_μ represents the half width at half maximum of the distributions. This case is realized, for example, in dilute spin-glass systems. The initial μ^+ depolarization is exponential [$G(t) \simeq \exp(-\lambda t)$ for $t < \lambda^{-1}$].

2. Fluctuations

In this subsection only the most common case of a time dependence of the Gaussian distribution of internal fields described by Eq. (25) will be discussed. This time dependence may arise from a fluctuation of the magnetic moments or from muon diffusion. In fluctuating fields, characterized by a fluctuation rate ν, the KT function is modified to the so-called dynamical KT function, which, with the exception of some limiting cases, cannot be expressed analytically. For slow fluctuations, i.e., when $\nu/\Delta \ll 1$, only the $\tfrac{1}{3}$ term of Eq. (26) will be modified to $\tfrac{1}{3}\exp(-\tfrac{2}{3}\nu t)$. On the other hand, for fast fluctuations ($\nu/\Delta \gg 1$) the depolarization function will be given by

$$G(t) = e^{-\lambda_1 t}. \tag{29}$$

This depolarization rate, describing the spin-lattice relaxation rate ($1/T_1$ processes with $1/T_1 = \lambda_1$), involves spin-flip transitions induced by the fluctuating magnetic fields with component perpendicular to $\mathbf{P}_\mu(0)$.

In this fast fluctuation limit, the depolarization rate λ_1 is given by (see, for example, Narath, 1973)

$$\lambda_1 = \gamma_\mu^2 k_B T \frac{1}{N} \sum_{\mathbf{q}} \sum_{\alpha\beta} [A_{hf}^{\alpha\beta}(\mathbf{q})]^2 \frac{\chi^{\beta\beta}(\mathbf{q})}{N_A \Gamma(\mathbf{q})}$$

$$(\alpha = x,y; \ \beta = x,y,z), \tag{30}$$

where $A_{hf}(\mathbf{q})$ represents the spatial Fourier transform of the hyperfine coupling tensor (e.g., $\vec{A}_{dip}$ or $\vec{A}_c$), $\vec{\chi}(\mathbf{q})$ is the $\mathbf{q}$-dependent static molar susceptibility, and $\Gamma(\mathbf{q})$ is proportional to the fluctuation rate of excitations with wave vector $\mathbf{q}$.

Neglecting the $\mathbf{q}$ dependence of the fluctuation rate, the transformation of Eq. (30) into real space leads to

$$\lambda_1 = \gamma_\mu^2 k_B T \sum_{\mathbf{r}} \sum_{\alpha\beta} [A_{hf}^{\alpha\beta}(\mathbf{r})]^2 \frac{\chi^{\beta\beta}(\mathbf{r})}{\nu N_A}. \tag{31}$$

For uncorrelated spin fluctuations, and after performing the sum over α and β and taking the powder average, the depolarization rate can be simply written as

$$\lambda_1 = \frac{1}{T_1} = \frac{4}{3}(\gamma_\mu \gamma_N \hbar)^2 \frac{J(J+1)}{\nu} \sum_{\mathbf{r}} \frac{1}{r^6} = 2\Delta^2 \frac{1}{\nu}, \tag{32}$$

where Δ^2/γ_μ^2 is the second moment of the field distribution along one cartesian axis perpendicular to the initial μ^+ polarization [see Eq. (27)]. Moreover, it can be shown that for very fast dynamics $T_1 \simeq T_2$ [see Eq. (22) and Slichter, 1978].

For intermediate values of ν, the depolarization function $G(t)$ is obtained numerically (see, for example, Hayano et al., 1979).

E. Longitudinal-field (LF) μSR technique

1. Static-field distributions

When a longitudinally [i.e., parallel to $\mathbf{P}_\mu(0) = (0,0,P_z)$] oriented field is applied, some decoupling of the μ^+ spin from the randomly oriented internal static fields occurs. For internal fields that are Gaussian distributed, $f(B_z)$ in Eq. (25) will be replaced by

$$f(B_z) = \frac{1}{\sqrt{2\pi}} \frac{\gamma_\mu}{\Delta} \exp\left(-\frac{\gamma_\mu^2(B_z - H_{ext})^2}{2\Delta^2}\right). \tag{33}$$

Hayano et al. (1979) have derived the depolarization function $G_{KT}(t, H_{ext})$ as function of the applied field, which assumes the form

$$\begin{aligned} G_{KT}(t, H_{ext}) = 1 &- \frac{2\Delta^2}{\gamma_\mu^2 H_{ext}^2}[1 \\ &- \exp(-\tfrac{1}{2}\Delta^2 t^2)\cos(\gamma_\mu H_{ext} t)] \\ &+ \frac{2\Delta^3}{\gamma_\mu^3 H_{ext}^3} \int_0^{\Delta t} \exp(-\tfrac{1}{2}y^2) \\ &\times \cos\left(\frac{\gamma_\mu H_{ext}}{\Delta}y\right) dy. \end{aligned} \tag{34}$$

The effect of $\mathbf{H}_{ext}$ is to gradually remove the time dependence of the polarization. Eventually, by choosing $\mathbf{H}_{ext}$ to be stronger than the internal fields (i.e., $\gamma_\mu H_{ext}/\Delta \gg 1$), the muon's "up" and "down" states are eigenstates of the Zeeman Hamiltonian, and any inhomogeneous (static) distribution of the internal fields will not affect the time evolution of the μ^+ polarization, which will remain constant. This behavior reflects the decoupling of the μ^+ spin from the static internal fields.

2. Fluctuations

On the other hand, for fast fluctuations of the internal fields the spin-lattice relaxation regime is recovered, and induced spin-flip transitions (irreversible transitions between energy levels) will lead to a depolarization in longitudinal fields similar to the one observed in zero external field [see Eq. (29)]. However, spin-lattice relaxation may be affected by the applied longitudinal field (see Abragam, 1970; Slichter, 1978), and Eq. (32) assumes the form

$$\frac{1}{T_1} = \frac{2\Delta^2/\nu}{1 + (\gamma_\mu H_{ext}/\nu)^2}. \tag{35}$$

TABLE II. Selected properties and microscopic parameters characterizing the magnetic and superconducting states of the heavy-fermion superconductors (polycrystalline samples). $B_{c1,0}$: $B_{c1}(T\to0)$; $B_{c2,0}$: $B_{c2}(T\to0)$; λ: London penetration depth; ξ: Ginzburg-Landau coherence length. The other symbols have their usual meanings. See, for example, the review article of Grewe and Steglich (1991) for references and more details.

Compounds	T^* (K)	T_N (K)	μ_s (μ_B)	T_c (K)	m^*/m_e	$\Delta C/(\gamma(T_c)T_c)$	$B_{c1,0}$ (G)	$B_{c2,0}$ (kG)	λ (Å)	ξ (Å)	Space group
$CeCu_2Si_2$	10	~1	0.1–0.3	0.65	380	0–1.48	23	15–25	5000	90	$I4/mmm$
UBe_{13}	8	-	-	0.87	260	2.4	46	102	11000	95	$Fm3c$
UPt_3	80	5	0.02	0.52, 0.48	180	0.4–1.6	nd[a]	15	>15000	200	$P6_3/mmc$
URu_2Si_2	70	17	0.02	1.5	140	0.6	16	80	10000	100	$I4/mmm$
UNi_2Al_3	~100	4.3	0.2	1	48	0.5	nd	<10	3300	240	$P6/mmm$
UPd_2Al_3	15–50	14.5	0.85	~2	66	1.2	11	25–30	4000	85	$P6/mmm$

[a]Not determined.

Equations (34) and (35) clearly indicate that in longitudinal fields, and depending on the nature of the internal fields (static or fluctuating), the μ^+ depolarization function will assume drastically different forms. Hence, in order to pinpoint the origin of the depolarization, decoupling experiments in longitudinal fields are routinely performed.

III. HEAVY-FERMION SUPERCONDUCTIVITY

Probably the most fascinating aspect of heavy-fermion physics remains the observation of superconductivity, first detected in $CeCu_2Si_2$ (Steglich *et al.*, 1979). Together with the later observation of superconductivity in exotic materials such as layered cuprate compounds or fullerene systems, this discovery certainly constitutes a milestone in the study of superconductivity.

Two exciting aspects of the superconductivity of $CeCu_2Si_2$ are the facts that (i) it occurs in a system showing a Curie-Weiss-type magnetic susceptibility at high temperature, indicating the presence of local magnetic moments that are known to rapidly depress superconductivity in conventional systems; and (ii) it appears as a co-operative phenomenon involving heavy quasiparticles that form Cooper pairs below T_c. This latter deduction is based on the observed scaling of the huge linear coefficient of the electronic specific heat ($\gamma = C_p/T$) with the specific-heat jump at T_c, as well as with the initial slope of the upper critical field at T_c. Although $CeCu_2Si_2$ is still so far the only Ce-based heavy-fermion superconductor at ambient pressure, the same phenomenon was subsequently reported in several U-based heavy-fermion compounds (see Table II). Even at an early stage in the development of heavy-fermion physics, it was speculated from numerous experimental evidence that the superconductivity in these systems may not be of the usual s-state isotropic type, but may instead involve an unconventional superconductivity ($L \neq 0$) with anisotropic p or d states. This possible unusual type of superconductivity could result from the nature of the mechanism providing the attractive force necessary for the Cooper-pair formation. In conventional superconductors, the electrons are paired in a spin-singlet zero-angular-momentum state ($L = 0$),

which results from a phonon-mediated pairing mechanism. This isotropic state leads to the formation of a superconducting gap in the electronic excitations over the whole Fermi surface. The possible unconventional superconductivity in the heavy-fermion systems should, on the other hand, be characterized by the presence on the Fermi surface of points or lines with vanishing superconducting gap, leading to power-law temperature dependencies below T_c of excitation-dependent physical properties. In recent years, numerous studies have been devoted to this question (see, for example, Grewe and Steglich, 1991). However, it should be stressed that the observation of power-law temperature dependencies does not constitute a definitive proof for unconventional superconductivity (power-law dependencies can also reflect the presence of impurity scattering in conventional superconductors). In addition, some of the observations reported to date present severe inconsistencies from one property to another. In this context it was soon recognized that μSR could help to draw more definitive conclusions. As extensively reported (see, for example, Gor'kov, 1987), the order parameter of an unconventional superconductor will not remain invariant under all the transformations allowed by the physical symmetry group and will therefore lack either the full point symmetry of the crystal or time-reversal invariance. Since μSR is an ideal tool to investigate weak-magnetism phenomena in zero external field, it can be utilized to search for the occurrence of spontaneous magnetism below T_c, which would signal a possible breakdown of the time-reversal invariance. Moreover, μSR transverse-field measurements below T_c can furnish valuable information on the possible anisotropies of the temperature dependence of the London penetration depth, which could indicate a crystal symmetry breaking.

Another fascinating aspect of heavy-fermion superconductivity [with the exception of $(U,Th)Be_{13}$] is that it appears to coexist with some kind of static magnetism occurring above T_c. The coexistence in itself does not represent an astonishing observation, since magnetic superconductors such as the Chevrel phases (Fischer, 1978) and the rare-earth rhodium borides, in which the superconductivity is carried by conduction electrons interacting only weakly with the local moments respon-
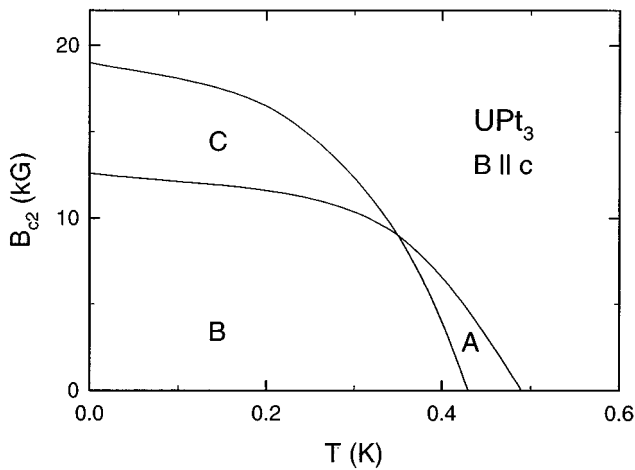
FIG. 3. Schematic $B - T$ phase diagram of UPt$_3$ for **B**‖**c**. The phases labeled A, B, and C refer to the three different superconducting phases.

FIG. 4. Temperature dependence of the μ^+ depolarization rate obtained in a polycrystalline UPt$_3$ sample (Cooke *et al.*, 1986). The zero-field results (open circles) were obtained by fitting a Kubo-Toyabe function [Eq. (26)] through the data, whereas the longitudinal-field μ^+ depolarization function (H_{ext}=5 kOe) is best described by a relaxing exponential function (open squares).

sible for the magnetism, have previously exhibited that phenomenon. The novel aspect of heavy-fermion superconductors is that both the quasiparticles forming the Cooper pairs as well as the electrons carrying the magnetism above T_c have unquestionably the same f character. Due to the local character of the μ^+ probe and its uniform implantation in a sample, μSR has been successfully utilized to check whether the coexistence of magnetism and superconductivity appears on a microscopic scale (as is usually only *assumed* from macroscopic measurements) or in different domains due to sample inhomogeneities, which are often present in heavy-fermion compounds and are known to hamper the interpretation of macroscopic measurements.

An overview of the μSR results obtained on the different heavy-fermion superconductors will be given in the following sections with special emphasis on the particular information provided by this microscopic technique.

A. UPt$_3$

Recently, the hexagonal heavy-fermion superconductor UPt$_3$ has appeared as the heavy-fermion compound for which the most indications for unconventional superconductivity have been reported. At an early stage, power-law temperature dependencies, as well as anisotropic responses of properties reflecting the electronic excitation spectrum, have been observed. Later, specific-heat studies (Fischer *et al.*, 1989) on high-quality crystals revealed the presence of two superconducting phase transitions (at T_{c+} and T_{c-}) in zero external field, interpreted as phases with different order parameters. Moreover, in an external magnetic field, one observes a multicomponent diagram with at least 3 superconducting phases meeting at a tetracritical point (see Fig. 3; Bruls *et al.*, 1990). The precise nature of the 3 superconducting phases remains an open question, but their occurrence is often interpreted as evidence that the supercon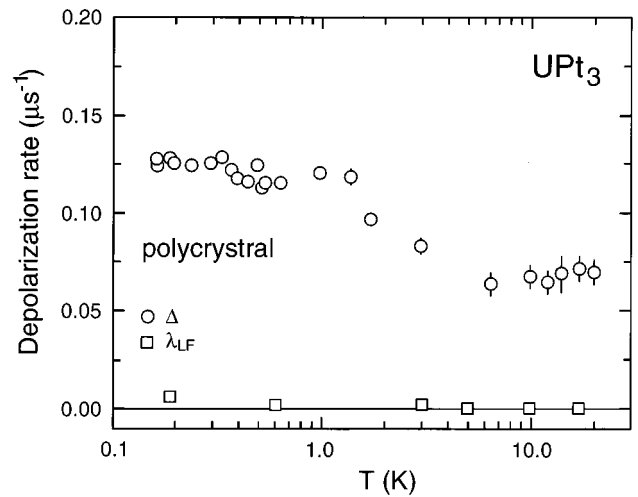ducting-gap function belongs to a two-dimensional (2D) representation (E_{1g}) of the rotation group D_{6h} (see Joynt, 1988; Machida and Ozuki, 1989). In this 2D scenario, the gap function, with even-parity pairing, is given by $\psi(\mathbf{k})$ = $\eta_x k_x k_z + \eta_y k_y k_z$, where the complex vector (η_x, η_y) determines the order parameter. The different superconducting phases would then correspond to the (1,0), (1,i), and (0,1) complex vectors. An alternative scenario (1D scenario; Machida and Ozuki, 1991) would be to consider two nearly degenerate one-dimensional representations of the rotation group corresponding to a gap function with odd parity. For both scenarios the presence of a symmetry-breaking field lifts the degeneracy of otherwise degenerate pairing states and leads to a splitting of T_c. Several experimental evidences, and notably the correlation between the splitting of T_c and the value of the magnetically ordered moments (Haiden *et al.*, 1992; Löhneysen *et al.*, 1992), demonstrate that the symmetry-breaking field originates from the weak antiferromagnetic order detected below $T_N \simeq 5$ K. This magnetic transition was first discovered utilizing μSR (Cooke *et al.*, 1986). The zero-field data recorded on a polycrystalline sample are reported on Fig. 4. Above 5 K, the value of the μ^+ depolarization rate is compatible with the depolarization arising from the field distribution at different possible μ^+ sites, which is solely created by the ^{195}Pt nuclear magnetic moments. The clear rise of the depolarization below 5 K is indicative of an increased field distribution at the μ^+ site, owing to the occurrence of static magnetic moments of electronic origin. The static character of these moments is proven by the essentially zero depolarization measured in longitudinal fields. Without knowledge of the exact μ^+ stopping site, Cooke *et al.* (1986) estimated the value of the static f moments to be of the order of $\mu_s \simeq 10^{-3}\ \mu_B$/U-atom. Later extensive neutron studies
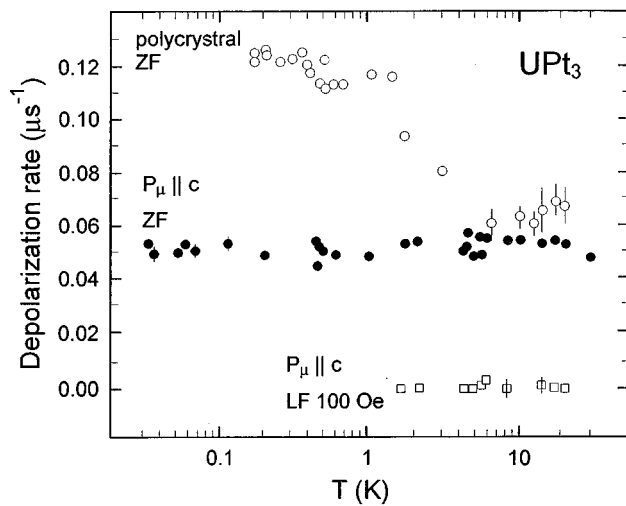
FIG. 5. Temperature dependence of the Kubo-Toyabe μ^+ depolarization rate obtained on a high-quality UPt$_3$ single crystal (solid symbols) in a configuration with the initial μ^+ polarization along the hexagonal c axis (Dalmas de Réotier *et al.*, 1995; Yaouanc *et al.*, 1994). Measurements performed with the initial μ^+ polarization along the a^* axis give very similar results. The exponential longitudinal-field (LF) μ^+ depolarization rate obtained in an external field $H_{ext}=100$ Oe is also reported (open squares) as well as the zero-field (ZF) depolarization rate obtained in a polycrystal (open circles; see also Fig. 4).

(Aeppli *et al.*, 1989) on the very same sample unravelled the antiferromagnetic structure formed by static moments of 0.02 μ_B ordered along the basal plane with an ordering vector $\mathbf{q}=(1/2,0,0)$. The small value of the static moment and the observation that $T_N \ll T^*$ (see Table II) indicates a magnetic state involving the renormalized heavy quasiparticles rather than the bare f moments (heavy-fermion band magnetism, see Sec. IV). Subsequent neutron studies always confirmed the presence of magnetic order, but several μSR studies presented conflicting results. The most relevant example is certainly furnished by the comprehensive study performed by Dalmas de Réotier *et al.* (1995) on a single crystal of very high quality. This high quality is illustrated by the clear double-peak structure of the specific heat due to the two superconducting transitions (Yaouanc *et al.*, 1994; see below, Fig. 10), and by the reported residual electrical resistivity, which was of the order of 0.1 $\mu\Omega$ cm. The most striking point of this μSR study is the observation of a temperature-independent zero-field depolarization rate (see Fig. 5) indicative of the lack of additional field distribution at the μ^+ site below 5 K. Since neutron-scattering studies on the very same sample clearly ascertain the antiferromagnetic transition at $T_N \simeq 5$ K, the present data appear in manifest contradiction with that reported in Fig. 4. A possible explanation would be to consider a μ^+ stopping site where the internal fields produced by the magnetic sublattices in the antiferromagnetic ordered state cancel. In such a scenario the increased μ^+ depolarization rate observed in some samples below T_N arises from distortions of the magnetic sublattices, producing a supplementary
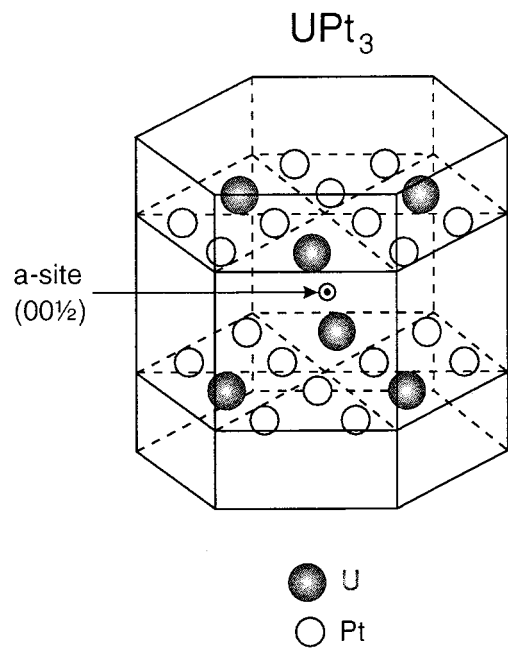

FIG. 6. Hexagonal structure of UPt$_3$ (space group $P6_3/mmc$) with the possible μ^+ stopping site (a site).

distribution of internal fields with zero mean at the muon site. The nonobservation of an increase of the depolarization rate below T_N should not be interpreted as an indication for the absence of magnetic order but rather as proof of the high quality of the investigated sample. In discussing possible μ^+ sites, we first recall that UPt$_3$ crystallizes in the close-packed hexagonal structure of the MgCd$_3$-type, corresponding to the low-temperature structure of SnNi$_3$ (Heal and Williams, 1955). This structure belongs to the space group $P6_3/mmc$ (D_{6h}^4), with U atoms at the c sites (Wyckoff notation) and Pt atoms at the h sites, with $x=\frac{5}{6}$ (see Fig. 6). The most likely μ^+ stopping site, with cancellation of the dipolar fields produced by the magnetic sublattices, can be identified as the a site ($00\frac{1}{2}$), which is located between two U-Pt planes.

At this point it is appropriate to mention the preliminary μSR studies on U$_{1-x}$Th$_x$Pt$_3$ with $x=0.05$ (Heffner *et al.*, 1989). It is known that the substitution of small concentrations of Th for U or Pd for Pt expands the unit-cell volume and therefore weakens the exchange interaction between the localized f electrons and the conduction electrons, which finally leads to the stabilization of the f local magnetic moment against the formation of the local Kondo singlets. Hence the substitution of a few atomic percents Th or Pd results in the occurrence of an antiferromagnetic order, with the same structure as in UPt$_3$ but a much larger value of the ordered moment ($\mu_s \simeq 0.5 \mu_B$; Goldman *et al.*, 1986; Frings *et al.*, 1987). The zero-field μSR results reported by Heffner *et al.* (1989) show a reduction of 80% of the amplitude of the μSR signal by cooling the sample below $T_N \lesssim 6.5$ K. Such an amplitude decrease indicates the presence of either an extremely fast depolarization or a
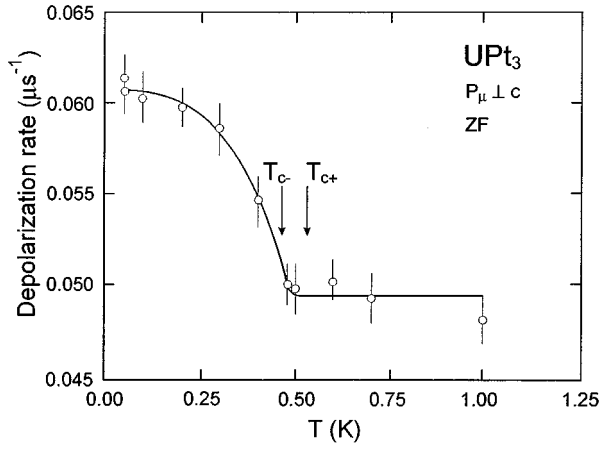
FIG. 7. Temperature dependence of the zero-field (ZF) exponential μ^+ depolarization rate obtained by Luke et al. (1993b) on a monocrystalline UPt$_3$ sample with the initial μ^+ polarization along the basal plan. The depolarization function was characterized by the product $G(t)=G_{KT}(t)\exp(-\lambda t)$ (see text).

very high frequency, neither of which could have been resolved in the experiment. Moreover, the remaining amplitude below 6.5 K is formed by two spontaneous-frequency components associated with large depolarization rates corresponding to linewidths larger than the precession frequencies. Such observations seem to indicate that more than two μ^+ sites are involved, unlike the observations with undoped UPt$_3$. However, the large observed μ^+ depolarization, as well as the presence of distinct components, could be indicative of defect-induced perturbations of the μ^+ sites and different domains in the sample. Therefore, before drawing any definitive conclusions from this latter study, additional measurements on samples with comparable quality as the undoped UPt$_3$ samples are advocated.

Another remarkable piece of information furnished by the μSR studies on UPt$_3$ was the observation in zero-field experiments of a supplementary very weak spontaneous magnetism below the superconducting transition temperature T_{c-} (Luke et al., 1993a, 1993b). To characterize the zero-field depolarization data Luke et al. (1993b) used a product of a temperature-independent Kubo-Toyabe function (arising from the ^{195}Pt nuclear moments) and an exponential relaxing function $\exp(-\lambda t)$ representing the additional μ^+ depolarization due to electronic magnetic moments. Such a product is legitimate for independent channels of depolarization. Figure 7 exhibits the exponential depolarization rate $\lambda(T)$ obtained in a single crystal, where the initial μ^+ polarization was along the basal plane. For this sample the increase in the depolarization, which is greater than that occurring below $T_N\simeq5$ K, appears to be linked with the lower superconducting transition and to indicate the presence of additional spontaneous internal fields of ~0.1 G at the μ^+ site.

In discussing the possible origins of this increased depolarization, Luke et al. (1993b) invoked first a reorientation of the ordered moments in the basal plane. Such a

reorientation was first suggested by Blount et al. (1990) to explain the observed reduction in the superconducting phase of the intensity of the neutron magnetic Bragg peaks, which was considered an indication of the coupling between the magnetic and the superconducting order parameter. The simplest reorientation would correspond to a simultaneous rotation of all the magnetic moments in the basal plane through a common angle. However, such a reorientation, corresponding to an admixture of longitudinal and transverse antiferromagnetic structure, would also lead, like the situation above T_c, to a cancellation of the internal fields at the above considered μ^+ stopping site. Consequently, for ideal crystals no change in the depolarization rate should be expected upon entering the superconducting phase. Under this assumption, the enhanced depolarization has to be linked to a side effect of the reorientation, generating, for a nonperfect crystal, an increase of the field distribution with zero mean at the μ^+ site. In this respect, the μSR data obtained on a high-quality single crystal and reported on Fig. 5 do not indicate a change of the depolarization below T_c.

A second possible origin for the increased depolarization is the occurrence below T_c of a superconducting state with no time-reversal symmetry, which creates an additional field at the μ^+ site. The magnitude of this supplementary field (0.1 G) has been taken by Ohmi and Machida (1993) as evidence for a lifting of the degeneracy in the spin space rather than in the orbital space. They thus argued for a spin-triplet odd-parity superconducting state belonging to the 1D scenario. However, the nonobservation by Dalmas de Réotier et al. (1995) (see Fig. 5) of an increase of the depolarization rate below T_{c-} in a high-quality single crystal, with the initial μ^+ polarization either along the c axis or the a^* axis, seriously questions this latter interpretation.

Several μSR studies have been devoted to determining the temperature dependence of the magnetic-field penetration depth in UPt$_3$. For transverse-field μSR measurements in type-II superconductors (with $H_{ext}>H_{c1}$), the presence of the flux-line lattice (FLL) causes an additional field distribution at the μ^+ site with a second moment given by (Brandt, 1988)

$$\langle\Delta B^2\rangle=\frac{3.706\times10^{-3}\phi_0^2}{\Lambda_{eff}^4},\qquad(36)$$

where ϕ_0 is the magnetic flux quantum. By assuming a triangular flux lattice, with interflux spacing $L\ll\Lambda_{eff}$ and a high value of the Ginzburg-Landau parameter κ, Barford and Gunn (1988) showed that for an uniaxial superconductor $\Lambda_{eff}=\sqrt{\lambda_\perp\lambda_\parallel}$ for $\mathbf{H}\perp\mathbf{c}$ and $\Lambda_{eff}=\lambda_\perp$ for $\mathbf{H}\parallel\mathbf{c}$ (where $\lambda_\perp$ and $\lambda_\parallel$ are the penetration depths perpendicular and parallel to the symmetry c axis). The presence of this supplementary field distribution at the μ^+ site produces an additional depolarization that is usually assumed to possess a Gaussian character with a depolarization rate $\sigma_{FLL}=\gamma_\mu\sqrt{\langle\Delta B^2\rangle}$. Such an oversimplification is known to introduce systematic uncertainties in the evaluation of the penetration depth from the fitted
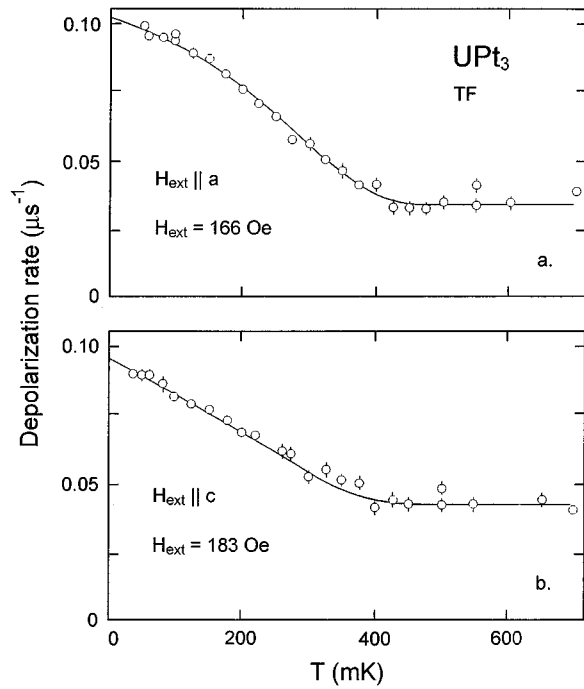
FIG. 8. Temperature dependence of the transverse-field (TF) μ^+ depolarization rate (Gaussian fits) in monocrystalline UPt$_3$ with (a) $\mathbf{H}_{ext}\|\mathbf{a}$ and H_{ext}=166 Oe, and (b) $\mathbf{H}_{ext}\|\mathbf{c}$ and H_{ext}=183 Oe. The solid lines are fits based on an anisotropic-gap function (for more details, see Broholm $et~al.$, 1990).

σ_{FLL}. Hence in the Gaussian approximation the high-field tail of the true spectral distribution is suppressed in the fit, resulting in too large Λ_{eff}. Thus the penetration depth obtained by such a fit must always be regarded as an upper limit.

Broholm $et~al.$ (1990) first measured the transverse-field depolarization rate on a UPt$_3$ single crystal (see Fig. 8) in the superconducting phase. The observed rise was interpreted as resulting from the values for the magnetic penetration depth of $\lambda_{\perp}(0)\simeq 7200$ Å and $\lambda_{\|}(0)$ $\simeq 6900$ Å. From the temperature dependence of the depolarization rate, $\lambda_{\perp}(T)$ and $\lambda_{\|}(T)$ were extracted and shown to be consistent with a superconducting gap possessing a line of nodes in the basal plane, which was ascribed to an even-parity superconducting state belonging to the above-described 2D scenario (with E_{1g} representation). However, one may notice that an order parameter belonging to the 2D E_{2u} representation has a similar topology of nodes as the E_{1g} order parameter, but with odd-parity state. Hence it appears that no definitive conclusions can be drawn from these μSR results.

This interpretation of the first μSR data was later questioned by Luke $et~al.$ (1993b). They noticed first that the reliable determinations of the penetration depth by bulk measurements (Gross $et~al.$, 1989; Signore $et~al.$, 1992) indicate values of $\sim$20 000 Å, which should lead to an increase of only 0.02 μs^{-1} in the μSR depolarization rate, a much smaller value than the one reported by Broholm $et~al.$ (1990). The second observation is the fact that the increase of σ takes place at temperatures clearly
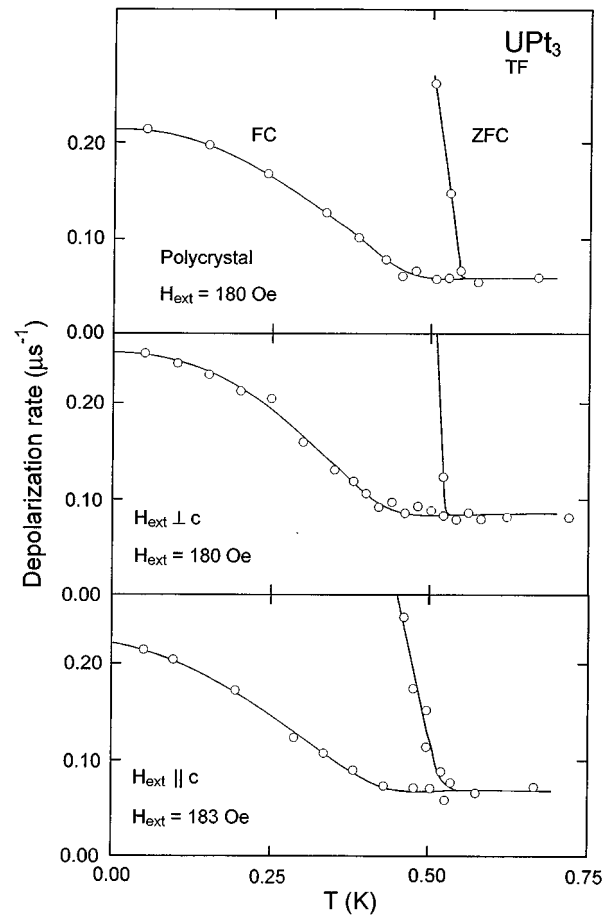

FIG. 9. Temperature dependence of the Gaussian transverse-field (TF) μ^+ depolarization rate obtained in field-cooling (FC) and zero-field-cooling (ZFC) procedures on polycrystalline and monocrystalline UPt$_3$ samples. Note that the temperatures where the depolarization rates start to increase do not coincide for the two procedures (from Luke $et~al.$, 1993b).

below the higher of the two superconducting transition temperatures T_{c+}. This was indisputably proven by the dissimilar behavior of the depolarization rate between zero-field-cooling (ZFC) and field-cooling (FC) measurements (see Fig. 9). At low temperature, σ_{ZFC} exceeds σ_{FC} due to flux pinning, which hampers the formation of a uniform flux-line lattice. The flux-depinning temperature, where $\sigma_{\text{ZFC}}\simeq\sigma_{\text{FC}}$, can be considered as a lower limit for the higher superconducting transition temperature T_{c+}. Figure 9 clearly establishes that the depolarization-rate rise, possibly due to the formation of the flux-line lattice, occurs at a temperature about 50 mK smaller than T_{c+}. Luke $et~al.$ (1993a) hence inferred that the increase of σ_{FC} was confined to the lower superconducting phase. Recently, Yaouanc $et~al.$ (1994) confirmed this observation on a single crystal, for which the specific heat was also measured (see Fig. 10). Unquestionably, the rise of the depolarization rate takes place at T_{c-}, whereas the flux-depinning temperature, as well as the reduction of the μ^+ frequency originating from the diamagnetic response of the sample, arise at T_{c+}. The problem emerges now to interpret the increase of the depolarization below T_{c-}.
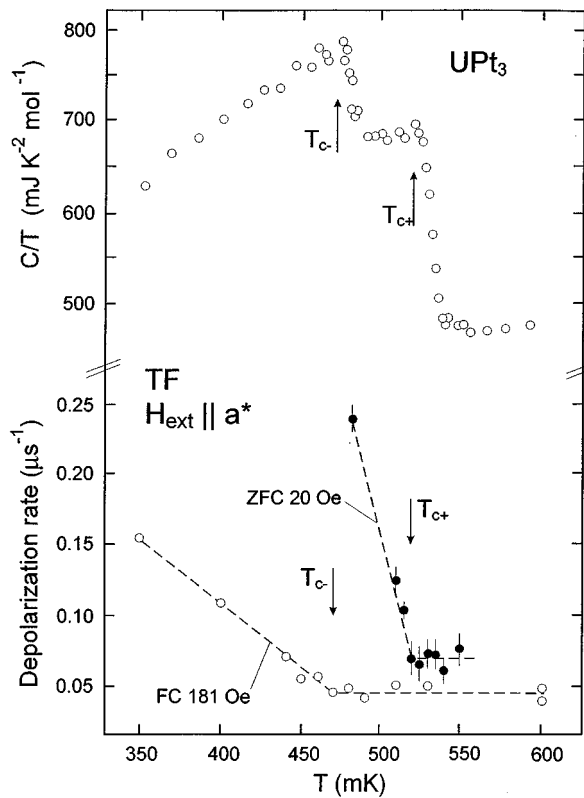
FIG. 10. Temperature dependence of the Gaussian transverse-field μ^+ depolarization rate in UPt$_3$ obtained in field-cooling (FC) and zero-field-cooling (ZFC) procedures in a high-quality single crystal ($\mathbf{H}_{ext}\|\mathbf{a}^*$). Note the coincidence between the two superconducting-transition temperatures (determined by specific heat on the same sample, see upper part of the figure) and the temperatures corresponding to the increase of the depolarization rates (see text). The high quality of the single crystal is underlined by the sharpness of both superconducting transitions (from Yaouanc *et al.*, 1994).

At this point, the reader should keep in mind the tentative character of the interpretation given below, owing to the absence of a complete picture of the behavior of the depolarization rate in external fields. It is tempting to associate the transverse-field depolarization rise with the increase reported in zero-field (see Fig. 7). However, two main objections could be formulated against this interpretation. First, the zero-field depolarization increase is substantially smaller than the one observed in a transverse field. Second, the rise in transverse-field depolarization is also reported for high-quality single crystals, for which the zero-field depolarization is temperature independent below T_{c-} (see Figs. 5 and 10). Another interpretation for the depolarization-rate increase is to invoke a drastic change of the flux-line lattice below T_{c-}. Indeed, several authors (Tokuyasu *et al.*, 1990, Garg and Chen, 1994) have postulated an unusual form of the flux-line lattice for time-reversal-breaking superconducting states, which therefore alters the relation between depolarization and magnetic penetration depth [see Eq. (36)]. As an example, Fig. 11 shows the possible stable flux-line lattices in the B phase as calculated by Garg and Chen (1994), considering the
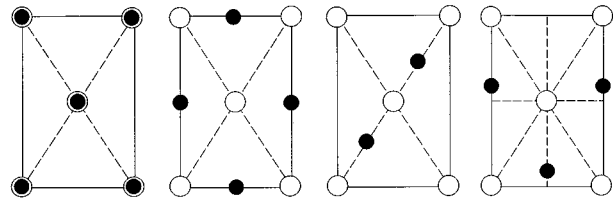

FIG. 11. Possible stable flux-line lattices for the superconducting B phase of UPt$_3$ calculating within the 1D scenario (see text; from Garg and Chen, 1994).

1D scenario. In this scenario, the B phase represents the region where both independent superconducting order parameters are nonzero. All possible cases represented in Fig. 11 lead to a modification of the field inhomogeneity at the μ^+ site, either by destroying the ideal triangular lattice or by doubling the vortex quantization. In this framework and opposite the usual situation, it is conceivable that a penetration depth as high as 20 000 Å could produce a detectable increase of the transverse-field depolarization rate. To verify this hypothesis, more transverse-field studies are urgently needed, notably in the superconducting C phase, where the presence of a single superconducting order parameter should be characterized by the recovery of a regular flux-line lattice.

Although the μSR studies on UPt$_3$ have left many questions unanswered and thus a complete understanding of the data is still lacking, among the heavy-fermion compounds UPt$_3$ undeniably constitutes a striking example wherein the highly sensitive μSR technique has uncovered unusual features, which have subsequently been "rediscovered" by more traditional techniques.

B. UBe$_{13}$

The system UBe$_{13}$ was the first U-based heavy-fermion superconductor discovered (Ott *et al.*, 1983), and, similar to UPt$_3$, it shows peculiar properties, pointing to an unconventional superconducting order parameter. The specific heat below $T_c \simeq 0.86$ K follows close to a T^3 law, compatible with the presence of points on the Fermi surface with vanishing superconducting gap. Josephson-effect studies (Han *et al.*, 1986) in a contact between UBe$_{13}$ and Ta [s-wave superconductor with $T_c(\text{Ta}) > T_c(\text{UBe}_{13})$] indicate that the s-wave order parameter induced by the proximity effect is strongly suppressed by the occurrence of the UBe$_{13}$ order parameter, suggesting that the latter might have odd parity. Finally, ultrasound attenuation (Golding *et al.*, 1985), as well as NMR spin-lattice relaxation time (MacLaughlin *et al.*, 1984), do not indicate an exponential temperature dependence below T_c. Nevertheless, no clear picture of the symmetry of the order parameter has emerged, and apparent inconsistencies still remain. The NMR relaxation rate, for example, follows a power law with exponent $n = 3$, which, contrary to the specific-heat data, is compatible with the presence of lines with vanishing superconducting gap.
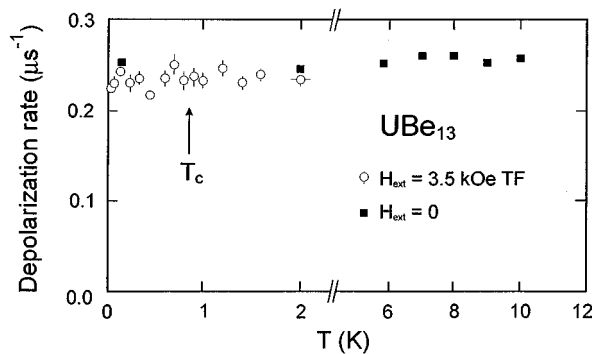
FIG. 12. Temperature dependence of the μ^+ depolarization rate obtained in a transverse-field (TF) (H_{ext}=3.5 kOe, Gaussian fit) and in zero field (Kubo-Toyabe fit) on a polycrystalline UBe$_{13}$ sample (from Luke *et al.*, 1991).

Early transverse-field μSR studies of polycrystalline UBe$_{13}$ were dedicated to the determination of the μ^+ Knight shift in the superconducting state. Heffner *et al.* (1989) first reported a strong reduction in absolute value of the Knight shift by cooling the sample below T_c. Since the Knight shift reflects the behavior of the conduction-electron spin susceptibility, such a decrease was interpreted as resulting from either even-parity pairing or odd-parity pairing, provided that the order parameter was strongly pinned to the lattice and therefore not free to rotate in the field. These results appeared to contradict ^{9}Be NMR data (MacLaughlin *et al.*, 1984), as well as induced-form-factor studies (Stassis *et al.*, 1986), which both indicated a temperature-independent spin susceptibility below T_c. This inconsistency was removed by subsequent μSR studies (Heffner, 1990; Luke *et al.*, 1991), for which the μ^+ Knight shift was found to be virtually unchanged in the superconducting state.[3] This behavior is compatible with odd-parity pairing and consistent with the observed power-law behavior of the specific heat.

A byproduct of the transverse-field μSR studies is the determination of the μ^+ depolarization, which, as we saw with Eq. (36), is related below T_c to the magnetic penetration depth. Typical results by Luke *et al.* (1991) are reported in Fig. 12. The lack of any increase of the depolarization below T_c demonstrates that the magnetic penetration depth is greater that 10 000 Å, in agreement with the value of ~11 000 Å obtained by flux confinement (Gross *et al.*, 1989). Furthermore, it is worth mentioning that measurements by magnetic induction (Einzel *et al.*, 1986) show that the penetration depth follows a T^2 power-law temperature dependence below T_c,

---

[3]Although Luke *et al.* (1991) extensively discussed the observation of a temperature-independent Knight shift in UBe$_{13}$, their experimental data show a slight frequency shift below T_c. Since this frequency shift is basically independent of the applied field [corresponding to $B_\mu(T=0) - B_\mu(T=T_c) \simeq 1$ G], it presumably does not reflect the spin susceptibility. So far no convincing explanation for the occurrence of this frequency shift has been provided.
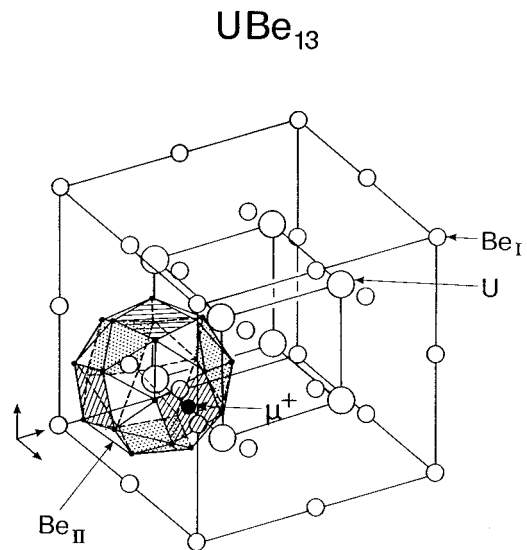
UBe$_{13}$

FIG. 13. Crystallographic structure of UBe$_{13}$ (space group $Fm3c$) with the possible μ^+ stopping site (d site) located between two nearest-U and four nearest-Be neighbors. 32 Be sites (Be$_{II}$) form a "snub cube" around each U site.

which again is compatible with an anisotropic gap function for an axial p-wave (odd-parity) superconducting state.

The possible occurrence of static magnetism in the superconducting phase has been checked by zero-field μSR studies (see, for example, Heffner *et al.*, 1989). The Kubo-Toyabe depolarization rate does not exhibit any detectable change, implying a complete absence of magnetic correlations with moments $\gtrsim 10^{-3}$ μ_B/U-atom down to at least 50 mK. In particular, the reported magnetic transition at $T_N \simeq 8.8$ K, which was observed by magnetostriction (Kleinman *et al.*, 1990), could not be confirmed within the high sensitivity of the μSR technique. The temperature-independent zero-field depolarization rate $\Delta = 0.245(2)$ μs^{-1} arises solely from the spread in dipolar fields due to the ^{9}Be nuclear magnetic moments. By comparing the measured value with calculated values for candidate interstitial sites, one observes an almost perfect agreement by assuming that the μ^+ stops at the d site (see Fig. 13). For this site of the cubic structure (space group $Fm3c$), a theoretical value of Δ_{theor}=0.246 μs^{-1} is calculated, very close to the observed value.

In order to check for the unconventional character of the superconducting order parameter, different studies on the influence of nonmagnetic impurities on the superconducting properties of UBe$_{13}$ have been undertaken. In conventional superconductors, elastic impurity scattering only affects the normal density of states, without affecting the superconducting critical temperature T_c. On the other hand, in unconventional superconductors nonmagnetic impurity scattering should act on the anisotropic orbital part of the superconducting wave function, leading to a depression in T_c. The observation of a clear-cut pair-breaking effect for U$_{1-x}$M$_x$Be$_{13}$ with M=La, Y, or Th has therefore been interpreted as sup-
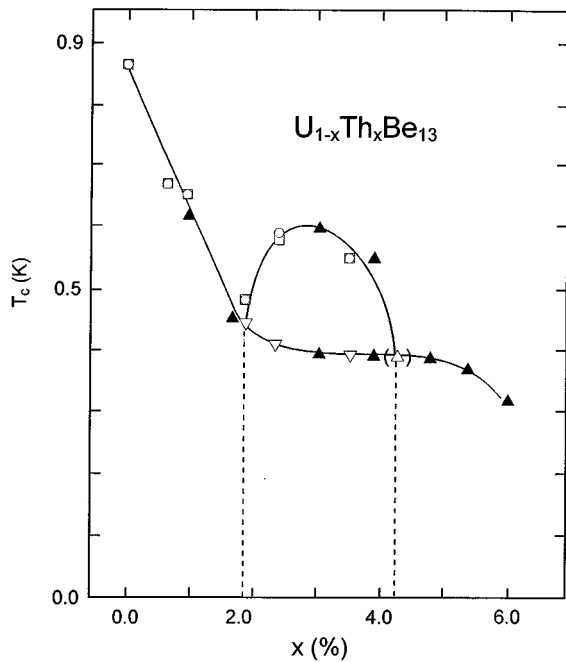
FIG. 14. Phase diagram of $U_{1-x}Th_xBe_{13}$. Note the second phase transition appearing for $0.019 \lesssim x \lesssim 0.043$ (see Heffner *et al.*, 1990, for more details).

FIG. 15. Temperature dependence of the zero-field μ^+ depolarization rate measured on polycrystalline $U_{1-x}Th_xBe_{13}$ sample with different Th concentrations (from Heffner *et al.*, 1990).

portive for an anisotropic order parameter. The most intriguing observation was probably done in the system $U_{1-x}Th_xBe_{13}$, where the substitution of the Th for U depresses the superconducting transition temperature in a strongly nonmonotonic fashion (Smith *et al.*, 1984). An even more astonishing phenomenon is the presence for $0.019 \lesssim x \lesssim 0.043$ of a second transition (T_{c2}) within the superconducting state, detected by a distinct anomaly in the specific heat (Ott, Rudigier, Fisk, and Smith, 1985; see Fig. 14) and by a clear change of slope of the lower critical field H_{c1} versus T^2. Several interpretations have been proposed for this second transition, invoking the occurrence of a spin-density-wave state resulting from the residual interactions between the heavy quasiparticles (Machida and Kato, 1988), magnetic moments on either the U (Fisk *et al.*, 1988), or Th sites (Moshchalkov, 1987), as well as a transition to a superconducting state exhibiting spin (Volovick and Gor'kov, 1985) or orbital magnetism (Sigrist and Rice, 1989).

In order to gain more insight into the nature of the phase below T_{c2}, several μSR studies have been performed, first on a limited number of samples (Heffner *et al.*, 1989), and later for a wide range of Th concentrations (Heffner *et al.*, 1990). For this latter study the temperature dependence of the zero-field depolarization rate is shown in Fig. 15. The values above $T \gtrsim 0.5$ K of Δ are determined by the dipolar field distribution produced by the ^{9}Be nuclei as described above for pure UBe_{13}. The small variation from sample to sample probably reflects systematic uncertainties in the data analysis. For all concentrations no change in $\Delta(T)$ was observed at T_{c1}. Moreover, for $x = 0.000$, 0.010, and 0.060, $\Delta(T)$ is constant down to at least 50 mK, suggesting a complete absence of static magnetic moments with μ_s
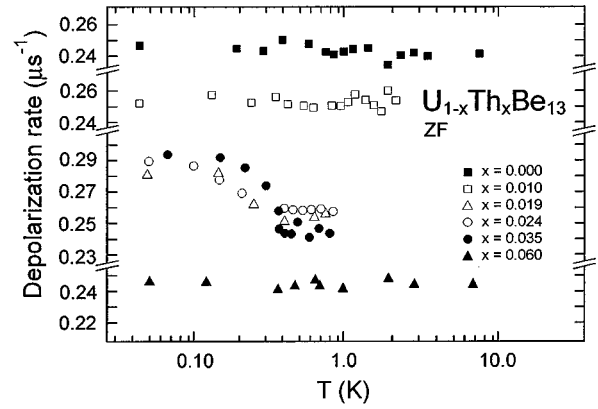
$\gtrsim 10^{-3}$ μ_B/U atom. The most striking observation is the increase in $\Delta(T)$ occurring only for Th concentrations $0.019 \lesssim x \lesssim 0.043$, i.e., in the concentration range for which the second transition is observed. Comparison with specific-heat and H_{c1} data (Heffner *et al.*, 1990) clearly indicates that $\Delta(T)$ starts to increase below T_{c2} (see Fig. 16). Such an increase arises from the onset of weak magnetism of electronic origin. By keeping in mind that the electronic and nuclear contribution to the total depolarization rate add in quadrature, one finds that (i) the temperature dependence of the electronic contribution $\Delta_e(T)$, which reflects the magnetic order parameter, is compatible with a second-order transition;
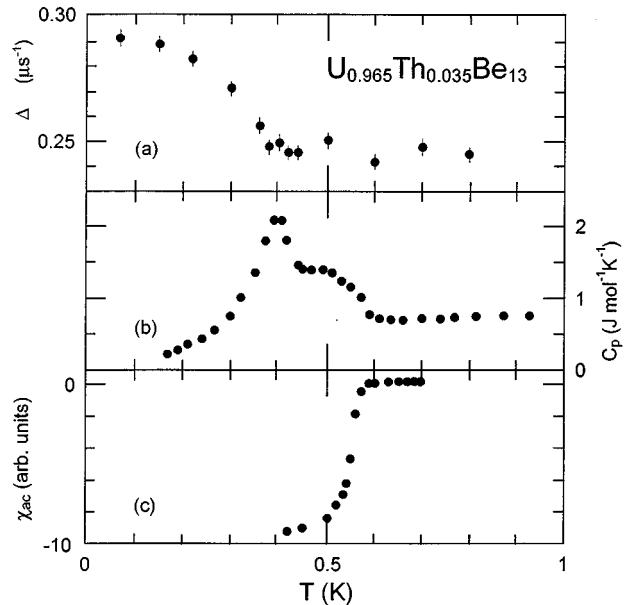

FIG. 16. Temperature dependence of (a) zero-field μ^+ depolarization rate (Kubo-Toyabe fit), (b) the specific heat, and (c) the AC susceptibility for $U_{0.965}Th_{0.035}Be_{13}$. Note the coincidence between the onset of the depolarization-rate increase and the lower specific-heat anomaly at T_{c2} (from Heffner *et al.*, 1990).

and (ii) $\Delta_e(T \to 0)$ increases sublinearly with the Th concentration. This sublinearity as well as the abrupt disappearance of magnetism below $x = 0.019$ indicate no formation of local Th moments. By assuming the μ^+ stopping site to be the d site, as deduced in the pure UBe$_{13}$, the static effective magnetic moments responsible for the depolarization-rate increase are of the order of $\sim 3 \times 10^{-3}$ μ_B/U atom. The occurrence of electronic magnetism with very small moments associated with a large specific-heat anomaly at T_{c2} appears to preclude the formation of a magnetic phase not interacting with the superconducting state. Therefore the plausible origins for the phase below T_{c2} include either the formation of a magnetic phase coupled with the superconducting order parameter, or the occurrence of a new superconducting phase violating time-reversal invariance. The former possibility is supported by the observation of a λ-shaped ultrasound-attenuation peak at T_{c2}, consistent with those expected near a magnetic transition (Batlogg et al., 1985). Knetsch, Nieuwenhuys et al. (1993) have also discussed the possibility that the spin fluctuations could be responsible for the electrical-resistivity and specific-heat maxima occurring just above T_c in pure UBe$_{13}$. With Th doping these maxima move lower in temperature and cross the superconducting-temperature transition at $x = 0.019$, i.e., at the concentration where the evolution of T_{c1} is reversed (see Fig. 14). It is therefore tempting to connect the anomaly at T_{c2} with the freezing of these spin fluctuations giving rise to some kind of weak-magnetism coupling with the superconducting order parameter. Heffner et al. (1990) argued that a loss of Fermi surface at a magnetic transition of spin-density-wave type should reduce the effective mass of the quasiparticles, which is compatible with the increase of $|dH_{c1}/dT^2|$ below T_{c2} (Rauchschwalbe, 1987). The coupling between a spin-density-wave state and the superconducting state has been theoretically investigated by Gulásci and Gulásci (1989). It was found to favor the occurrence of a superconducting order parameter breaking the translational symmetry.

As stated above, and as observed for UPt$_3$, the μSR results for UBe$_{13}$ are also consistent with a multicomponent complex superconducting order parameter. The phase transition at T_{c2} would be interpreted as the transition to a superconducting ground state violating time-reversal invariance. Under this assumption, several models predict the occurrence of orbital currents, induced when scattering from nonmagnetic impurities (Th) lead to inhomogeneities of the superconducting order parameter (see, for example, Mineev, 1989). However, in this framework the paramount problem is to understand why UBe$_{13}$ is changed by Th doping in such a drastic way and why La or Lu dopings merely result in a monotonic suppression of the superconductivity.

The substitution of B for Be represents another striking example of impurity-doping effects on the superconducting state of UBe$_{13}$ (Felder et al., 1989). A recent systematic study of UBe$_{13-y}$B$_y$ (Beyermann et al., 1995) indicates, on one hand, a modest reduction of T_c with B concentration and, on the other hand, a dramatic varia-
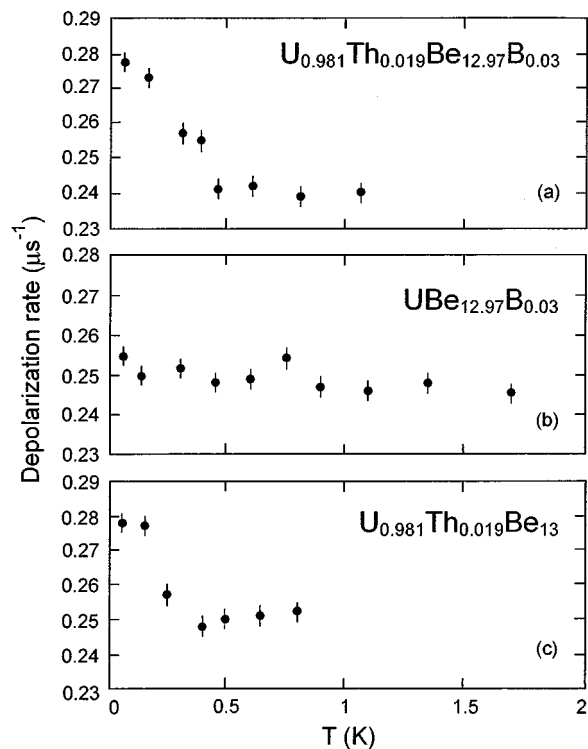

FIG. 17. Temperature dependence of (a) zero-field μ^+ depolarization rate (Kubo-Toyabe fit) measured in UBe$_{12.97}$B$_{0.03}$, U$_{0.981}$Th$_{0.019}$Be$_{12.97}$B$_{0.03}$, and U$_{0.981}$Th$_{0.019}$Be$_{13}$. Note the depolarization rate increases only in Th-doped samples (from Heffner et al., 1991).

tion of the normalized specific-heat jump $[\Delta C/(\gamma(T_c)T_c)]$ at the superconducting transition temperature, with a maximum value of $\Delta C/(\gamma(T_c)T_c) \simeq 3.76$ (for $y = 0.03$), which is the largest of any known material. Contrary to the results reported for Th doping, no indication for a second transition near T_c has been found.

The origin of the increased specific-heat jump at T_c has first been discussed as arising from a magnetic phase transition concomitant with the superconducting transition. However, zero-field μSR data on a $y = 0.03$ sample (Heffner et al., 1991) do not support this interpretation (see Fig. 17). The temperature-independent behavior of Δ implies the virtual absence of static magnetism below T_c, similar to what was observed in pure UBe$_{13}$. Moreover, additional Th doping (for example, U$_{0.981}$Th$_{0.019}$Be$_{12.79}$B$_{0.03}$) leads again to a second transition in the specific heat, below which μSR unquestionably detects magnetism in a similar way as in the B free U$_{0.981}$Th$_{0.019}$Be$_{13}$ (see Fig. 17). Hence B doping does not appear to alter the Th-induced magnetic feature. Recently, Beyermann et al. (1995) discussed the specific heat and electrical resistivity of UBe$_{13-y}$B$_y$ systems in terms of strong-coupling theories of unconventional superconductivity. The temperature T^* characterizing the renormalized quasiparticles is reduced with B doping and seems to be accompanied by a reduction of the frequency ω_0 characterizing the bosonic excitation mediating the pairing interaction. This could be consistent if

the superconducting pairing mechanism was mediated by spin fluctuations. However, in this framework the problem is to understand why T_c is not as significantly reduced as ω_0. Another possible scenario for the increased specific-heat jump would be to consider a change of the superconducting state and therefore of the nodal structure of the superconducting gap. Clearly, more theoretical work is required to explain how such small dopings can trigger such dramatic changes of the superconducting state.

C. UPd$_2$Al$_3$ and UNi$_2$Al$_3$

The most recently discovered heavy-fermion superconductors UPd$_2$Al$_3$ and UNi$_2$Al$_3$ (Geibel, Shank *et al.*, 1991; Geibel, Thies *et al.*, 1991) exhibit coexistence between superconductivity and a magnetic state with relatively large ordered moments. In this new variant of the interplay between heavy-fermion superconductivity and magnetism, much excitement arose from the potential to observe a strong interaction between the magnetic and superconducting order parameters. Furthermore, the detection of large static magnetic moments contradicted the picture that small values of these moments ($\mu_s \lesssim 10^{-2} \mu_B$) were a prerequisite for a coexistence of both types of ground states. Therefore this discovery has provided a fascinating opportunity to extend the comprehension of the heavy-fermion compounds, and extensive experiments have been carried out on these compounds. Both systems crystallize in a rather simple hexagonal structure $P6/mmm$ (D_{6h}^1, PrNi$_2$Al$_3$-type structure). Whereas UNi$_2$Al$_3$ forms peritectally, UPd$_2$Al$_3$ has a congruent melting, resulting in the availability of large single crystals. As a consequence, most results were first obtained in the latter compound.

UPd$_2$Al$_3$ was found to exhibit a simple antiferromagnetic structure [wave vector $\mathbf{q}=(0,0,\frac{1}{2})$] below $T_N \simeq 14.5$ K (Krimmel *et al.*, 1992) and static magnetic moments of U lying in the basal plane. The neutron-scattering data are consistent with an ordered magnetic moment $\mu_s \simeq 0.85 \mu_B$, reduced compared to the effective moment obtained from the high-temperature susceptibility, but exceeding by up to two orders of magnitude the small moments found, for example, in UPt$_3$ (see Sec. III.A). Hence, in contrast to UPt$_3$, a picture of local-moment magnetism seems to describe the magnetic state in UPd$_2$Al$_3$. Surprisingly, this large-moment magnetism was found to coexist with heavy-fermion superconductivity exhibiting the highest T_c reported to date.

Early zero-field μSR measurements on polycrystals indicated the absence of a precessing component in the zero-field μSR spectra (see Fig. 18; Amato, Feyerherm, Gygax *et al.*, 1992), indicating that even below T_N the internal field has an average value of zero at the μ^+ site, which must therefore be symmetric with respect to the antiferromagnetic sublattices. The magnetic transition is nevertheless characterized by the change of behavior of the μ^+ depolarization. Whereas above T_N the μ^+ depolarization only reflects the field spread caused by the
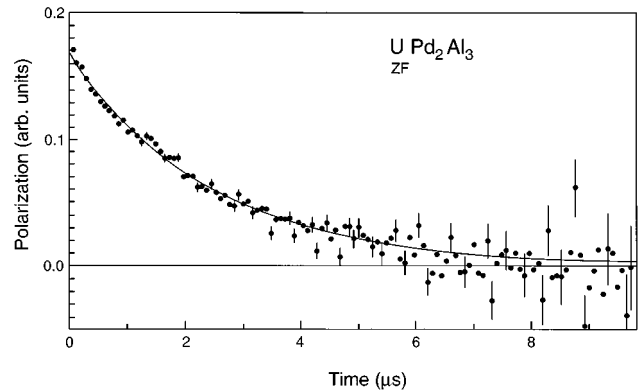

FIG. 18. Time evolution of the μ^+ polarization measured in zero-field (ZF) in a polycrystalline UPd$_2$Al$_3$ sample below T_N. Note the absence of spontaneous precession and the exponential depolarization (from Amato, Feyerherm, Gygax *et al.*, 1992).

nuclear dipole fields of the ^{27}Al nuclei, a slight increase is observed below T_N, caused by imperfections of the magnetic sublattices producing an enhancement of the field distribution at the μ^+ site. Furthermore, the depolarization is unchanged below T_c, indicating that the magnetic state is not affected by the onset of superconductivity. Considering the above-described magnetic structure observed by neutrons, the zero-field μSR data indicate that solely the b site $(00\frac{1}{2})$ is occupied in UPd$_2$Al$_3$ (see Fig. 19). This site determination was later confirmed by transverse-field μSR measurements in a single crystal (Amato, Feyerherm, Geibel *et al.*, 1992). Figure 20 shows the angular dependence of the μ^+ frequency for which the shape and amplitude are only compatible with the occupation of the symmetric b site.

If the nonobservation of spontaneous μ^+ frequencies below T_N has, on one hand, impeded a μSR study of the magnetic structure, it nevertheless gave the opportunity
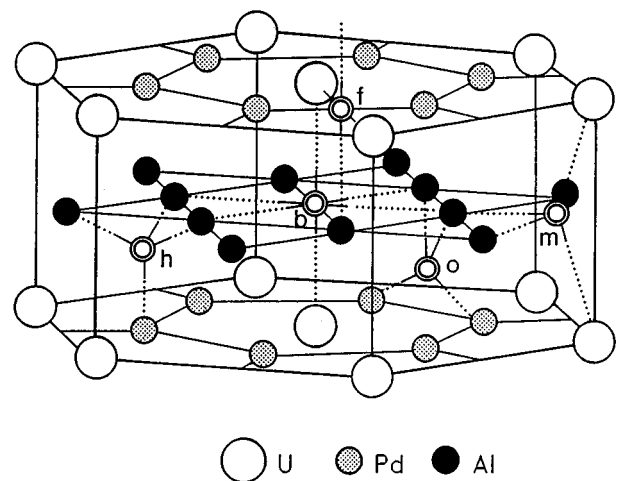

FIG. 19. Crystalline structure of UPd$_2$Al$_3$ (and UNi$_2$Al$_3$), where different interstitial sites are indicated by their Wyckoff notation. The μ^+ stopping site in UPd$_2$Al$_3$ is located between two U ions along the c axis.
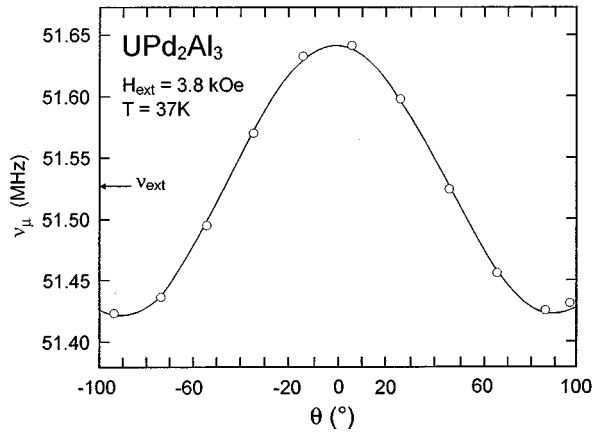
FIG. 20. Angular dependence of the μ^+ frequency measured in a monocrystalline UPd$_2$Al$_3$. $\mathbf{H}_{ext}$ is rotated in the a^*-c plane and θ denotes the angle between $\mathbf{H}_{ext}$ and the c axis (from Amato, Geibel et al., 1992).

to perform transverse-field measurements in the magnetic phase. In particular the behavior of the μ^+ depolarization rate as well as the μ^+ Knight shift could be investigated for $T \ll T_N$, i.e., in the superconducting phase.

Early transverse-field measurements by Amato, Feyerherm, Gygax et al. (1992), performed with a relatively low external field ($H_{ext} = 117$ Oe) on a polycrystal, show that for all temperatures the μSR spectra are composed of only one component. This indicates the absence of volume segregation and therefore implies that in UPd$_2$Al$_3$ magnetism and superconductivity coexist at a microscopic level. Additional transverse-field μSR studies of the magnetic and superconducting phase have been reported by Feyerherm, Amato, Gygax, Schenck, Geibel et al. (1994) for monocrystalline samples. An extensive analysis of the data obtained below T_c has provided valuable information on the nature of the superconducting phase and will therefore be briefly described. Below T_c the field spread at the μ^+ site caused by the magnetic phase coexists with the field inhomogeneity due to the flux-line lattice ($H_{ext} > H_{c1}$). The different nature of these field distributions results in two independent channels of depolarization acting on the muon ensemble. The time evolution of the μ^+ polarization can therefore be written as

$$G(t) = \exp(-\lambda_0 t) \cdot G_{FLL}(t), \qquad (37)$$

where λ_0 represents the width of the field distribution created by the magnetic order and $G_{FLL}(t)$ reflects the depolarization due to the flux-line lattice. An additional complication arises from the smallness of the upper critical field H_{c2} in UPd$_2$Al$_3$. For measurements with relatively high external magnetic fields, and keeping in mind that the coherence length is small compared to the penetration depth, the inhomogeneity of the superconducting order parameter (and therefore of the change of the μ^+ Knight shift due to the formation of the Cooper pairs) has to be taken into account in the analysis. Feyerherm, Amato, Gygax, Schenck, Geibel et al. (1994)
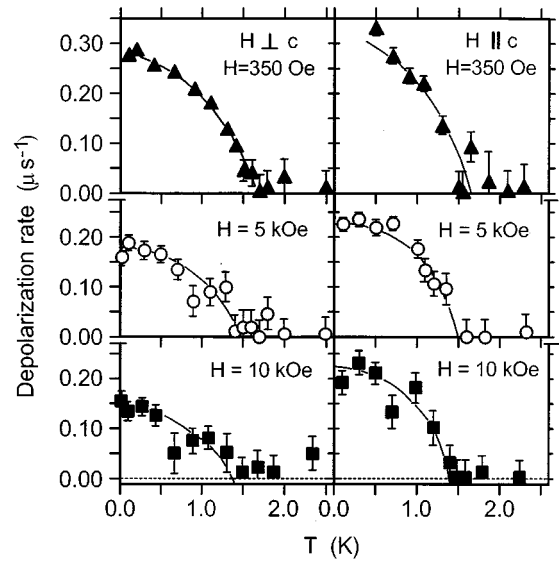

FIG. 21. Temperature dependence of the transverse-field μ^+ depolarization rate σ_{FLL} measured in UPd$_2$Al$_3$ for $\mathbf{H}_{ext}\|\mathbf{c}$ (r.h.s.) and $\mathbf{H}_{ext}\perp \mathbf{c}$ (l.h.s.). σ_{FLL} is caused by the field distribution due to the flux-line lattice ($H_{ext} \gg H_{c1}$, see text for fitting procedure). The observed field dependence is well in line with theoretical predictions (see, for more details, Feyerherm, Amato, Gygax, Schenck, Geibel et al., 1994).

have approximated the spatial variation of the gap function ψ by setting $\psi = 0$ in the vortex cores (normal regions) and $\psi = \psi_{max}$ in the intercore regions. For high field measurements, a two-component fit was applied with

$$G_{FLL}(t) = \mathcal{A}_c \cos(\omega_c t) + \mathcal{A}_{ic} \exp\left(-\frac{\sigma_{FLL}^2 t^2}{2}\right) \cos(\omega_{ic} t),$$
$$(38)$$

where $\mathcal{A}_c$ and $\mathcal{A}_{ic}$ represent the volume occupied by the core and intercore regions, respectively ($\mathcal{A}_c + \mathcal{A}_{ic} = 1$ and $\mathcal{A}_c / \mathcal{A}_{ic} \simeq H_{ext}/H_{c2}$). The temperature dependence of the μ^+ depolarization arising from the FLL is reported in Fig. 21. A comparison with simulated data yields a penetration depth $\lambda_\perp(0) = 4800 \pm 500$ Å and $\lambda_\|(0) = 4500 \pm 500$ Å. This μSR data provided the first indication of the isotropic character of the penetration depth in UPd$_2$Al$_3$. Furthermore, the μ^+ Knight shift was found to manifest a peculiar behavior below T_c. For the axially symmetric b site, the relative shifts of the μ^+ frequency (in the intercore regions) are given by [see also, Eq. (18)]

$$\frac{\Delta \omega_{ic,\|}}{\omega_{ext}} = K^*_{\mu\|} = (A_c + A^{zz}_{dip})\chi_{5f,\|} + (\text{D.F.} + \text{L.F.}),$$

$$\frac{\Delta \omega_{ic,\perp}}{\omega_{ext}} = K^*_{\mu\perp} = (A_c - \tfrac{1}{2}A^{zz}_{dip})\chi_{5f,\perp} + (\text{D.F.} + \text{L.F.}).$$
$$(39)$$

The last terms represent the demagnetization and Lorentz fields, which again essentially mirror the $5f$ magnetic susceptibility χ_{5f}. The temperature dependencies of $K^*_{\mu\|}$ and $K^*_{\mu\perp}$ are reported in Fig. 22 for $H_{ext} = 10$ kOe.
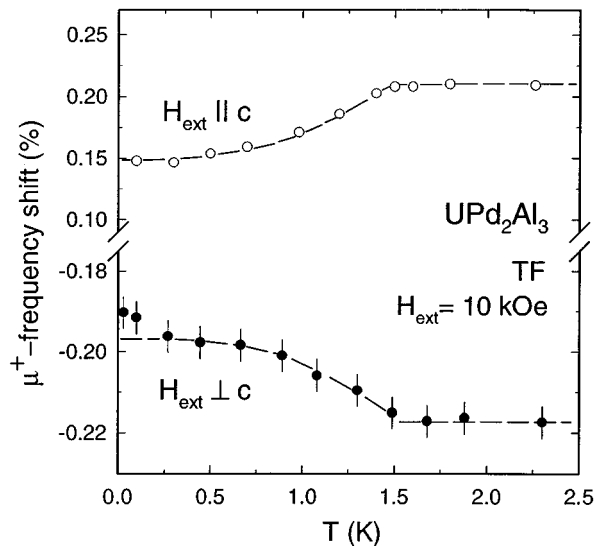
FIG. 22. Temperature dependence of the μ^+-frequency shifts in UPd$_2$Al$_3$ with H_{ext}=10 kOe applied along and normal to the c axis. The data are not corrected for demagnetization and Lorentz fields (adapted from Feyerherm, Amato, Gygax, Schenck, Geibel et al., 1994).

In discussing the possible origins for the decrease in absolute value of the μ^+ frequency shift below T_c, Feyerherm, Amato, Gygax, Schenck, Geibel et al. (1994) noticed that (i) the diamagnetic shift due to the flux expulsion was estimated to be much smaller than 0.01% and would be negative independent of the orientation of $\mathbf{H}_{ext}$; (ii) a change of the hyperfine coupling constant would also lead to a change of the μ^+ frequency in the same direction for both crystallographic orientations; and (iii) the dipolar coupling constant is only given by the lattice geometry and accordingly has to be considered constant for all temperatures. Therefore the observed partial reduction of the μ^+ frequency shift can only reflect a reduction of χ_{5f} below T_c. This observation, which is compatible with singlet pairing of the superconducting state, is supported by the strong paramagnetic effects on the critical field $H_{c2}(T)$ (Amato Feyerherm, Gygax et al., 1992). Surprisingly, the derived reduction of χ_{5f} is *isotropic* ($\Delta\chi_{5f,\perp} \simeq \Delta\chi_{5f,\parallel} \gtrsim 1.7 \times 10^{-3}$ emu/mole), in sharp contrast with the highly *anisotropic* total 5f susceptibility. Since UPd$_2$Al$_3$ is unquestionably in the clean limit (Amato, Feyerherm, Gygax et al., 1992), the residual susceptibility below T_c ($\chi_{5f} - \Delta\chi_{5f}$) cannot arise from impurity scattering. It is therefore tempting to develop a physical picture of two rather independent electron subsets where $\Delta\chi_{5f}$ must be associated with the susceptibility of the electron subsystem formed by the heavy quasiparticles condensing into Cooper pairs below T_c, yet the anisotropic residual susceptibility ($\chi_{5f} - \Delta\chi_{5f}$) should be ascribed to the electron subsystem associated with the local antiferromagnetism, which is unaffected in the superconducting state. Furthermore, the isotropy of $\Delta\chi_{5f}$ could reflect the itinerant character of the heavy-quasiparticle subsystem. Interestingly, polarized neutron-scattering studies (Pa-

olasini et al., 1993) indicate that the delocalized electron susceptibility amounts to $\chi \simeq 2.1 \times 10^{-3}$ emu/mole, close to the value extracted by μSR. Additional support for the coexistence of two distinct electron subsets was provided by specific-heat measurements under pressure (Caspary et al., 1993), which demonstrated that the itinerant subsystem accounts for only 80% of the linear coefficient of the specific heat. From these results, and using a rudimentary free-electron model, an estimation of the susceptibility of the itinerant subsystem yields $\chi \simeq 1.6 \times 10^{-3}$ emu/mole, which again appears in close agreement with the μSR results. Finally, one should mention the recent ^{27}Al NMR Knight-shift data (Kyogaku et al., 1993), for which, by *assuming* (in contrast to the μSR data) a temperature-independent hyperfine contact coupling constant, a similar picture with independent electron subsets can be deduced. Furthermore, the temperature dependence of the nuclear-spin-lattice relaxation $1/T_1$ obtained by nuclear quadrupole resonance (NQR) shows a T^3 behavior (over four orders of magnitude), compatible with a line of zero superconducting gap on the Fermi surface. This behavior has been ascribed to a d-wave even-parity superconducting state, compatible with the reduction of the spin susceptibility observed by μSR.

Despite the fact that the idea of a coexistence of different electron subsystems in heavy-fermion compounds is still controversial, some theoretical models have been proposed to explain the apparent duality of these systems. Kuramoto and Miyake (1990) have developed a phenomenological model that introduces two electron components: itinerant and localized, with the latter retaining a large part of the spin degree of freedom. This model has been utilized to qualitatively explain heavy-fermion magnetism with strongly reduced static moments (see Sec. IV), which is usually embedded in a state with strong paramagnetic response. It remains to be seen whether such an approach could account for the observed coexistence between local-moment magnetism and superconductivity. Caspary et al. (1993), on the other hand, favor a picture where the appearance of different subsystems arises from an anisotropic hybridization between the f moments and the conduction electrons, resulting in the formation of different states coexisting in the $\mathbf{k}$ space. However, in this framework the difficulty is to understand the occurrence of a perfectly isotropic superconducting state.

For the parent system UNi$_2$Al$_3$, early μSR data on polycrystalline probes (Amato, Geibel et al., 1992) have been performed with the aim of unravelling the magnetic structure. The zero-field spectra below $T_N \simeq 4.3$ K (see Fig. 23) show a complex signal, in sharp contrast with the situation observed in UPd$_2$Al$_3$ (see Fig. 18). Unfortunately, such a complex signal prohibits a μSR study of the superconducting state, and therefore only information about the magnetic phase could be provided. Regardless of the exact underlying magnetic structure and μ^+ stopping sites, the magnitude of the observed frequencies has furnished evidence for a relatively moderate value of the ordered moments of the
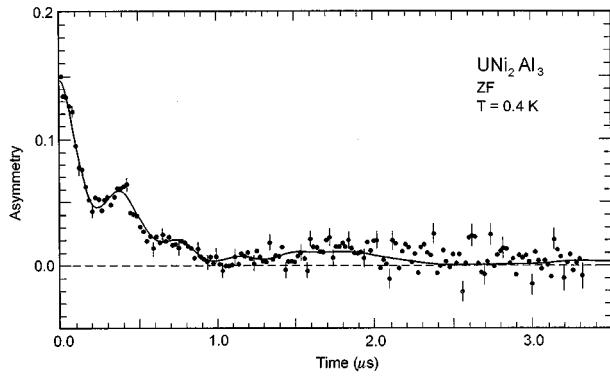
FIG. 23. Time evolution of the μ^+ polarization measured in zero field (ZF) in a polycrystalline UNi$_2$Al$_3$ sample below T_N. Solid curve: best-fit curve obtained by the sum of two J_0 Bessel functions and a relaxing $\frac{1}{3}$ term (see text).

order of $\mu_s \simeq 0.1 \ \mu_B$. No sizable change of the spontaneous frequencies was detected below $T_c \simeq 1$ K, implying that the magnetic order microscopically coexists with and is not appreciably affected by superconductivity below T_c.

Later neutron-diffraction measurements (Krimmel *et al.*, 1992) performed on powder samples indirectly confirmed the order of magnitude of μ_s found by μSR by failing to detect any evidence of static magnetism and setting an upper limit of $\sim 0.2 \ \mu_B$ for μ_s. Subsequent zero-field investigations on a single crystal demonstrated the similarity between the spectra obtained on UNi$_2$Al$_3$ and those of the incommensurate-spin-density-wave organic system (TMTSF)$_2$PF$_6$ (see Fig. 24). This resemblance strongly suggests the likelihood of a magnetic state with incommensurate spin structure in UNi$_2$Al$_3$. For an incommensurate magnetic structure (IMS) described by one **q** wave vector, the local-field distribution $n_{IMS}(B)$ at the μ^+ site can be analytically computed (Major *et al.*, 1986). Whereas, for commensurate magnetic structure sharp distributions are present due to the
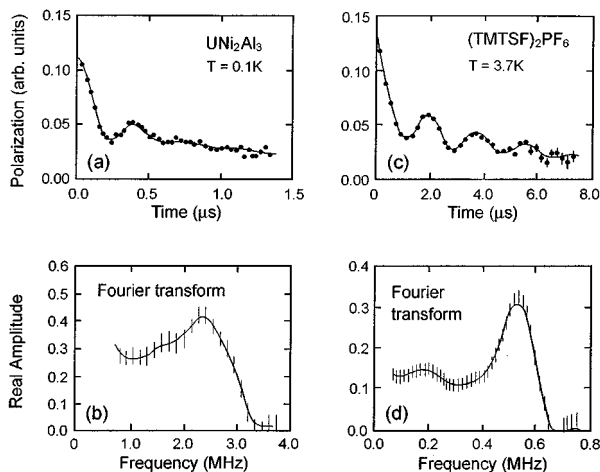

FIG. 24. Zero-field μSR signals and their Fourier transforms recorded below T_N in UNi$_2$Al$_3$ and (TMTSF)$_2$PF$_6$ (from Uemura and Luke, 1993).
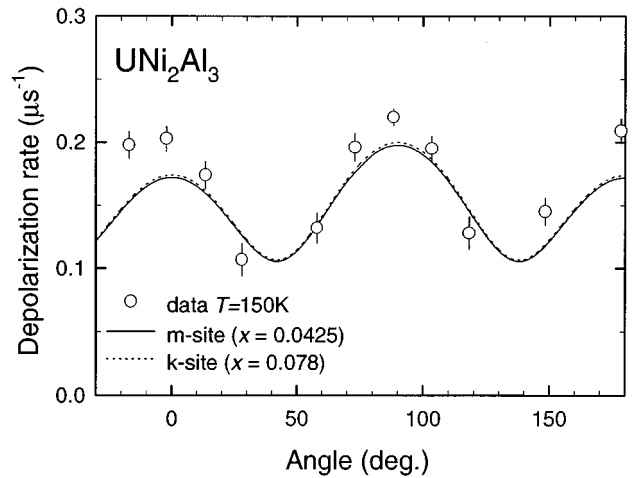

FIG. 25. Angular dependence of the transverse-field Gaussian μ^+ depolarization rate in UNi$_2$Al$_3$. The lines are calculations assuming that the μ^+ stops either at the k site ($x \ x \ \frac{1}{2}$) or the m site ($2x \ x \ \frac{1}{2}$) with the parameter x chosen such as to reproduce the spontaneous frequencies below T_N (see text).

constant phase between the μ^+ site and the spin modulation, for incommensurate structure $n_{IMS}(B)$ represents a sinusoidal distribution of the internal field and is given by

$$n_{IMS}(B) = \begin{cases} \dfrac{2}{\pi} \dfrac{1}{\sqrt{B^2 - B_{max}^2}} & \text{for } B < B_{max}, \\ 0 & \text{otherwise.} \end{cases} \quad (40)$$

Combining Eq. (13) with Eq. (40), and assuming that the initial μ^+ polarization is perpendicular to the internal fields, one can easily calculate that the time evolution of the μ^+ polarization is given by the Bessel function

$$G(t) = J_0(2\pi\nu_{max}t), \quad (41)$$

where $\nu_{max} = \gamma_\mu B_{max}/(2\pi)$ represents the cutoff field of $n_{IMS}(B)$. The presence of an incommensurate magnetic state in UNi$_2$Al$_3$ was later confirmed by neutron-scattering measurements on single crystals that determined an ordering wave vector $\mathbf{q} = (\frac{1}{2} \pm \delta, 0, \frac{1}{2})$ with $\delta = 0.110 \pm 0.003$ and ordered moments ($\mu_s \simeq 0.2 \ \mu_B$) in the basal plane. These results, in apparent contradiction with the early μSR data (Amato, Geibel *et al.*, 1992), for which a commensurate structure was deduced, motivated additional μSR studies (Amato, Feyerherm, Gaulin *et al.*, 1994) to determine precisely the μ^+ stopping site by analyzing the angular dependence of the μ^+ Knight shift and of the μ^+ depolarization rate induced by the ^{27}Al nuclei (see Fig. 25). From the observed angular dependence one concludes that either the m sites ($2x \ x \ \frac{1}{2}$) or the k sites ($x \ x \ \frac{1}{2}$) are occupied by the muon. Both sites are located very close to the b site, which has been found to be solely occupied in UPd$_2$Al$_3$. A secondary criterion for the determination of the free parameter x of both sites was to reproduce the observed spontaneous frequencies below T_N, assuming the value of μ_s found by neutron-scattering studies. In the mag-
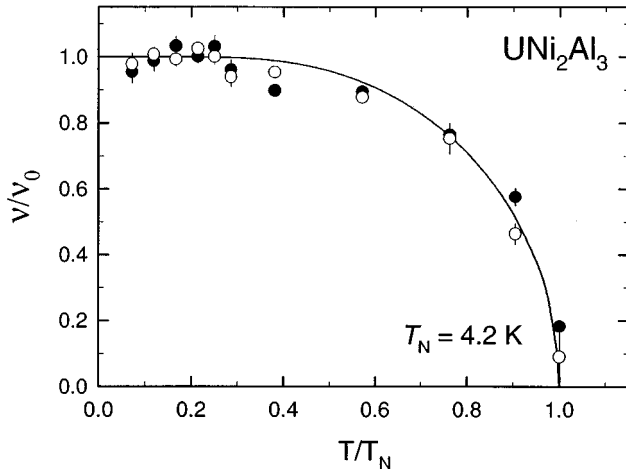
FIG. 26. Temperature dependence of the cutoff frequencies obtained by fitting the zero-field μSR signal of UNi_2Al_3 with the sum of two J_0 Bessel functions (see text). The frequencies are normalized to their values for $T \to 0$ (solid symbols: 2.78 MHz, open symbols: 0.62 MHz).

FIG. 27. μ^+ frequency shifts ($\mathbf{H}_{ext}\|\mathbf{c}$ and $\mathbf{H}_{ext}\perp\mathbf{c}$) obtained in UNi_2Al_3 plotted as function of the bulk susceptibility with the temperature as an implicit parameter (from Amato, Feyerherm, Gaulin et al., 1994).

netic phase, the μSR spectra can be satisfactorily fitted by the sum of two J_0 Bessel functions (see solid line on Fig. 23), for which the cutoff frequencies are reported on Fig. 26. The ratio $\mathcal{A}_{low}/\mathcal{A}_{high}=2/1$ between the amplitudes of the two components suggests magnetically inequivalent μ^+ sites with respect to the magnetic structure, which is indeed the case for the m and k sites if the ordered moments lie in the basal plane. The assumption that the static moments are polarized along the a^* axis, as proposed by Schröder, Musser et al. (1994), implies that the k site is solely occupied with $x=0.078$. On the other hand, assuming the moments aligned along the a axis implies a localization of the muons at the m site with $x=0.0425$.

Besides a rather accurate μ^+ site determination, the most interesting result of this study was furnished by the temperature dependence of the μ^+ frequency shift. Considering that both k and m sites are close to the b site and, hence, possess a nearly perfect axial symmetry (the difference $|A_{dip}^{xx}-A_{dip}^{yy}|$ is calculated to be less than 5%), the μ^+ frequency shift for the two main crystallographic directions can be written as in Eq. (39). Figure 27 exhibits the μ^+ frequency shift plotted versus the magnetic susceptibility (Clogston-Jaccarino plot). From the slopes, one obtains the dipolar coupling constant $A_{dip}^{zz}=1.52$ kG/μ_B, which is much smaller than the calculated values $[A_{dip,theor}^{zz}(k-site)=3.89$ kG/μ_B and $A_{dip,theor}^{zz}(m-site)=3.94$ kG/$\mu_B]$. The contact hyperfine constant is estimated within the range $0.53 \lesssim A_c \lesssim 1.3$ kG/μ_B, which is the same order of magnitude as the value observed in UPd_2Al_3 ($A_c=1.1$ kG/μ_B; Feyerherm, Amato, Gygax, Schenck, Geibel et al., 1994). The huge discrepancy between A_{dip}^{zz} and $A_{dip,theor}^{zz}$ constitutes a very peculiar feature, considering that A_{dip}^{zz} is exclusively determined by the lattice geometry and the assumed μ^+ site. However, the measured value A_{dip}^{zz} is obtained by considering that the moments at the U sites
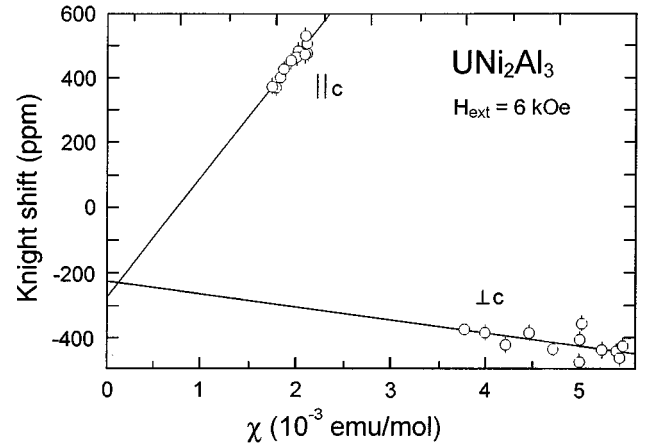
induced by the external magnetic field are directly proportional to the bulk susceptibility. Alternatively, assuming that a sizable part of the induced magnetization is located at the Ni sites and/or in the interstitial volume, these results could be readily understood. Furthermore, such explanation appears in line with the picture that UNi_2Al_3 has a more pronounced itinerant character than UPd_2Al_3. The stronger delocalization of the $5f$ electrons in UNi_2Al_3 was notably inferred by the absence of a Curie-Weiss law in the susceptibility (see, for example, Geibel et al., 1993) and the nonobservation of Kondo-like behavior in the electrical resistivity. Hence the substitution of Ni for Pd, which is accompanied by a reduction of the unit-cell volume, increases the hybridization of the f electrons with the conduction electrons, driving the system away from a localized-moments behavior.

D. URu_2Si_2

URu_2Si_2 is the first heavy-fermion system for which the coexistence between magnetism ($T_N \simeq 17.5$ K) and superconductivity ($T_c \simeq 1.3$ K) was reported (Schlabitz et al., 1984). Additional interest was created by the apparent contradiction between the large entropy loss at T_N and the extremely small value of the ordered moment detected by neutron scattering ($\mu_s \simeq 0.02$ μ_B; Broholm et al., 1987).

1. Paramagnetism

Several μSR studies have been devoted to the measurements of the μ^+ Knight shift at high temperature with the aim to determine the μ^+ site (MacLaughlin et al., 1988; Knetsch, Menovsky et al., 1993). Figure 28 exhibits a Jaccarino-Clogston plot of the μ^+ Knight shift (K_μ versus χ with the temperature as an implicit parameter) and shows that $K_{\mu\|}$ is large and negative for $\mathbf{H}_{ext}\|\mathbf{c}$. On the other hand, for $\mathbf{H}_{ext}\perp\mathbf{c}$ no temperature dependence of $K_{\mu\perp}$ is measured, in line with the obser-
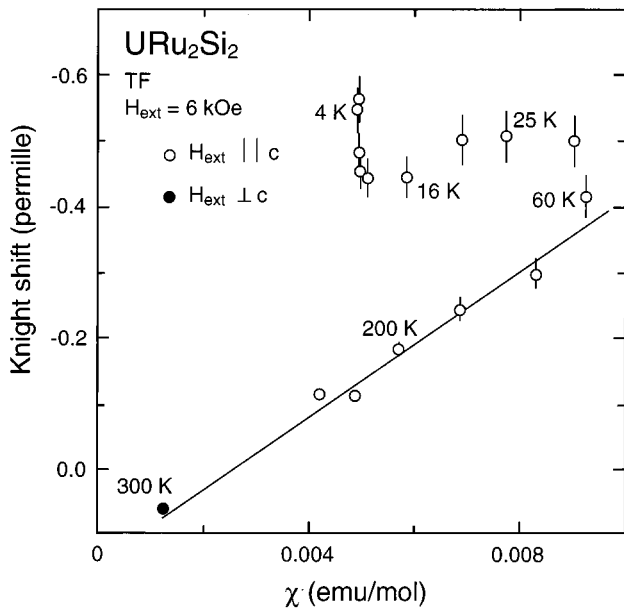
FIG. 28. μ^+ Knight shifts ($\mathbf{H}_{ext}\|\mathbf{c}$ and $\mathbf{H}_{ext}\perp\mathbf{c}$) obtained in URu$_2Si_2$ plotted as function of the bulk susceptibility with the temperature as an implicit parameter. Note the negative scale for the Knight shift (adapted from Knetsch, Menovsky *et al.*, 1993).

FIG. 29. Temperature dependence of the transverse-field μ^+, depolarization rate obtained in URu$_2$Si$_2$ with $\mathbf{H}_{ext}\|\mathbf{c}$. The inset gives the situation at low temperature. The lines are to guide the eye.

vation of a constant $\chi_\perp$. The value of $K_{\mu\perp}$ can be considered as the high-temperature limit of $K_{\mu\|}$ [$\chi_\|(T)$ $=\chi_\|^0+\chi_{5f}(T)$ with $\chi_\|^0\simeq\chi_\perp$], which is confirmed by the extrapolation of $K_{\mu\|}$ for $\chi_\|\to\chi_\|^0$ (see Fig. 28). Unfortunately, the absence of a sizable f-electron contribution in $\chi_\perp$ impedes an independent determination of the dipolar and contact coupling constants, resulting in the impossibility of unambiguously deducing the μ^+ stopping site. A remarkable observation, contained in Fig. 28, is the loss of scaling between $K_{\mu\|}$ and $\chi_\|$ occurring below 50 K, i.e., for a temperature below which $\chi_\|$ exhibits a broad peak usually ascribed to the crystal-electric-field (CEF) splitting of the $^3H_4$ Hund's-rule ground-state multiplet. Several possibilities have been invoked to explain such behavior. It may, for example, reflect the build up of the Kondo screening of the localized moments. If the Kondo cloud is spatially extended, with a characteristic radius larger than the μ^+-U distance, the bulk susceptibility χ_{bulk} will appear lower than the atomic susceptibility probed by the muon, hence breaking the scaling between the μ^+ Knight shift and χ_{bulk}. However, the observation by ^{29}Si NMR of a perfect scaling between Knight shift and χ_{bulk}, combined with the fact that the distances μ^+-U and Si-U are of the same order, seriously questioned this interpretation. As another possible origin for the unusual behavior of the μ^+ Knight shift below 50 K, one could consider a slight perturbation of the CEF by the implanted μ^+, causing a modification of the atomic susceptibility of the neighboring U atoms. Such a μ^+-induced effect has been observed on the singlet ground-state system PrNi$_5$ (Feyerherm, Amato, Gygax, Schenck, Zimmerman *et al.*, 1994), where the implanted
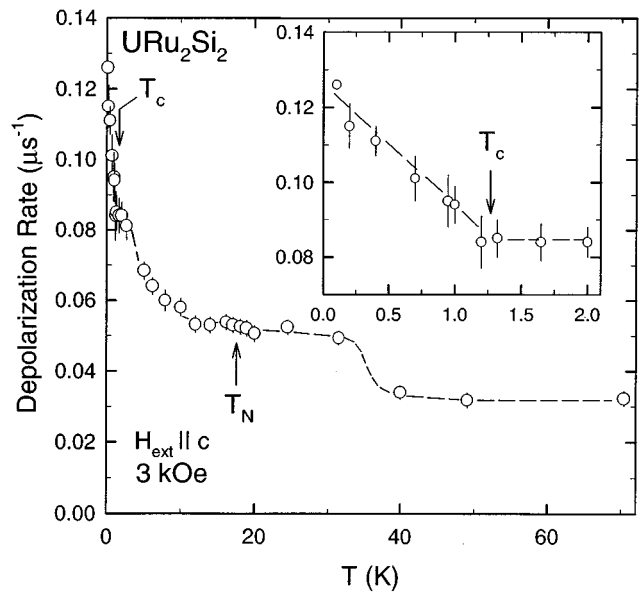
μ^+ appears to lower the local symmetry, causing a pronounced rearrangement of the low-lying CEF levels. However, in this case one also observes a dramatic μ^+-induced change of the spin dynamics of the Pr $4f$ moments, which does not seem to have a counterpart in URu$_2$Si$_2$. Finally, it is worth mentioning that the μ^+ Knight shift loses its scaling with χ_{bulk} near the temperature for which a weak ferromagnetic transition has been reported (Ramirez *et al.*, 1991) and which was ascribed to stacking-fault defects along the c axis, leading to ordered moments of $\sim10^{-4}$ μ_B/(U atom). For a sensitive technique like μSR it is plausible that the presence of such a ferromagnetic signal could deeply alter the μ^+ Knight shift behavior. Interestingly, the μ^+ depolarization rate obtained in transverse-field studies (see Fig. 29) exhibits a clear increase below ~40 K, where magnetization measurements in a SQUID magnetometer on the same sample reveal the presence of a weak ferromagnetic signal.

Several μSR studies have been dedicated to the characterization of the antiferromagnetic phase. Whereas the large majority of these studies reveal that magnetism occurs homogeneously below $T_N\simeq17.5$ K throughout the sample, signs for a spatially inhomogeneous development of magnetism have been recently reported. Since the conclusions drawn by these two kinds of observations are diametrically opposed, they will be separately addressed in the following.

2. Magnetism—homogeneous picture

Several μSR studies reveal the presence of antiferromagnetism below $T_N\simeq17.5$ K by an increase of the μ^+ depolarization rate in zero-field and transverse-field measurements (MacLaughlin *et al.*, 1988; Luke *et al.*,

1990; Knetsch, Menovsky *et al.*, 1993; see Fig. 29). Several indications can be extracted from these data: (i) the increase occurs for few samples already at a temperature above T_N; (ii) the temperature dependence of the μ^+ depolarization rate and therefore of the magnetic order parameter strongly differs from sample to sample; and (iii) no change of the zero-field depolarization rate is detectable at the superconducting transition (Knetsch, 1993a).

The first two observations are probably related and have to be linked to similar inferences from neutron measurements. Recently, Fåk *et al.* (1995) clearly established the influence of the sample preparation on the temperature dependence of the magnetic order parameter. However, independent of the sample quality, T_N and $\mu_s(T\rightarrow 0)$ are rather stable, indicating that the small-moment magnetism is intrinsic. Finally, the third μSR observation suggests that the coupling between the superconducting and antiferromagnetic order parameter must be weak (if it exists at all), contrary to observations for UPt$_3$ (see Sec. III.A).

The increase of the μ^+ depolarization observed in zero external field can be interpreted either as indicating a real broadening of the field distribution with zero mean at the μ^+ site or as reflecting the early-time evolution of the μ^+ polarization precessing in a small magnetic field. With this latter picture, one extracts a value of $B_\mu \simeq 1-2$ G for the field at the μ^+ site. On the other hand, when the weak Bragg peaks observed by neutron scattering are interpreted as arising from ordered moments along the c axis with ordering vector $\mathbf{q}=(0,0,1)$, one obtains small ordered moments $\mu_s \simeq 0.03\ \mu_B$. Assuming this value, the calculated dipolar local fields at the possible μ^+ sites are of the order of $B_{dip} = 50-100$ G with the exception of the f site $(\frac{1}{4}\frac{1}{4}\frac{1}{4})$, which is symmetric between the two magnetic sublattices and for which the dipolar fields cancel. In view of the large discrepancy between B_μ and B_{dip}, one is confronted with two possibilities: either (i) the μ^+ stops at the f site where $B_{dip}=0$ and the μ^+ depolarization-rate enhancement is caused by sublattices imperfections; or (ii) the magnetic order is destroyed locally around the implanted μ^+. The former possibility appears to contradict the μSR results on the isostructural compound URh$_2$Si$_2$ (Yaouanc *et al.*, 1990), which possesses an analogous antiferromagnetic structure and for which a spontaneous μ^+ frequency is observed below T_N, ruling out an occupation of the f site. Before discussing the second possibility, it is appropriate to mention the quadrupolar model of the 17.5 K phase transition developed by Ramirez *et al.* (1992) and Santini and Amoretti (1994). In this approach the fundamental order parameter of the 17.5 K transition is not the tiny staggered magnetic moment (which is only a secondary effect of the symmetry-breaking perturbation), but the ordering of the localized f quadrupoles. This model has been shown to qualitatively reproduce the order temperature, the loss of entropy, and the linear susceptibility, as well as the peculiar anomaly of the nonlinear susceptibility at the transition temperature. Referring to the latter possi-

bility stated above, one may speculate that a μ^+-induced perturbation of the crystal electric field at the U^{4+} ions next to the μ^+ results in a quenching of the static magnetism at the neighboring U sites. Interestingly, assuming that the μ^+ does not occupy the f site, the observed dipolar field B_μ roughly corresponds to the contribution expected from the magnetically ordered next-nearest-neighbor U ions.

3. Magnetism—inhomogeneous picture

At this point, it is fitting to mention the peculiar μSR results obtained by Luke, Keren, Le, Uemura *et al.* (1994) on a particular single crystal that shows a completely different picture than the one reported by other groups and described above. The key point of this latter zero-field μSR study of the magnetic phase was the observation of a clear two-component structure of the μSR signal below T_N. Whereas the predominant component (component 1, $\sim$90% of the total amplitude) exhibits a behavior similar to what was observed in other μSR studies (i.e., lack of spontaneous μ^+ frequency, weak increase of the μ^+ depolarization rate), component 2 exists only in the magnetic phase and shows clear oscillations, implying large internal fields in a fraction of the sample. The temperature dependencies of the amplitude ($\mathcal{A}_2$) and frequency (ν_2) of this latter component are reported in Fig. 30. The abruptness of the frequency transition was taken as evidence of a first-order transition, whereas the flat temperature dependence for $T \ll T_N$ seems to imply the suppression of the low-energy magnetic excitations, in agreement with the observation of a spin-wave gap with neutron-scattering data (Broholm *et al.*, 1987). The rise of the amplitude $\mathcal{A}_2$ below T_N indicates that the fraction of the muon ensemble experiencing the large internal field increases and reaches a maximum of about 10% for $T\rightarrow 0$. These peculiar results were interpreted as follows: the slowly relaxing component 1 was related to the nonmagnetic fraction of the sample that coexists below T_N with a magnetic fraction occupying at the most 10% of the sample and identified with component 2. Luke, Keren, Le, Uemura *et al.* (1994) therefore conjectured that the smallness of the magnetic Bragg-peak intensity I_B in neutron-scattering experiments arose from a reduced magnetic volume fraction rather than from a reduced static magnetic moment, as is usually assumed. Interestingly, the quantity $\mathcal{A}_2 \nu_2^2$ is proportional to the observed Bragg-peak intensity. Within this picture, an estimation of $\mu_s \simeq 0.2\ \mu_B$ for the static magnetic moment is extracted from the μ^+ frequency value ν_2, which would roughly correspond to the value of μ_s extracted from I_B, assuming that only 10% of the sample volume is magnetically ordered.

The two above described pictures of the magnetism in URu$_2$Si$_2$ are completely incompatible, and one is now faced with the delicate task to critically evaluate them. An ingenuous statistical approach would strongly favor the homogeneous picture in view of the amount of data supporting it. Beyond this simple argument, several measurements seem incompatible with an inhomoge-
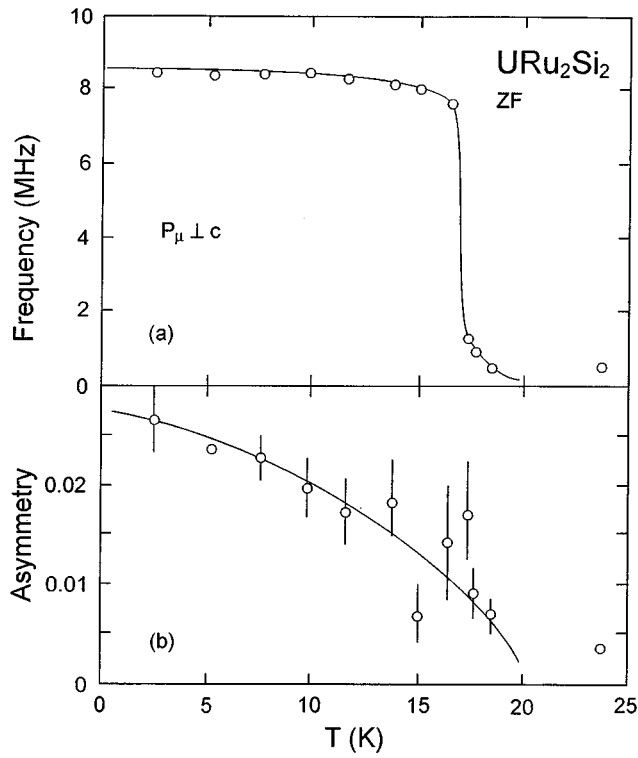
FIG. 30. Temperature dependence of the spontaneous zero-field μ^+ frequency detected below T_N by Luke, Keren, Le, Uemura et al. (1994) in a particular URu_2Si_2 monocrystalline sample ($\mathbf{P}_\mu \perp \mathbf{c}$). The asymmetry (amplitude) of this component is shown in the lower part of the figure. The value of the asymmetry for $T \rightarrow 0$ corresponds to about 10% of the total signal amplitude.

neous picture, as, for example, (i) the electrical resistivity can be accurately described, assuming an energy-gap antiferromagnet, without the need to invoke a large nonmagnetic contribution (Palstra et al., 1986); (ii) the entropy loss at T_N and the temperature dependence of the specific heat for $T < T_N$ are inconsistent with the ordering of a strongly reduced portion of the sample (Palstra et al., 1985); and (iii) the ^{29}Si $1/T_1$ NMR relaxation rate presents a clear deviation from a Korringa law for $T < T_N$ (Kohara et al., 1986; the Korringa law for $T \ll T_N$ is related to the residual density of states arising from ungapped regions of the Fermi surface). Although a number of data appears to rule out the inhomogeneous picture, the origin of the high-frequency component in the data reported in Fig. 30 should nevertheless be clarified, in particular its possible connection with stacking faults, and further studies are certainly warranted.

4. Superconducting phase

Transverse-field μSR measurements below T_c have been undertaken by several groups to study the coexistence between magnetism and superconductivity and obtain information about the magnetic penetration depth. Figure 29 exhibits the transverse-field depolarization rate obtained in a single crystal with $\mathbf{H}_{ext} \| \mathbf{c}$. In addition

to the increase below T_N discussed above, a second increase of the depolarization rate occurs below T_c, caused by the formation of the flux-line lattice, which generates a supplementary field distribution at the μ^+ site [see Eq. (36)]. The key information furnished by μSR is that down to the lowest temperature the μSR spectra contain only one signal which establishes that magnetism and superconductivity, which are responsible for the μ^+ depolarization, increases below T_N and below T_c, occur in the whole sample volume and therefore microscopically coexist below T_c. Interestingly, the μ^+ depolarization-rate increase below T_c is only observed for $\mathbf{H}_{ext} \| \mathbf{c}$, whereas for $\mathbf{H}_{ext} \perp \mathbf{c}$ the depolarization appears to be constant (Heffner, 1990; Luke et al., 1990). This implies that the magnetic penetration depth is much smaller in the basal plane than along the c axis (for this latter value a lower limit of $\sim$12 000 Å can be roughly estimated). From the increase with $\mathbf{H}_{ext} \| \mathbf{c}$, a penetration depth $\lambda_\perp(0) \simeq 9500$ Å is calculated, which is in agreement with estimations from thermodynamic properties (Schlabitz et al., 1986). If, on one hand, the presence of a strong anisotropy is in line with the temperature dependencies of $\lambda(T)$ determined from AC susceptibility data (Knetsch et al., 1992), it appears, on the other hand, to be in sharp contrast with lower-critical-field data, which show an isotropic character of H_{c1} (Knetsch, 1993b). From Eq. (36) one finds for the increase of the depolarization rate below T_c,

$$\sigma_{FLL} \propto \frac{1}{\lambda^2} = \frac{4\pi n_s e^2}{m^* c^2}, \tag{42}$$

where n_s is the superfluid density and m^* the effective mass of the heavy quasiparticles. Since $H_{c1} \propto n_s/m^*$ as well, one might expect a similar anisotropy for both quantities. However, the H_{c1} data should be considered with caution, since surface effects are known to considerably hamper the determination of H_{c1} and might well be related to the observed lack of anisotropy.

A more serious observation is the indication by tunnelling spectroscopy (Aarts et al., 1994) of a strongly anisotropic energy gap on part of the Fermi surface due to the formation of magnetic order below T_N. While no gap is found along the c direction, a sizable gap is detected in the basal plane, which should imply the lack below T_c of necessary currents in the basal plane able to screen vortices along the c axis. This simple picture therefore appears to contradict the μSR data. Nevertheless, it is doubtful whether a straightforward connection can be made between the size of the antiferromagnetic gap and the penetration-depth value. A similar anisotropic topology of the antiferromagnetic gap has, for example, been reported in UPd_2Al_3, which is nevertheless found by numerous techniques to possess isotropic superconducting properties as also observed by μSR (see Sec. III.C).

The evolution of the μ^+ frequency shift below T_c is reported in Fig. 31. The absence of a diamagnetic shift, characterized by a decrease of the frequency below T_c, has to be traced back to flux-pinning effects preventing
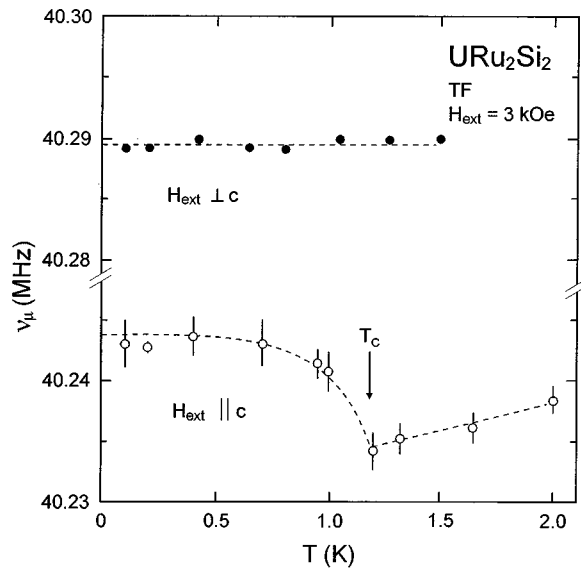
FIG. 31. Temperature dependence of the μ^+ frequency measured near T_c for $\mathbf{H}_{ext}\|\mathbf{c}$ and $\mathbf{H}_{ext}\perp\mathbf{c}$ in URu_2Si_2. The increase of the frequency observed below T_c for $\mathbf{H}_{ext}\|\mathbf{c}$ corresponds to a decrease of the μ^+ Knight shift (see also Fig. 28).

FIG. 32. Phase diagram of $CeCu_2Si_2$ deduced by different techniques (see, for example, Grewe and Steglich, 1991; Bruls et al., 1994) showing the superconducting phase (SC) and the magnetic phase (A). The magnetic phase (B) was determined by elastic constants and thermal-expansion measurements (Bruls et al., 1994).

the expulsion of flux in the field-cooling procedure. The most interesting effect is the increase of the frequency, signaling a decrease in absolute value of the μ^+ Knight shift, which tracks the conduction-electron spin susceptibility. As already discussed in Sec. III.C, such reduction is reminiscent of a Yosida-type decrease of the spin susceptibility below T_c and is often taken as an indication for even-parity pairing. This appears in line with the observation of a T^2 behavior of the specific heat in the superconducting state (see, for example, Maple et al., 1986), hinting at a line node in the superconducting energy gap at the Fermi surface, which is taken as an indication for d-wave (even-parity) superconductivity. However, it has been shown that this interpretation is not unambiguous (Brison et al., 1994), since for an even-parity s-wave pairing in a clean superconductor, a line node can be generated by the presence of a large antiferromagnetic molecular field. Within this model, when the molecular-exchange field exceeds T_c, a gapless region appears on an equatorial line perpendicular to the wave vector **q** characterizing the magnetic structure (in the basal plane for URu_2Si_2), and the calculated temperature dependence of the specific heat is in better agreement with the experimental observations than the d-wave calculations. This model does not exclude d-wave pairing, but emphasizes that the effect of magnetism has to be taken into account independent of the symmetry of the superconducting order parameter.

E. CeCu$_2$Si$_2$

Although $CeCu_2Si_2$ was the first heavy-fermion superconductor discovered (Steglich et al., 1979), many questions concerning its properties still remain unresolved. Several problems are certainly connected to metallurgi-
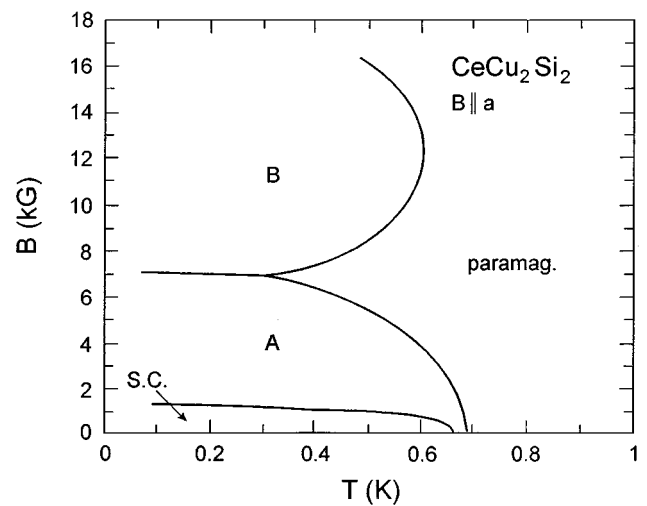
cal difficulties arising from its incongruent melting. Hence large variations in the properties of $CeCu_2Si_2$ have been reported, depending on the sample preparation, exact stoichiometry, and annealing conditions. For example, the presence of magnetism and/or superconductivity in this system is known to be extremely sensitive to the stoichiometry even in monocrystalline samples. It is usually believed that the superconducting properties of $CeCu_2Si_2$ are stabilized through a slight Cu excess, which by some mechanism produces a source of positive internal pressure. On the other hand, Cu deficiency causes an apparent spin-glass order at $T_g \simeq 2$ K.[4]

An additional problem arises from the fact that the superconducting phase appears embedded in a relatively stable magnetic phase (see Fig. 32). The magnetic character of this latter phase was first revealed by zero-field μSR measurements (Uemura et al., 1988; see Fig. 33) and subsequently confirmed by NMR (Nakamura, Kitaoka, Asayama, and Flouquet, 1988). Figure 33 indicates that below $\sim$0.9 K (a temperature much higher than $T_c \simeq 0.65$ K) a strong increase of the zero-field depolarization rate occurs due to the presence of magnetic correlations with static character, as demonstrated by the absence of μ^+ depolarization in longitudinal-field μSR studies. The absence of oscillations as well as the Gaussian character of the μSR signal was taken as evidence of a dense spin-glass type of ordering of the Ce moments with values of the static moment ranging from $\mu_s = 0.1-0.3$ μ_B/Ce atom, depending on the μ^+ stopping site considered.

---

[4]Recent studies (Geibel, 1995) strongly suggest that the magnetic anomaly at 2 K is extrinsic and arises from the parasitic phase $Ce_2Cu_{1+x}Si_{3-x}$.

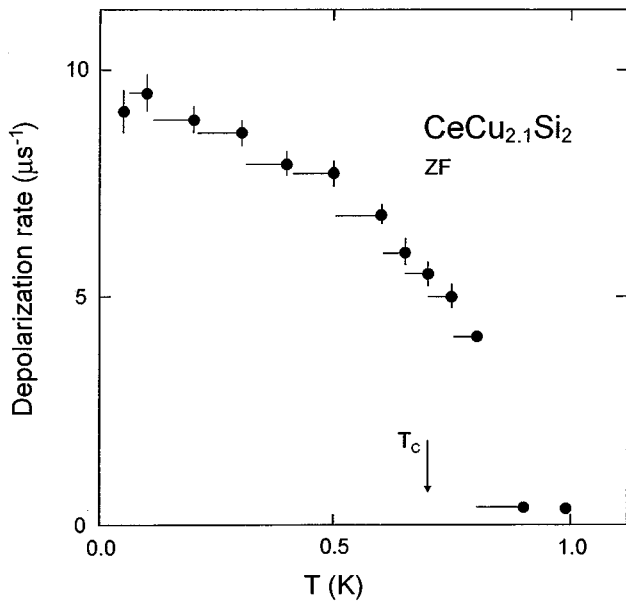FIG. 33. Temperature dependence of the zero-field μ^+ depolarization rate (Gaussian fit) obtained in a CeCu$_{2.1}$Si$_2$ sample. The superconducting critical temperature of this sample is also reported (from Uemura et al., 1988).

A capital additional contribution of the μSR technique was obtained from early zero-field studies performed on a CeCu$_{2.2}$Si$_2$ sample (Luke, Keren, Le, Sternleib et al., 1994), as well as more recently on a CeCu$_{2.05}$Si$_2$ sample (Amato, 1994). Both studies gave strong evidence *against* a microscopic coexistence between magnetism and superconductivity. The conclusions drawn from the μSR data are based on the observation of the occurrence of a clear two-component structure in the μSR spectra when lowering the temperature below T_c (see Fig. 34). The μ^+ depolarization function $G(t)$ is best described by
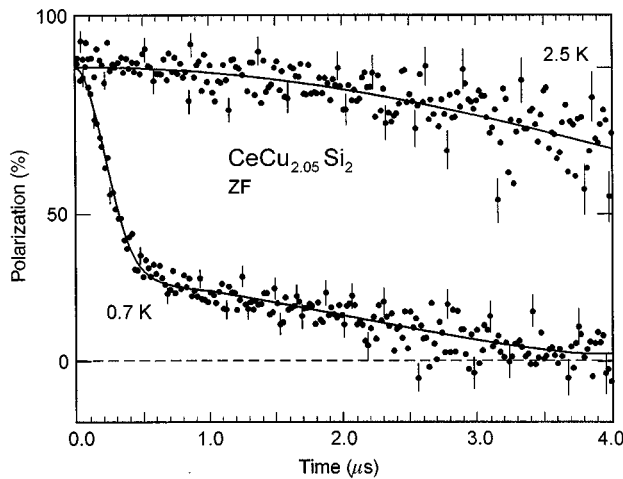

FIG. 34. Time evolution of the μ^+ polarization measured in zero field in a CeCu$_{2.05}$Si$_2$ sample at low temperature. Note the clear two-component structure of the signal measured at low temperature.

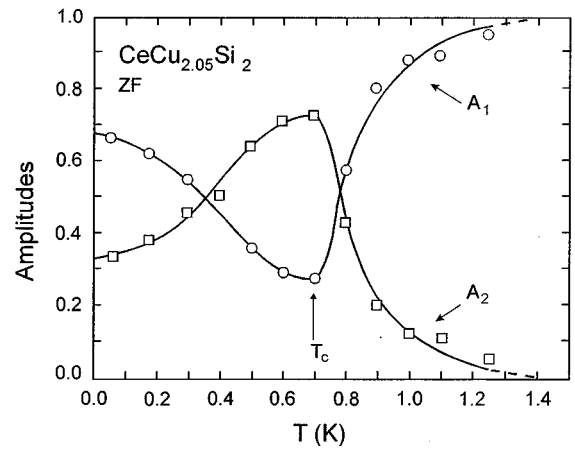FIG. 35. Temperature dependence of the amplitudes $\mathcal{A}_1$ and $\mathcal{A}_2$ of the zero-field μSR signal in CeCu$_{2.05}$Si$_2$, corresponding to the magnetic and nonmagnetic volume fractions [see Eq. (43)].

$$G(t) = \mathcal{A}_1(T)G_{KT}(T) + \mathcal{A}_2(T)\exp\left(-\frac{\sigma^2 t^2}{2}\right), \qquad (43)$$

where the amplitudes $\mathcal{A}_i$ represent a direct measure of the sample volume fractions related to the two components and G_{KT} is the usual Kubo-Toyabe function [see Eq. (26)]. Component 1 represents domains in the paramagnetic regime (which become superconducting below T_c; see below) and for which the μ^+ depolarization function is best described by the Kubo-Toyabe function solely caused by the ^{63,65}Cu and ^{29}Si nuclei. The fast Gaussian component 2 is ascribed to the presence of the magnetic domains. Figure 35 exhibits the temperature dependence of the volume fractions measured in a CeCu$_{2.05}$Si$_2$ sample. Below 1.2 K the magnetic volume fraction increases significantly, reaches a maximum exactly at T_c ($\simeq 690$ mK for this sample), and finally strongly decreases for $T \to 0$. Therefore these data show that, on one hand, magnetism is *not* a bulk phenomenon, and, on the other hand, that, at least in domains where the condensation energy of the magnetic phase is not too large, magnetism and superconductivity compete for volume with one another. A similar picture has been provided recently by elastic-constant and thermal-expansion measurements (Bruls et al., 1994). The exact mechanism leading to a reduction below T_c of the magnetic volume fraction is still unclear and has led to speculations about a collapse of the RKKY interactions due to the absence of unpaired conduction electrons or a more effective Kondo screening in the superconducting state (Luke, Keren, Le, Sternleib et al., 1994).

Comprehensive μSR studies on a series of Ce$_{1+x}$Cu$_{2+y}$Si$_2$ polycrystalline samples have been recently undertaken by Feyerherm et al. (1995) in order to possibly elucidate the underlying causes of the observation of different types of ground states. The analysis of the μSR spectra indicates that the size of the magnetic volume fraction (i.e., the amplitude of the "fast" Gaussian component of the μ^+ depolarization function) is strongly sample dependent (see Fig. 36). However, the
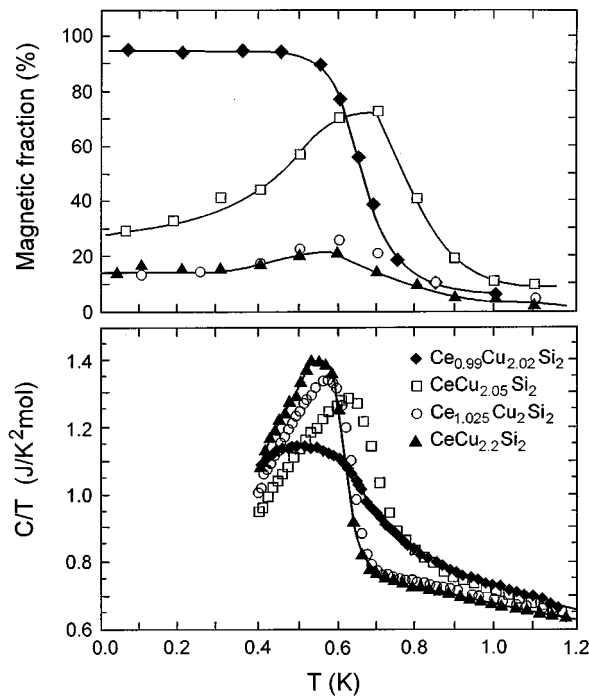
FIG. 36. Comparison between μSR and thermodynamic measurements. *Upper part*: Temperature dependence of the magnetic volume fraction determined by the zero-field μSR signal for different $Ce_{1+x}Cu_{2+y}Si_2$ samples. *Lower part*: Specific-heat data measured in the same samples (adapted from Modler *et al.*, 1995 and Feyerherm *et al.*, 1995).

depolarization rate of the fast signal is similar for all investigated samples (see Fig. 37), suggesting that the nature of the magnetic correlations is not affected by the actual size of the magnetic domains. Again, the static character of the magnetism was demonstrated by the lack of μ^+ depolarization in longitudinal-field measurements. Furthermore, specific-heat data on the same samples (Modler *et al.*, 1995; see Fig. 36) show the close relationship between the sample-dependent size of the specific-heat jump at T_c and the paramagnetic volume fraction at T_c determined by μSR. Transverse-field μSR
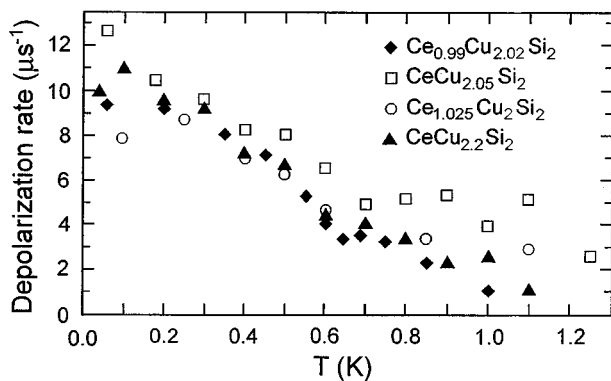

FIG. 37. Temperature dependence of the μ^+ depolarization rate of the zero-field μSR component characterizing the magnetic volume fraction, measured for the same $Ce_{1+x}Cu_{2+y}Si_2$ samples shown in Fig. 36.

studies with field-cooling and zero-field-cooling procedures have also unambiguously proven that the entire paramagnetic volume becomes superconducting below T_c. Figure 36 shows again that, for all samples, the competition between magnetism and superconductivity is characterized by a decrease of the magnetic volume fraction below T_c. In discussing the large sample dependencies, Feyerherm *et al.* (1995) first remark that, although the starting chemical compositions are quite different, the actual composition obtained by microanalysis is almost sample independent without a sizable trend. The microanalysis also reveals an apparent increase of the density of microcracks in samples with a large magnetic volume fraction, which could act as a release mechanism for internal strains arising from the incongruent melting of $CeCu_2Si_2$. Assuming the amount of internal pressure is the underlying mechanism for the large sample dependence, the variation of the ratio between the magnetic and paramagnetic volumes could be explained in a simple Doniach model (Doniach, 1977). In this model, describing the competition between the RKKY and Kondo interaction, the application of pressure delocalizes the f electrons and increases their exchange interaction with the conduction electrons. This leads to a relative decrease of the indirect magnetic interactions with respect to the Kondo interaction. Since $CeCu_2Si_2$ is located at the borderline of magnetism and paramagnetism, as, for example, shown by band-structure calculations (Endstra *et al.*, 1993), a slight change of the exchange interaction could possibly result in a collapse of the magnetic fraction to the benefit of the paramagnetic one. Additional support for this picture is furnished by the high sensitivity of T_c to external pressure p (Jaccard *et al.*, 1985; Thomas *et al.*, 1993). At low p, T_c is strongly reduced, most likely by the presence of strong spin fluctuations. As this low-p regime, characterized by anomalous values of the Grüneisen parameter (Γ), is destroyed with increasing p at about 30 kbar (which could possibly correspond to the point where the magnetic fluctuations are completely suppressed), a second regime is reached with high T_c (~ 2 K) and negative value of $\Gamma(T_c)$, as observed in the U-based heavy-fermion superconductors. In contrast, the presence of negative chemical pressure, achieved by substitution of La for Ce, is found to rapidly depress the superconducting properties.

The presence of different domains has seriously hampered the characterization by μSR of the superconducting state in $CeCu_2Si_2$. Hence no reliable information could be extracted from the μ^+ frequency shift below T_c. An estimation of the magnetic penetration depth of $\lambda \simeq 10\,000$ Å is obtained from the small increase of the transverse-field μ^+ depolarization rate (due to the flux-line lattice), observed in the component that reflects the superconducting fraction. Former bulk determinations of λ, which gave a much lower value ($\lambda \simeq 5000$ Å), were calculated from the slope of the higher critical field H_{c2} at T_c and the linear term (γ) of the specific heat. It is nevertheless conceivable that such bulk determinations are biased by the large sample depen-

dence of $|dH_{c2}/dT|$ and by the difficulty to reliably determine γ due to the presence of domains with different ground states.

In summary, μSR has furnished a completely new picture of the interplay between magnetism and superconductivity in CeCu$_2$Si$_2$, indicating that both types of ground states do not coexist at the microscopic level and that they arise from instabilities of the same subset of electrons, namely those involved in the heavy-fermion state. Whether the difference between CeCu$_2$Si$_2$ and the U-based heavy-fermion superconductors (where magnetism, if present, microscopically coexists with superconductivity) has a fortuitous character, or whether it reveals a more fundamental difference between $4f$ and $5f$ heavy-fermion compounds, is still an open question.

IV. MAGNETIC PROPERTIES

As already mentioned in Sec. I.B, the condition of formation of a magnetic ground state in heavy-fermion compounds is governed by the delicate balance between the characteristic energies of the Kondo and RKKY interactions.

Several authors have theoretically investigated the magnetic response of heavy-fermion systems. A systematic overview on the possible forms of magnetism has been presented by Grewe (1988), who considers the Anderson lattice model investigated in the frame of perturbation theory. In a similar way, as in conventional band magnetism, the wave-number and frequency-dependent magnetic susceptibility is expressed via a Stoner's formula

$$\chi(\mathbf{q}, \nu) = \frac{\chi_0(\mathbf{q}, \nu)}{1 - \chi_0(\mathbf{q}, \nu) K(\mathbf{q}, \nu)}, \qquad (44)$$

where the noninteracting term χ_0 is corrected by an additional term K accounting for the quasiparticle interactions. The processes contributing to K are of the RKKY type (high-energy processes) and those involving exchange interaction between the heavy quasiparticles (low-energy processes). Hence, if the denominator on the right-hand side of Eq. (44) becomes small for temperature $T > T^*$, high-energy processes will be dominant, and a RKKY instability occurs with moderately renormalized local magnetic moments. [The systems presenting this type of ground state will be thereafter labeled local-moment magnets (LMM).] On the other hand, if the characteristic temperature T^* is larger than the temperature of the magnetic instability, the magnetic degrees of freedom associated with the localized moment are essentially transferred to the itinerant heavy quasiparticles. Hence the high-energy processes contributing to K are integrated out and implicitly contained in the renormalization of the quasiparticles. Low-energy processes (i.e., the residual interactions of the quasiparticles) will then become dominant and may drive the system toward a magnetic instability via exchange splitting of the heavy-quasiparticle band, characterized by strongly renormalized static moments ($\mu_s \simeq 10^{-2} - 10^{-3} \mu_B$). [Such systems are usually called

heavy-fermion band magnets (HFBM).] As pointed out by Grewe and Welslau (1988), low-energy processes are connected to interband transitions over the hybridization gap of the heavy-fermion band and favor incommensurate magnetic structures with modulations of several crystal-lattice spacings. Furthermore, the occurrence of complicated magnetic structures could be favored by the competition of small-$\mathbf{q}$ and $2\mathbf{k}_F$ instabilities (the latter characterizing RKKY interactions).

In the following, magnetic heavy-fermion systems investigated by μSR (see Table III) are tentatively classified as members of the above described classes (LMM and HFBM). Special emphasis will be placed on novel magnetic features revealed by the μSR spectroscopy.

A. Heavy-fermion band magnetism

One of the most outstanding contributions of μSR to the comprehension of heavy-fermion phenomena has been the discovery of weak static magnetism in systems that were long considered examples of Fermi-liquid paramagnets. This has considerably modified the phenomenological classification of the heavy-fermion compounds, where a paramagnetic ground state appears now to be an exception at best.

Due to its local character, the muon itself cannot determine whether the observed small static magnetic moments are the characteristic feature of an itinerant band magnetism, or, alternatively, if they result from local f moments only partially compensated by the Kondo effect. However, several aspects of this weak static magnetism indicate that it reflects an instability of the heavy quasiparticle band. In addition to the strongly reduced value of the static moments, this magnetism occurs at very low temperature (well below T^*), i.e., at temperatures for which the heavy quasiparticle band is fully developed. Moreover, this magnetic state is shown to compete with the heavy-fermion superconducting state (see, for example, the case of CeCu$_2$Si$_2$: Secs. III.E and IV.A.3), which has been proven to be a cooperative phenomenon in the system of heavy quasiparticles. It therefore appears natural to assume a similar picture for the peculiar magnetic states described in the following sections.

1. CeAl$_3$

CeAl$_3$ was considered for a long time to be the archetypical example of a heavy-fermion Fermi-liquid paramagnetic, which exhibits a giant electronic specific-heat coefficient $\gamma \simeq 1.62$ J/(K^2 mol), an almost temperature-independent magnetic susceptibility below 1 K, and a huge T^2 term in the electrical resistivity. Neutron-diffraction studies did not reveal long-range magnetism (Murani et al., 1980). Furthermore, the shallow maxima observed in the specific heat at $\sim$0.5 K and in the magnetic susceptibility were ascribed to the occurrence of a Fermi-liquid state formed by the narrow band of quasiparticles (Flouquet et al., 1982). Theoretically, the modification of the density of states at the Fermi level, which could explain these anomalies, was predicted by Martin

TABLE III. List of the magnetic and paramagnetic heavy-fermion systems discussed in this review. The different parts of the table contain local-moment paramagnets, heavy-fermion band magnets, and paramagnets. For the references, further properties, and details, the reader is referred to review articles (for example, Grewe and Steglich, 1991; Steglich *et al.*, 1992) and to the text.

Compounds	T_c (K)	T^* (K)	T_N (K)	μ_s (μ_B)	Space group
$CeAl_2$		3.5	3.9	0.63	$Fd\bar{3}m$
CeB_6		3	2.3	0.65	$Pm\bar{3}m$
$CeCu_5$		4.8	4.1	0.42	$P6/mmm$
$CeCu_5Au$		~3	2.2	~0.8	$Pnma$
$CePtSn$		10	7.6 (5)	0.6 (0.8)	$Pn2_1a$
$CePdSn$		10	7.5	0.82	$Pn2_1a$
UCu_5^{HT}		nd	15	0.9–1.55	$F\bar{4}3m$
U_2Zn_{17}		nd	9.7	0.8	$R\bar{3}m$
UNi_4B		7	20	0.6	$P6/mmm$
UCd_{11}		10	5	~1	$Pm\bar{3}m$
UPd_2Al_3	~2	15–50	14.5	0.85	$P6/mmm$
$CeAl_3$		4	1.6^a	~0.1	$P6_3/mmc$
$CeRu_2Si_2$		15	2^a	~0.001	$I4/mmm$
$CePd_2Al_3$		19	2.7	0.47	$P6/mmm$
$CeCu_2Si_2$	0.65	10	$~1^a$	0.1–0.3	$I4/mmm$
UCu_5^{LT}		nd	1^b	0.01	$F\bar{4}3m$
UPt_3	0.52,0.48	80	5^a	0.02	$P6_3/mmc$
UNi_2Al_3	1	~100	4.3	0.2	$P6/mmm$
URu_2Si_2	1.5	70	17	0.02	$I4/mmm$
$YbBiPt$		~1	0.4	0.1	$F\bar{4}3m$
$CeCu_6$		4	-	-	$Pnma$
$CePt_2Sn_2$		1	(?1)	(?)	$P4/nmm$

[a]Discovered by μSR technique.
[b]Magnetic nature determined by μSR.

(1982). In the Kondo model the position of the Kondo resonance is fixed by the Friedel sum rule (Friedel, 1952). Below T^* this resonance will appear as a real band with a proper dispersion function $E(\mathbf{k})$, which therefore strongly contributes to the number of states at the Fermi surface. Martin suggested that in order to obey the Luttinger sum rule (Luttinger, 1960), determining the number of states of the Fermi surface with or without interactions, a pseudo-gap should appear in the Kondo resonance at E_F, possibly resulting in anomalies, for example, in the specific heat or the magnetic susceptibility. Similar arguments were applied to describe the change of sign of the thermoelectric power below 0.5 K.

Undoubtedly, the observation by μSR of static magnetism in $CeAl_3$ by Barth *et al.* (1987) has constituted a remarkable reversal of heavy-fermion research. The key point of these zero-field μSR studies was the observation below 0.7 K of a clear spontaneous oscillating μSR signal, which unambiguously indicated the presence of a static finite magnetic field at the μ^+ site (see Fig. 38). Different fitting procedures were adopted to describe in particular the rapid loss of polarization observed for short times. To describe the fraction of the μSR signal arising from the magnetic volume of the sample, Barth *et al.* (1987) utilized the sum of one oscillating signal and one rapidly depolarized Kubo-Toyabe component. The rapidly depolarized Kubo-Toyabe component was as-

cribed to domains exhibiting random or extremely short-range order reminiscent of a spin-glass order. They were thought to coexist with domains that show coherent magnetic order and are responsible for the signal showing precession pattern. However, a basic problem with this analysis was the occurrence of an unrealistic phase shift in the oscillating component.
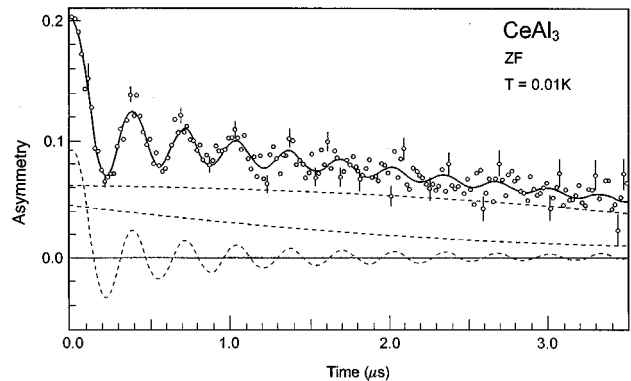

FIG. 38. Time evolution of the μ^+ polarization measured in zero-field in a $CeAl_3$ sample at low temperature. The clear spontaneous oscillations indicate a finite static magnetic field at the μ^+ site at low temperature. The solid line represents a fit to the data of the $G(t)$ function defined in Eq. (45). The broken lines are the different components of $G(t)$.

Recent measurements on a high-quality polycrystal (Amato, Feyerherm, Gygax, Schenck, and Jaccard, 1994) exhibit very similar results, pointing to the intrinsic character of the magnetism. For this new study the presence of the rapid depolarization at short times was tentatively attributed to the transition from a precursor μ^+ state to a final μ^+ state sensitive to the static magnetism. A more recent description of the data (Amato, 1995a) seems to furnish a more straightforward picture of the static magnetism in CeAl$_3$. Hence the presence of a phase shift and rapid depolarization at early times are reminiscent of a J_0 Bessel function. This function, as we saw in Sec. III.C, is characteristic of an incommensurate magnetic structure and possesses an inherent fast relaxation at early time as well as a phase shift when its oscillations are tentatively fitted by a simple cosinusoidal component. Excellent fits of the CeAl$_3$ data below 0.7 K are obtained by describing the time evolution of the μ^+ polarization with

$$G(t) = \mathcal{A}_m[\tfrac{2}{3}J_0(2\pi\nu_{max}t)\exp(-\lambda_1 t) + \tfrac{1}{3}\exp(-\lambda_2 t)]$$
$$+ \mathcal{A}_{nm}G_{KT}(t), \qquad (45)$$

where $\mathcal{A}_{nm}$ and $\mathcal{A}_m$ represent the nonmagnetic and magnetic volume fraction of the sample ($\mathcal{A}_{nm}+\mathcal{A}_m=1$); the Kubo-Toyabe function G_{KT} characterizing the nonmagnetic volume describes the field spread created by the dipole fields of the ^{27}Al ions ($\Delta \simeq 0.2\ \mu s^{-1}$); the $\tfrac{1}{3}$ term of the magnetic component is caused by the fraction of the muon ensemble ($\tfrac{1}{3}$ for a polycrystal) for which the static internal field at the μ^+ site is parallel to the initial μ^+ polarization, and for which the depolarization rate λ_2 reflects inhomogeneous broadening as well as spin-lattice relaxation; and finally, the term containing the Bessel function describes the muons precessing in a modulated internal field, and the depolarization rate λ_1 is caused by both homogeneous and inhomogeneous broadenings.

Figure 39 shows the temperature dependence of the magnetic volume fraction and of the cutoff frequency ν_{max}. It should be stressed that almost identical behaviors for these parameters are obtained using the different fitting procedures described above, indicating that the main conclusions drawn from the μSR data are independent of the adopted model. The main indication furnished by these data is the absence of a clearcut cooperative magnetic transition. Unlike usual magnetic transitions, static magnetism first appears below $\sim$2 K in a vanishingly small fraction of the sample volume and seems to be characterized by a rapidly damped Kubo-Toyabe function (not shown), indicating short-range random static magnetism. Below 0.7 K, the increase of the magnetic volume is concomitant with the occurrence of a well-resolved oscillatory behavior of the μSR signal. The value of the residual paramagnetic volume for $T\to 0$ is a sample-dependent feature, and, for example, Barth et al. (1987) found no persisting paramagnetic volume at zero temperature. On the other hand, similar temperature dependences of the cutoff frequency were observed for all investigated samples, indicating a maximum local
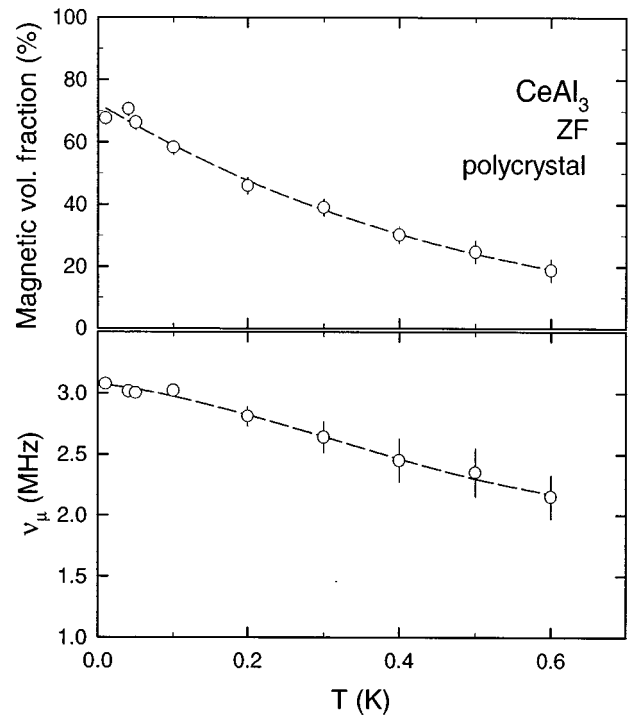

FIG. 39. Zero-field μSR measurements on a polycrystalline CeAl$_3$ sample. *Upper-part*: Temperature dependence of the magnetic volume fraction ($\mathcal{A}_m$) as deduced from μSR data. *Lower part*: Temperature dependence of the cutoff frequency ν_{max} of the J_0 Bessel function [see Eq. (45)].

field of the order of $B_\mu = 200$ G at the μ^+ site. The sharp appearance of the frequency is reminiscent of spin-density-wave transitions in antiferromagnetic chromium (Arrot, Werner, and Kendrick, 1965) or the Beechgaard salt (TMTSF)$_2$PF$_6$ (Le et al., 1991) and may be an indication of a first-order transition.

The occurrence of a magnetic transition in CeAl$_3$ was subsequently confirmed by several techniques. Nakamura, Kitaoka, Asayama, and Flouquet (1988) observed that the ^{27}Al NMR linewidth increases markedly below 1.2 K, where the nuclear spin-relaxation $1/T_1$ also exhibits a maximum. The complicated lineshape of the NMR spectra was ascribed to the appearance of some complex spin structures such as an incommensurate spin-density wave. Electrical-resistivity studies on tiny single crystals showed a clear anomaly for $T\gtrsim 1$ K and a T^3 dependence between 0.3 K and 1 K, from scattering spin excitations of an incommensurate modulated structure (Jaccard, Cibin, and Sierro, 1988). Finally, and contrary to what was observed in polycrystals, specific-heat and magnetic-susceptibility measurements on single crystals exhibit large anomalies for temperatures ranging from $\sim$1 K to $\sim$2.2 K (Lapertot et al., 1993).

The absence of anomalies in the bulk properties of polycrystals could be explained by the peculiar peritectoidic formation of CeAl$_3$, which could induce large strains inside polycrystalline samples. In a similar way as discussed for CeCu$_2$Si$_2$ (Sec. III.E), the presence of internal sources of pressure could deeply affect the ground state of CeAl$_3$ by promoting a paramagnetic ground

state. The removal of the internal strains, either by powdering the sample as for NMR studies, or by obtaining single crystals, is thought to reduce the hybridization between f moments and conduction electrons, which leads to stable magnetic ground states. The large sensitivity to pressure of CeAl$_3$ is also demonstrated by the dramatic decrease of the specific heat ($\sim$40%) under an external pressure as low as 0.4 kbar (Brodale *et al.*, 1985). It is also plausible that the presence of internal strains is responsible for the absence of clearcut transitions as observed by μSR, creating a spread of the condensation energy of the magnetic phase throughout the sample.

Without precise knowledge of the μ^+ stopping site, no definitive conclusions could be drawn on the value of the static Ce moment. Tentative estimations furnished moderate values ranging from $\mu_s=0.11\,\mu_B$/Ce atom to $\mu_s=0.5\,\mu_B$/Ce atom, in line with the clear anomaly of the specific heat observed on single crystals. If the more realistic spin-density-wave picture is adopted, no unambiguous determination of the static-moment value can be furnished by the μSR data, since the cutoff frequency is closely dependent on both the wave vector $\mathbf{q}$ and the value of μ_s of the static moment. Additional information concerning the magnetic structure could be provided by investigating the angular dependence of the cutoff frequency in a single crystal. Hopefully, and despite the smallness of the currently available single crystals, such experiments will be possible in the near future owing to new capabilities to investigate reduced-size samples by μSR (see, for example, Kiefl *et al.*, 1994).

2. CeRu$_2$Si$_2$

Until very recently, the tetragonal system CeRu$_2$Si$_2$ was still classified as one of the last heavy-fermion systems exhibiting a Fermi-liquid paramagnetic ground state. New μSR studies on well characterized single crystals have drastically changed this picture (Amato, Feyerherm, Gygax, Schenck, Flouquet, and Lejay, 1994).

CeRu$_2$Si$_2$ appears to be close to a local-moment-magnetism transition, as can be seen by its extreme sensitivity to internal pressure. The substitution of $\sim$10% of Si by Ge expands the unit cell and thereby decreases T^*, resulting in the occurrence of long-range magnetism with a moderate value of the static Ce moment. For the pure system, dynamical magnetic intersite correlations, characterized by incommensurate wave vectors, start to develop below 60 K, but on-site fluctuations (Kondo fluctuations) were considered to prevent the divergence of the magnetic correlation length (Regnault *et al.*, 1987).

μSR studies were first dedicated to the determination of the μ^+ site in transverse-field experiments by measuring the angular and temperature dependence of μ^+ Knight shifts (see Fig. 40). From 300 K down to at least 10 K, and along both main crystallographic directions, K_μ scales nicely with the magnetic-susceptibility contribution χ_f from the f moment (where χ_f is obtained by subtracting the magnetic susceptibility of the reference compound LaRu$_2$Si$_2$ from the total susceptibility). Con-
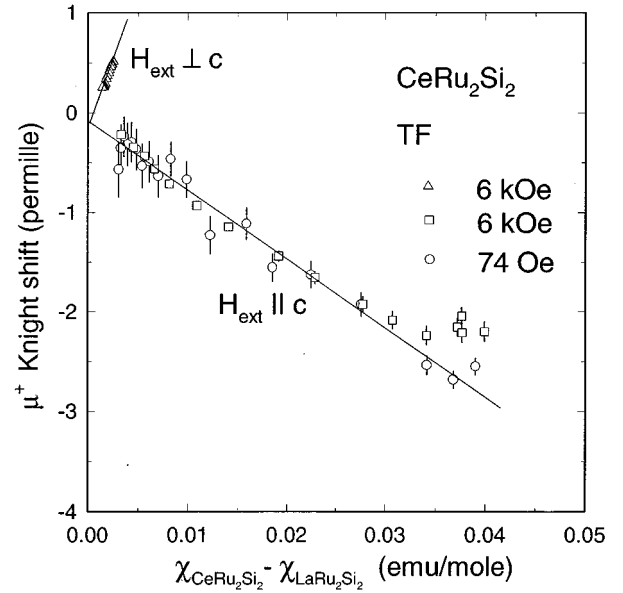

FIG. 40. μ^+ Knight shift plotted versus the magnetic susceptibility (Clogston-Jaccarino plot) for the principal directions in CeRu$_2$Si$_2$ with the temperature as an implicit parameter. The susceptibility of the reference compound LaRu$_2$Si$_2$ has been subtracted.

sidering an axial symmetry for the μ^+ site, and in analogy to Eq. (18), the μ^+ Knight shift can be written as

$$K_{\mu\parallel}=(A_c+A_{\rm dip}^{zz})\chi_{f,\parallel},$$
$$K_{\mu\perp}=(A_c-\tfrac{1}{2}A_{\rm dip}^{zz})\chi_{f,\perp}. \quad (46)$$

From the observed scaling $A_c=0.86$ kG/μ_B and $A_{\rm dip}^{zz}=-1.24$ kG/μ_B are obtained. Among the possible μ^+ sites of the structure (space group $I4/mmm$), only the b site ($\frac{1}{2}\frac{1}{2}0$) has a compatible dipole coupling constant $A_{\rm dip,theor}^{zz}=-1.30$ kG/μ_B. The small difference between $A_{\rm dip}^{zz}$ and $A_{\rm dip,theor}^{zz}$ suggests an outward displacement (with respect to the interstitial μ^+) of $\sim$1.5% of the Ce nearest neighbors, due to the usual lattice distortion around the interstitial μ^+ (Camani *et al.*, 1977).

Zero-field studies at very low temperature were undertaken to probe for the occurrence of static magnetism (Amato, Feyerherm, Gygax, Schenck, Flouquet, and Lejay, 1994). Owing to the slow decay of $P(t)$ ($\mathbf{P}_\mu(0)\|\mathbf{c}$), no unambiguous determination of the best-fit function could be made, and an exponential depolarization function was adopted for all the temperatures. Above 2 K and up to 200 K (where μ^+ diffusion sets in), the measured μ^+ depolarization rate is small, as expected from the computed linewidth due to the nuclear dipole fields from ^{29}Si, ^{99}Ru, and ^{101}Ru nuclei. As seen in Sec. II.D, such a depolarization process is better described by a Kubo-Toyabe function [see Eq. (26)], for which the short-time behavior is quite different from the exponential function. However, the relative short temporal window of the μSR technique compared with the observed depolarization time, as well as the presence in the depolarization process of a non-negligible contribution arising from fast electronic-spin
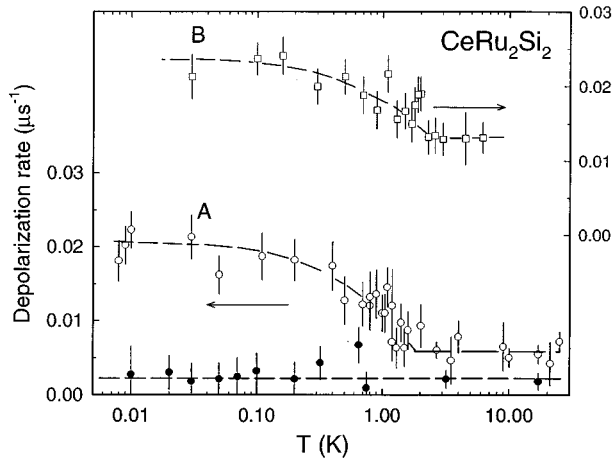
FIG. 41. Temperature dependence of the zero-field (open symbols) and longitudinal-field ($H_{ext}=6$ kOe solid symbols) depolarization rates in CeRu$_2$Si$_2$ measured in two monocrystalline samples. The arrows indicate which y axis the points are plotted on. The initial μ^+ polarization was along the tetragonal c axis.

FIG. 42. Comparison of the transverse-field μSR relaxation time $T_2 = 1/\lambda_{TF}$ and linewidth Γ_{ss} and Γ_{is} obtained from inelastic neutron scattering in CeRu$_2$Si$_2$. Γ_{ss} refers to single-site (Kondo) fluctuations and Γ_{is} to intersite fluctuations (from Amato, Baines et al., 1993).

fluctuations (see discussion below), could explain the reasonably good exponential fits obtained in this temperature range.

Below 2 K, the depolarization rate exhibits a significant increase (see Fig. 41), corresponding to an enhancement of the field spread at the μ^+ site of the order of 0.2 G, which originates from the electronic moments. The static nature of the local fields was proven by the strong reduction of the μ^+ depolarization observed in longitudinal fields. Additional transverse-field measurements indicates the isotropic character of the field spread, which disfavors the presence of a unique, albeit very small, field at the μ^+ site. Considering that the different magnetic structures observed in isostructural compounds with light rare earths led to nonzero net dipole field at the b site (Szytula and Leciejewicz, 1989), Amato, Feyerherm, Grygax, Schenck, Flouquet, and Lejay (1994) concluded that the field distribution with zero average value detected by μSR in CeRu$_2$Si$_2$ was due to static Ce moments of the order of $\mu_s \simeq 10^{-3}$ μ_B/Ce ordering in a complicated (possibly incommensurate) structure. Such an ultrasmall value for a static moment is the lowest ever detected by μSR. The extremely small entropy with such a small value of μ_s could explain the nonobservation of any kind of anomaly in the specific-heat data (Fisher et al., 1991). The thermoelectric power is the only macroscopic property exhibiting a change of behavior for $T \lesssim 2$ K (Steglich et al., 1985). Such an anomaly is similar to the ones observed in CeAl$_3$ and for nonsuperconducting samples of CeCu$_2$Si$_2$, which were first interpreted as signatures of coherent Kondo scattering (Sparn et al., 1985). The discovery of static magnetism by μSR in these systems necessitates a reinterpretation of the thermoelectric-power anomalies as a possible manifestation of magnon drag effects.

Owing to the very small depolarization due to nuclear dipole fields, CeRu$_2$Si$_2$ presents a unique possibility to
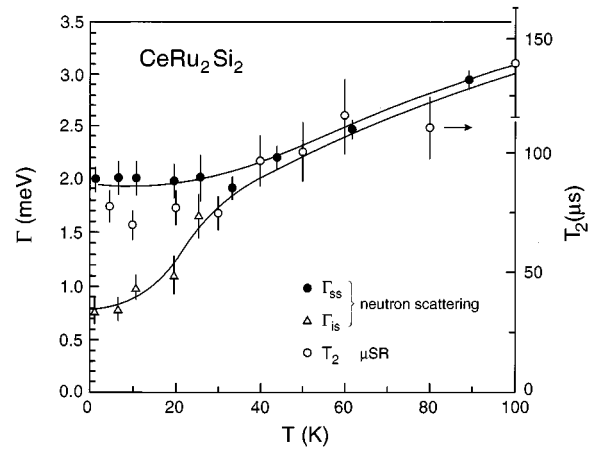
investigate the dynamics of the f moments at high temperature. Transverse-field studies in very small applied fields (Amato, Baines et al., 1993) indicated that the depolarization above 6 K is formed by 2 independent channels: (i) the spread caused by the nuclear dipole fields leading to a very small Gaussian depolarization; and (ii) the effect of the $4f$ spin fluctuations (with a characteristic time τ_c), which produces an exponential decay of the polarization. For fast fluctuations $1/T_2 \simeq 1/T_1 = 2M_2\tau_c$ (see Sec. II), where M_2 is the van Vleck second moment of the dipole-field distribution at the μ^+ site, assuming that the Ce moments are randomly frozen. Since the μ^+ spin is mainly affected by magnetic excitations with zero energy transfer, τ_c can be obtained from the width $\Gamma_{ss} = \hbar/\tau_c$ of the quasielastic neutron-scattering signal corresponding to single-site (Kondo) fluctuations. Figure 42 shows that the relaxation time T_2 scales with Γ_{ss} as expected, since $1/T_2 = 2M_2\tau_c = 2M_2\hbar/\Gamma_{ss}$. From the observed scaling, an estimated size of ~ 0.6 μ_B for the fluctuating Ce moments can be extracted. This value is much higher than the static moment found below 2 K, demonstrating the importance of the Kondo effect in the renormalization of the moment of the quasiparticles.

Although the μ^+ depolarization rate is strongly reduced in longitudinal-field measurements at low temperature (see Fig. 41), a small contribution λ_{LF} persists. This very small contribution, which is close to the instrumental resolution of the continuous muon beam available at the Paul Scherrer Institute (Villigen, Switzerland), where the experiments were carried out, has recently been confirmed by experiments performed at the ISIS Facility (Rutherford Appleton Laboratory, Chilton, U.K.), where the background is virtually zero because of the pulsed nature of this muon source (see Amato et al., 1996). This contribution also suggests the presence of fast f-spin fluctuations below 2 K. The contribution $\lambda_{LF} = 1/T_1$ is of the same order as $\lambda_{TF} = 1/T_2$ observed in the transverse-field data, as expected for fast fluctuations. Hence the μSR data seem to indicate the
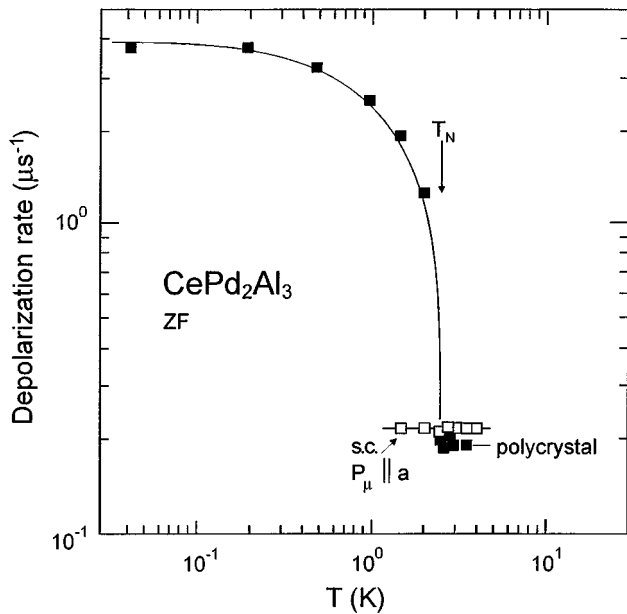
FIG. 43. Temperature dependence of the zero-field depolarization rate (Kubo-Toyabe fits) in $CePd_2Al_3$ measured in a single crystal ($\mathbf{P}_\mu \| \mathbf{a}$) and an annealed polycrystal. Note the drastic difference below T_N=2.7 K.

coexistence at low temperature of static ultrasmall-moment magnetism and dynamical f-spin fluctuations involving much higher moments. Such an observation could be in qualitative agreement with the picture of two different subsets of electrons in the ground state of some heavy-fermion compounds as discussed, for example, for UPd_2Al_3 in Sec. III.C.

3. Other Ce-based systems

$CePd_2Al_3$ constitutes another system that could tentatively be classified as a heavy-fermion band magnet. For annealed polycrystals an antiferromagnetic transition is observed at $T_N \simeq 2.7$ K in the bulk properties (Kitazawa et al., 1992). This transition occurs at a temperature much lower than the estimation of $T^* \simeq 19$ K. The static Ce moment of ~ 0.4 μ_B lying in the basal plane [wave vector $\mathbf{q}=(0,0,\frac{1}{2})$] is much lower than the final ground-state moment of the $|\pm \frac{1}{2}\rangle$ doublet, which is calculated to be 1.28 μ_B/Ce. Therefore a large exchange constant $\mathcal{J}$ has been invoked to explain the reduced ordered moment and rather large Kondo temperature (see, for example, Mentink, 1994). The low ordering temperature as well as the observation of intermediate-valence behavior in the smaller isoelectronic system $CeNi_2Al_3$ indicates that $CePd_2Al_3$ lies close to a magnetic-to-nonmagnetic boundary. This is also demonstrated by the pronounced sample dependence of the magnetism. Thus no magnetism is detected in monocrystalline samples as illustrated by zero-field μSR measurements, which indicate a temperature-independent Kubo-Toyabe depolarization rate (see Fig. 43). Similarly, as-cast polycrystals do not exhibit an indication of magnetism when bulk properties are investigated, and annealing procedures are necessary

to stabilize the magnetism, which is nevertheless not systematically observed. Figure 43 shows zero-field μSR data obtained on an annealed polycrystalline sample, which does not present obvious anomalies in its bulk properties at the expected transition temperature. The clear increase of the μ^+ depolarization rate below 2.7 K indicates the occurrence of short-range static magnetic correlations that become visible with a microscopic technique like μSR. For this sample, the huge value of $\Delta(T \to 0)$ corresponds to an almost completely random distribution of static Ce moments with $\mu_s \simeq 0.3$ μ_B, i.e., a value comparable to the one extracted by neutron studies on samples exhibiting long-range order.

The peculiar differences in magnetic behavior between the different types of samples have been discussed in terms of Al order. Annealed polycrystals possess a stoichiometric amount of Al, producing a well-defined electronic environment that promotes long-range order generated by magnetic exchange coupling via the aluminum layer. In as-cast polycrystals and as-grown single crystals, two Al sites are present (slightly shifted along the c axis compared to the g site of the hexagonal $P6/mmm$ structure) without altering the lattice symmetry. Random occupation of these sites for polycrystals and Al deficiency for single crystals leads to an irregular local electronic environment, deeply reducing the average coupling strength between planes and preventing the divergence of the magnetic correlation length.

The occurrence of magnetism in the system $CeCu_2Si_2$ was already discussed in Sec. III.E. Several aspects of this magnetism indicate that it is an instability of the heavy-quasiparticle band. Namely, one observes (i) a strongly reduced value of the static moment; (ii) a very low transition temperature; and (iii) a competition with the superconducting phase. Since the Cooper pairs are unambiguously composed of the heavy quasiparticles, this latter point clearly shows that both cooperative phases are formed out of the coherent heavy-fermion Fermi-liquid state.

This picture is supported by the calculations of the exchange-interaction parameter between the f and conduction electrons for $(Ce,U)T_2X_2$ compounds (where T denotes transition metals and X is silicon and/or germanium; Endstra et al., 1993). Considering that the conduction electrons in these compounds have significant d character, the f-ligand hybridization is governed by the f-d hybridization (i.e., $V \simeq V_{df}$), the strength of which is calculated via the Harrison formalism (Harrison, 1983), which combines Andersen's muffin-tin orbital theory and transition-metal pseudopotentials. Figure 44 shows schematically the evolution of the magnetic order as a function of the exchange-coupling parameter $\mathcal{J} \simeq \mathcal{J}_{df}$ obtained by the Schrieffer-Wolf transformation [see Eq. (3)]. As expected, $CeCu_2Si_2$ appears close to a local-moment magnetic instability. Furthermore, $CeRu_2Si_2$, which is situated on the right-hand side of $CeCu_2Si_2$, has been found, as discussed above, to display heavy-fermion band magnetism with extremely small static moment. In view of its weaker hybridization, the occur-
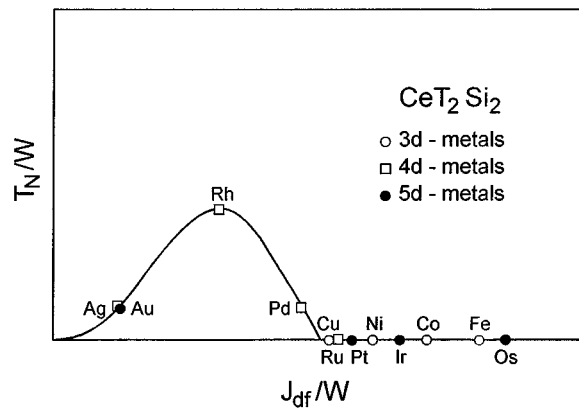
FIG. 44. Schematic phase diagram for the Kondo lattices of the CeT_2Si_2 family (ordering temperature versus the hybridization strength; both these quantities are normalized by the conduction-electron bandwidth W to allow comparison; adapted from Endstra *et al.*, 1993).

FIG. 45. Temperature dependence of the spontaneous μ^+ frequencies measured below T_N in UCu_5. The μSR signal also contains a nonoscillating component (from Barth *et al.*, 1986).

rence of heavy-fermion band magnetism in $CeCu_2Si_2$ appears therefore conceivable. Moreover, the observation of competition between magnetism and superconductivity indicate that both phases are almost degenerate. This raises the question of the real nature of the ground state in $CeCu_2Si_2$, which will require further microscopic and metallurgical studies to be definitively settled.

4. UCu_5

The face-centered-cubic system UCu_5 (space group $F\bar{4}3m$) orders antiferromagnetically below $T_N \simeq 15$ K. Early neutron-diffraction measurements identified the antiferromagnetic structure of the U sublattice as consisting of ferromagnetically ordered (111) planes coupled antiferromagnetically along the body diagonal (Murasik *et al.*, 1974). The exact determination of the size of the ordered U moments, pointing along the [111] direction, suffers from the large and still unexplained discrepancy between the value $\mu_s \simeq 0.9\ \mu_B$, reported by Murasik *et al.* (1974), and the value $\mu_s \simeq 1.55\ \mu_B$, determined by Schenck *et al.* (1990). In addition, the determination of the magnetic structure is not ambiguous, and, for example, a quadruple-**q** structure (Nakamura *et al.*, 1990) is also compatible with the neutron data.

At this point the reader could wonder about the classification of UCu_5 in the section devoted to heavy-fermion band magnetism. In fact the large value of μ_s, as well as the rather simple magnetic structure determined by neutron scattering unambiguously indicate that UCu_5 is a local-moment heavy-fermion magnet. However, UCu_5 exhibits a second transition at $T \simeq 1$ K $\ll T_N$, for which μSR studies, as we will see below, clearly demonstrated its unusual magnetic nature.

Specific-heat data (Ott, Rudigier, Felder *et al.*, 1985) have shown that the heavy-fermion state in UCu_5 develops at temperatures well below T_N. This situation is in contrast with the majority of the other local-moment-magnetic heavy-fermion compounds (see Sec. IV.B), for
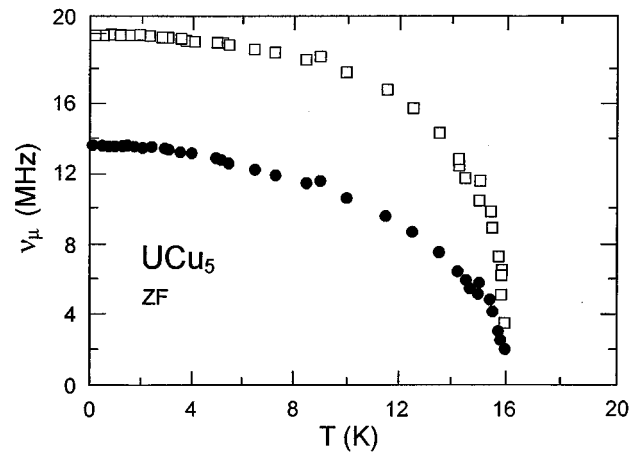
which the usually assumed picture implies that the spin fluctuations of the f moments are frozen out below T_N. Since these spin fluctuations are the necessary mechanism for the Kondo effect responsible for the occurrence of the heavy quasiparticles, one could expect that the presence of static magnetism impedes the formation of a heavy-fermion state at low temperature. Furthermore, the specific-heat data reveals a second phase transition at ~ 1 K, displaying hysteretic behavior but not latent heat, which is only observed in samples considered to be high-quality samples. This transition is also visible in the transport properties with, for example, an increase by an order of magnitude of the electrical resistivity below ~ 1 K.

Barth *et al.* (1986) first investigated the magnetic phase of UCu_5 by zero-field μSR on a sample not exhibiting the 1 K transition. Below $T_N \simeq 15$ K, they observed a three-component μSR signal, one nonoscillating component (1) associated with a μ^+ site with zero-average field, and the other two components, which display spontaneous spin precessions with $\bar{\nu}_{\mu,2}(T\rightarrow0)=19.8$ MHz (B_μ=1.46 kG) and $\bar{\nu}_{\mu,3}(T\rightarrow0)=13.6$ MHz ($B_\mu \simeq 1$ kG; see Fig. 45). If, on one hand, the nonoscillating component can be attributed to muons stopping at the b site ($\frac{1}{2}\frac{1}{2}\frac{1}{2}$), for which the dipole-field calculations show that $B_\mu=0$ for both proposed magnetic structures, on the other hand, the presence of two precession frequencies cannot be explained by either structure, assuming high-symmetry μ^+ stopping sites. A possible explanation would be to consider that the muons stopping at the ($\frac{3}{4}\frac{3}{4}\frac{3}{4}$) site are responsible for component 2 and that component 3 arises from muons stopping at vacancy Cu sites or defect sites, which is corroborated by the relatively small amplitude connected with this latter component. Regardless of the exact muon location, these data clearly indicate an absence of anomaly around 1 K in the temperature dependencies of both the μ^+ frequencies and μ^+ depolarization rates (see Figs. 45 and 46).

Schenck *et al.* (1990) investigated, by zero-field μSR below 2 K, a high-quality sample showing the 1 K tran-
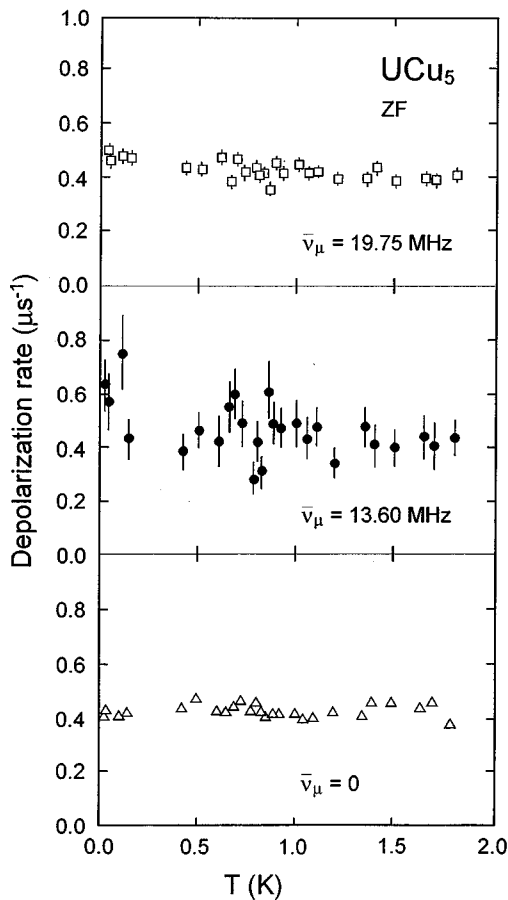
FIG. 46. Temperature dependence near 1 K of the μ^+ depolarization rates connected to the three components detected in the zero-field data on a UCu$_5$ sample not showing the 1 K transition (Gaussian fits for $\bar{\nu}_\mu \neq 0$, Kubo-Toyabe fit for $\bar{\nu}_\mu=0$; from Barth et al., 1986).

FIG. 47. Temperature dependence near 1 K of the μ^+ depolarization rates connected to the three components of the zero-field μSR signal recorded in a high-quality UCu$_5$ single crystal [(a) component with $\bar{\nu}_\mu \simeq 19.8$ MHz, (b) component with $\bar{\nu}_\mu \simeq 13.6$ MHz, (c) component with $\bar{\nu}_\mu=0$; above $T \simeq 1.15$ K: same fits as for Fig. 46; below $T \simeq 1.15$ K: exponential fits; from Schenck et al., 1990].

sition. The temperature dependence of the spontaneous frequencies showed a similar behavior as the one reported previously for the sample without a 1 K transition described above. No change of the spontaneous μ^+ frequencies was observed, indicating that the 1 K phase transition is not associated with a change in magnetic structure. This is in line with neutron-diffraction results that showed no change in the magnetic Bragg peaks when changing the temperature across the 1 K transition (Schenck et al., 1990). The most dramatic effect is seen in the μ^+ depolarization rates, which rise drastically as the temperature is lowered below ~ 1.15 K and change in appearance from Gaussian (or Kubo-Toyabe for the component 1 with $\bar{\nu}_{\mu,1}=0$) above 1.15 K to exponential for lower temperatures (see Fig. 47). Whereas the μ^+ depolarization above 1.15 K can be attributed to just the ^{63,65}Cu nuclear dipole fields, the increased depolarization rate for lower temperatures reflects an increased inhomogeneous linebroadening, i.e., an increased static-field spread experienced by the muon ensemble. Since the neutron results also imply that the 1 K transition is not associated with a structural phase transition, the increased field spread must reflect the occurrence of small static moments ($\sim 10^{-2}$ μ_B) of electronic origin, which
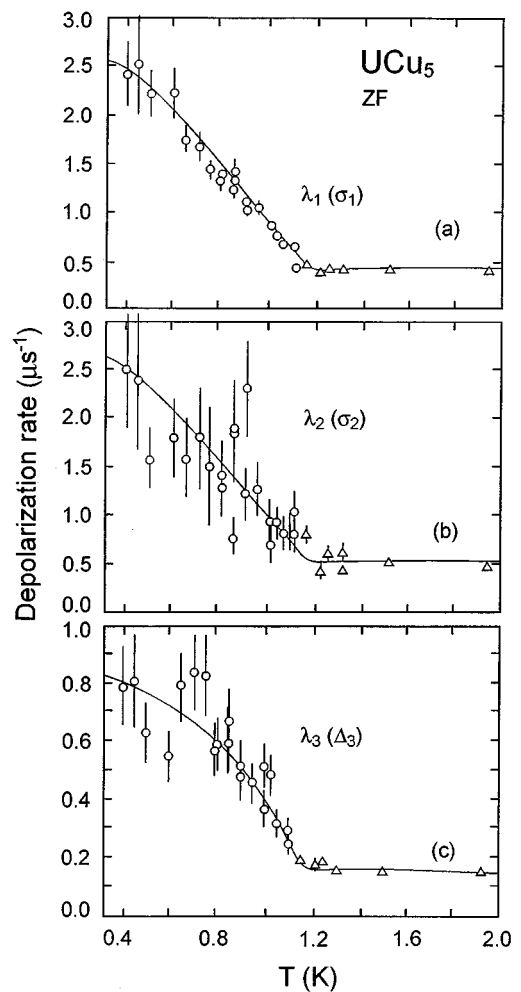
order in a complex fashion (incommensurate spin-density wave or even random order). The observations that the 1 K transition occurs at temperatures for which the heavy-fermion state is fully developed and that the value of the static moments is strongly reduced, suggest that this magnetic state involves an ordering of the heavy quasiparticles existing in parallel to the ordinary U-localized 5f moments, which are responsible for the antiferromagnetic state below 15 K. This implies that the ground state of UCu$_5$ is determined by the coexistence of two rather independent subsets of electrons. Hence the situation of UCu$_5$ is similar to the one observed in UPd$_2$Al$_3$ (see Sec. III.C), for which the heavy-quasiparticle state was found to be unstable against a superconducting transition. For UPd$_2$Al$_3$, the presence of both a more localized and more itinerant electron subsystem could result from anisotropic hybridization between localized and conduction electrons, possibly leading to portions of the Fermi surface being character-

ized by a different value of $k_B T^*$. Such a simple explanation cannot be applied to the cubic system UCu$_5$, and obviously more theoretical work will be required to understand the fascinating properties revealed by μSR.

5. Other U-based heavy-fermion band magnets

As discussed in detail in Sec. III, the heavy-fermion superconductors UPt$_3$, UNi$_2$Al$_3$, and URu$_2$Si$_2$ show antiferromagnetic transitions at $T_N \gg T_c$, which are characterized by strongly reduced values of the static moments. Furthermore, the magnetic transitions occur at temperatures much lower than the characteristic temperature T^* of the Kondo effect (see Table III), i.e., in a regime where the magnetic degrees of freedom have been transferred to the heavy quasiparticles. These indications strongly point to a heavy-fermion magnetism picture, where the magnetic properties are determined by the residual interactions between the heavy quasiparticles.

6. YbBiPt

This cubic system (MgAgAs structure type, space group $F\bar{4}3m$) has attracted considerable interest due to the record high linear coefficient of its electronic specific heat [$C/T(T\to 0) \simeq 8$ J/(K^2 mol), Fisk *et al.*, 1991], indicating the presence of extremely massive quasiparticles. Measurements of thermodynamic properties at low temperature suggested the occurrence of some kind of anomaly at ~0.4 K, the magnetic nature of which has been identified by μSR.

Zero-field μSR data, obtained on crushed powder and crystalline samples (Amato, Canfield *et al.*, 1992; 1993), show that the μ^+ depolarization function at low temperature is described by two relaxing but nonoscillating components

$$G(t) = A_f g_f(t) + A_s \exp(-\lambda_s t). \tag{47}$$

The form of $g_f(t)$ changes from exponential at high temperature to Gaussian [$g_f(t) = \exp(-\sigma^2 t^2/2)$] for temperatures below 0.5 K and is characterized by a large μ^+ depolarization rate ("fast" component, see Fig. 48). The Gaussian character at low temperature can arise either from static fields random in direction and magnitude, corresponding to a dense spin-glass-like order, or from an ordered magnetic state (with possibly incommensurate structure) sufficiently disturbed to lead to a rapid μ^+ depolarization. The second component, showing a slow exponential depolarization, is ascribed to dynamical fluctuations of the f moments sensed by the muons. The presence of two components at low temperature was first interpreted in terms of different magnetic regions with different characteristic μ^+ depolarization rates. In this vein the "fast" component would be associated with domains showing some static magnetic order below 0.5 K, whereas the "slow" component would arise from paramagnetic domains persisting down to the lowest temperature.

Alternatively, Heffner *et al.* (1994) suggested that both components describe the μ^+ depolarization occurring for a complicated incommensurate spin-density
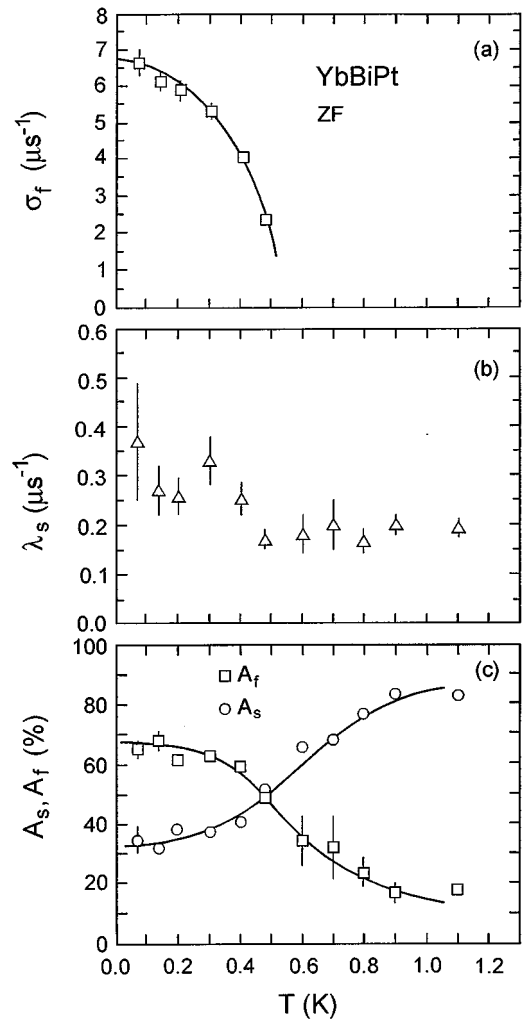

FIG. 48. Zero-field μSR measurements on a polycrystalline YbBiPt sample. (a) Temperature dependence of the "fast" Gaussian depolarization below 0.5 K, and (b) of the exponential depolarization rate characterizing the "slow" component. (c) Amplitudes of the "fast" and "slow" components of the μSR signal. At higher temperature the "fast" component vanishes (from Amato, Canfield *et al.*, 1993).

wave. Within this model the whole sample volume undergoes the magnetic transition. Interestingly, in the system Cr$_{85}$Mo$_{15}$, which possesses an incommensurate spin-density wave, one finds μSR signals that are again perfectly fitted with the sum of two components (Telling *et al.*, 1994). In any case, and as observed in several heavy-fermion systems, magnetism in YbBiPt develops in a spatially inhomogeneous form without a clearcut cooperative phase transition.

A tentative determination of the μ^+ stopping site was obtained from transverse-field μSR measurements where an asymmetric broadening typical of an anisotropic Knight-shift powder pattern was observed. Comparison with simulated data indicated that the muon is located at an off-center position shifted 0.4 Å from the $(\frac{1}{2}\frac{1}{2}\frac{1}{2})$ point toward a nearest-neighbor Bi ion. Adopting this μ^+ stopping site, one estimates a value of $\mu_s \simeq 0.1$ μ_B for the static Yb moment below 0.5 K respon-

sible for the fast depolarization. This low value is consistent with the absence of a nuclear Schottky anomaly in the specific heat (Thompson *et al.*, 1993), as well as with neutron-diffraction studies where the nondetection of magnetic Bragg peaks sets an upper limit of 0.25 μ_B for any ordered magnetic moments (Robinson *et al.*, 1994).

Longitudinal-field μSR experiments show that the rapid Gaussian depolarization does not change in fields up to H_{ext}=20 kOe. This is in sharp contrast with resistivity measurements below 0.4 K, where an anisotropic anomaly, ascribed to a Fermi surface that is gapped by a spin-density wave, is destroyed in a field of 3 kOe. Thus Heffner *et al.* (1994) proposed a model in which both the Yb local moments and the itinerant conduction electrons undergo ordering at $T \simeq 0.4-0.5$ K and in which an applied field of 3 kOe is sufficient to destroy the spin-density wave formed by the itinerant electrons but not the Yb ordering. Hence this implies that the electronic ground state is made up of rather independent electronic subsystems (localized and itinerant), in close similarity with the situations already observed in UPd$_2$Al$_3$ and UCu$_5$ (see Secs. III.C and IV.A.4).

B. Local-moment magnetism

Since heavy-fermion local-moment magnets are characterized by the occurrence of magnetism with moderately renormalized values of the static moments, it appears that neutron-scattering studies are more adapted than μSR to unravel the magnetic properties of the members of this class. It is the author's belief that μSR has not played a leading role in determining the basic mechanism for the appearance of moderately renormalized magnetism in these Kondo lattices. Nevertheless, the following examples will demonstrate that, due to local character of the information provided by the implanted muons, μSR should be considered a valuable complementary tool, which has furnished outstanding indications of the sometimes nonconventional character of heavy-fermion local-moment magnetism.

1. CeAl$_2$

This face-centered system (space group $Fd\overline{3}m$) is often considered as the archetypical example of a heavy-fermion local-moment magnet ($T_N \simeq 3.4-3.9$ K), exhibiting a moderate value of the linear coefficient of the specific heat $\gamma = C/T(T \to 0) \simeq 135-270$ mJ/(K^2 mol). Gavilano *et al.* (1993) showed that a large part of the γ coefficient for $T \ll T_N$ could arise from the spectra of low-energy magnetic excitations of an incommensurate magnetic structure. However, a substantial contribution to γ arising from the excitations of the itinerant electron system formed by the heavy quasiparticles has to be considered as well. Such a contribution is also reflected by the large NMR spin-lattice relaxation rate $1/T_1$ and the observation of a Korringa law [where $(TT_1)^{-1}$ is a constant] for $T \ll T_N$.

The determination of the magnetic structure was strongly hampered by the coexistence of two magnetic phase transitions, with comparable transition temperatures, in some investigated samples. For high-quality single crystals, neutron-diffraction measurements (see, for example, Barbara *et al.*, 1980) indicate the presence of only an incommensurate sinusoidally modulated spin structure [wave vector $\mathbf{q} = (\frac{1}{2} + \tau, \frac{1}{2} - \tau, \frac{1}{2})$, with $\tau = 0.112$; ordered moments $\mu_s \simeq 0.63$ μ_B directed along the [111] direction]. For samples of lower quality, one observes the presence of a second magnetic phase characterized by a simple type-II antiferromagnetism. It is believed (Schefzyk *et al.*, 1985) that the type-II structure appears in disturbed regions of a sample where the modulated structure is quenched.

Transverse-field μSR studies on a single crystal were first undertaken to determine the μ^+ site (Hartmann *et al.*, 1989). From the angular dependence of the μ^+ depolarization rate, the μ^+ site was identified as the "2-2" site (corresponding to the center of the 2Ce-2Al tetrahedra; g site in Wyckoff notation), which is also found to be occupied by hydrogen (Fisch *et al.*, 1979).

Measurements at low temperature revealed the presence in the μSR signal of a second component below 3.9 K, characterized by a fast depolarization rate and related to the occurrence of magnetic domains in the sample. The fast depolarization ($\lambda \simeq 20$ μs^{-1}) is consistent with a large static-field spread at the μ^+ site due to the incommensurate magnetic structure and the high number of magnetically inequivalent μ^+ sites (the g site has a multiplicity of 96). The amplitudes of this fast component ($\mathcal{A}_m$), which represents the magnetic volume fraction, and of the slowly damped component ($\mathcal{A}_{pm}$), which reflects the volume of the domains in the paramagnetic state, are reported in Fig. 49. The temperature dependence of $\mathcal{A}_m$ and $\mathcal{A}_{pm}$ indicate that the magnetic order does not immediately involve the total volume of the sample, but rather appears in a volume fraction that grows gradually from zero for $T \gtrsim 3.9$ K to ~80% at low temperature. Recent zero-field studies on a powdered sample (MacLaughlin *et al.*, 1993) have furnished, essentially, a similar picture.

It is plausible that the two-component structure of the μSR signal in CeAl$_2$ around T_N is somehow related to the large spread of the transition temperature observed in different samples (T_N=3.4–3.9 K). Such a large spread of the transition temperature could indicate slight differences of internal pressure in different samples. Schefzyk *et al.* (1985) have demonstrated the strong influence of the external pressure on the transition temperature, observed by thermal-expansion and specific-heat measurements, as well as by the dependence of bulk property anomalies at T_N on the sample quality. Finally, the observation by μSR of a residual paramagnetic volume fraction below T_N could provide a straightforward interpretation of the large and sample-dependent linear coefficient of the electronic specific heat observed for $T \ll T_N$, which, as discussed above, reflects a Fermi-liquid behavior.
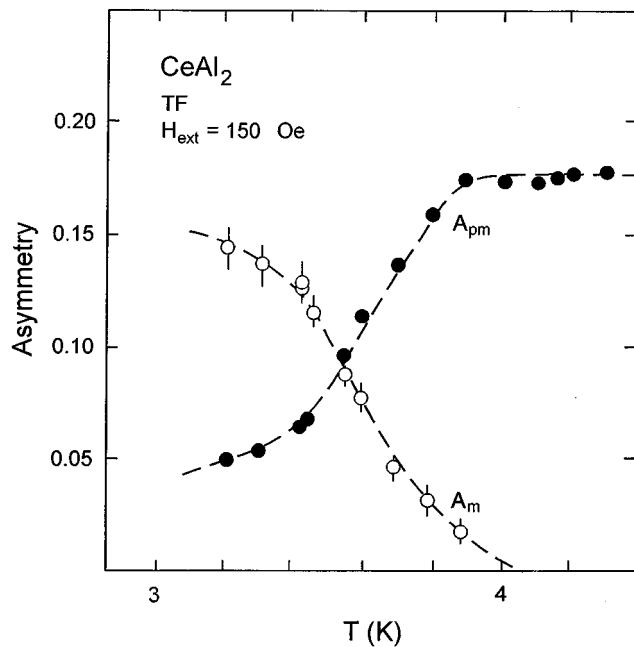
FIG. 49. Temperature dependence of the amplitudes (asymmetries) of the components of the transverse-field μSR signal in CeAl$_2$. The amplitudes are associated with the paramagnetic ($\mathcal{A}_{pm}$) and magnetic ($\mathcal{A}_m$) volume fractions (see text; from Hartmann et al., 1989).

2. CeB$_6$

This cubic system (space group $Pm\bar{3}m$) shows antiferroquadrupolar order below $T_Q \simeq 3.2$ K and an antiferromagnetic state below $T_N \simeq 2.3$ K (Komatsubara et al., 1983). The magnetic structure was found by neutron measurements to be described at 1.3 K by a wave vector $\mathbf{q}=(\frac{1}{4},\frac{1}{4},\frac{1}{2})$ with a relatively small static Ce moment of $\mu_s \simeq 0.28\,\mu_B$ (Effantin et al., 1985). However, no attempt was made to measure the temperature dependence of the magnetic ordering parameter. The antiferroquadrupolar ordering has been identified by inducing antiferromagnetic order by an external magnetic field, but controversial results are inferred from ^{11}B-NMR and neutron scattering (Takigawa et al., 1983; Erkelens et al., 1987). Whereas a complicated triple-$\mathbf{q}$ structure is derived from the angular dependence of the NMR results, a simple antiferromagnetic structure with $\mathbf{q}=(\frac{1}{2},\frac{1}{2},\frac{1}{2})$ is found for $\mathbf{H}_{ext}\|[111]$ by neutron measurements.

From the angular dependence of the μ^+ Knight shift measured in a single crystal, Amato, Feyerherm, Gygax, $\bar{\text{O}}$ nuki et al. (1993) demonstrated that the μ^+ stop solely at the d site $[(\frac{1}{2}00)$, see Fig. 50]. On the basis of this μ^+ site determination, and of the antiferromagnetic structure suggested by neutron measurements, one predicts from dipolar-field calculations that three different spontaneous fields should appear in the magnetic phase at the μ^+ sites (due to the presence of magnetically inequivalent sites below T_N). Surprisingly, zero-field measurements below T_N displayed a very complex μSR signal with 8 distinct spontaneous μ^+ frequencies ranging
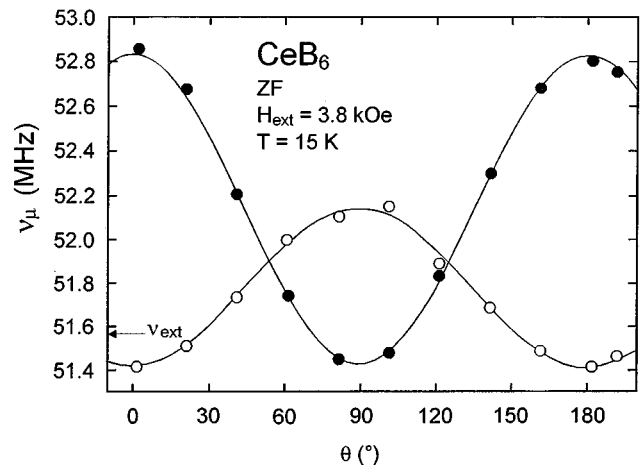

FIG. 50. Angular dependence of the two frequencies observed in the transverse-field μSR signal in CeB$_6$ (H_{ext}=3.84 kOe, T=15 K). The field was rotated around the [110] axis. The two signals have an amplitude ratio of 2:1 corresponding to the $(\frac{1}{2}00)$ and $(0\frac{1}{2}0)$ sites (open symbols) and the $(00\frac{1}{2})$ site (solid symbols). The angle θ corresponds to the angle between $\mathbf{H}_{ext}$ and the c axis.

from $\sim$2 to $\sim$77 MHz (see Fig. 51). Furthermore, several of the frequencies show strange temperature dependencies that were tentatively ascribed to a gradual change of the magnetic structure with temperature (e.g., turn of the static moments within the a-b plane; see Feyerherm, Amato, Gygax, Schenck, $\bar{\text{O}}$ nuki, and Sato,
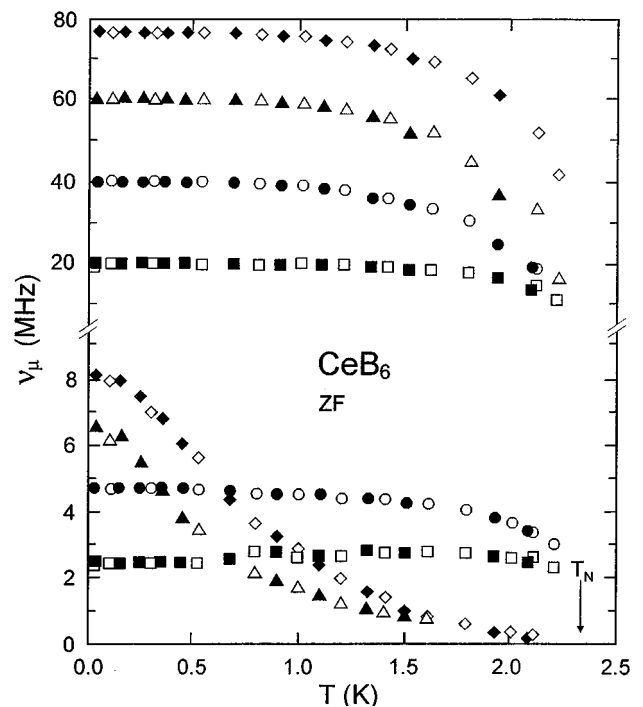

FIG. 51. Temperature dependence of the observed spontaneous μ^+ frequencies in the zero-field μSR signal below T_N in CeB$_6$. The two sets of symbols correspond to different sets of data (from Feyerherm, Amato, Gygax, Schenck, $\bar{\text{O}}$ nuki et al., 1994).

1994). A description of the magnetic state based on the μSR data cannot be given yet, but it clearly appears that these results are incompatible with the magnetic structure proposed from the analysis of the neutron-scattering data. In particular, the high μ^+ frequency components are not explained if the static Ce moment is as small as $0.28\,\mu_B$, as deduced by neutron-scattering measurements, and require ordered moments of the order of $1\,\mu_B$.

Finally, μ^+ Knight-shift measurements for the temperature range $T_N < T < T_Q$ also appear incompatible with the antiferromagnetic structure induced by an external field that was proposed on the basis of the NMR data. Hence from NMR results it was concluded that for $\mathbf{H}_{ext} \| [110]$ antiferromagnetic moments perpendicular to $\mathbf{H}_{ext}$ are induced. Such a structure should have led to an additional splitting of the μ^+ frequencies of the transverse-field μSR signal below T_Q, which were not observed (Feyerherm, Amato, Gygax, Schenck, Ō nuki, and Sato, 1994).

Due to their complexity, the μSR data on CeB$_6$ are still poorly understood. However, the peculiar observations seriously question the conclusions based on neutron scattering and should entice further studies utilizing these two techniques.

3. CeCu$_5$

This system crystallizes in the hexagonal CaCu$_5$-type structure (space group $P6/mmm$), which is similar to that of UNi$_2$Al$_3$, UPd$_2$Al$_3$, and CePd$_2$Al$_3$ (PrNi$_2$Al$_3$ type; see Secs. III.C and IV.A.3) but with Cu atoms placed at the inequivalent g and c sites. Specific-heat measurements at low temperature (Goremychkin et al., 1987) revealed an electronic linear term of roughly $\gamma \simeq 120$ mJ/(K^2 mol), comparable to those found typically for heavy-fermion local-moment magnets like CeAl$_2$. Inelastic neutron-scattering measurements have shown that the crystal electric field splits the sixfold degenerate state of the Ce^{3+} such that the ground state is constituted by the $|\pm\frac{1}{2}\rangle$ doublet, while the $|\pm\frac{3}{2}\rangle$ state is about 17 meV above the ground state and the $|\pm\frac{5}{2}\rangle$ state lies above the $|\pm\frac{3}{2}\rangle$ doublet (see, for example, Alekseev et al., 1992). Recent elastic neutron-scattering measurements suggest that the magnetic structure below $T_N \simeq 4$ K is a simple antiferromagnetic type, with a propagation vector $\mathbf{q} = (0,0,\frac{1}{2})$ (Bauer et al., 1994). Whereas the hexagonal heavy-fermion compounds with the parent PrNi$_2$Al$_3$ structure show static moments parallel to the basal plane, CeCu$_5$ was found to possess static moments parallel to the c axis with $\mu_s \simeq 0.36\,\mu_B$. This result appears surprising since the $|\pm\frac{1}{2}\rangle$ ground state implies that the direction of the easy magnetization is within the basal plane. To circumvent this problem, a model with strong anisotropic exchange had to be considered. Unfortunately, the difficulty in growing single crystals, owing to the formation of CeCu$_5$ through a peritectic reaction, has so far prevented a verification of this model by measurements on single crystals.
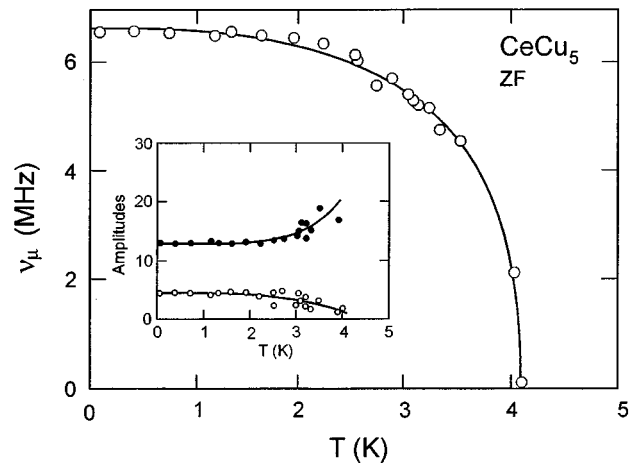

FIG. 52. Temperature dependence of the spontaneous μ^+ frequency of the zero-field μSR signal below T_N in CeCu$_5$. The inset shows the temperature dependence of the amplitudes of the oscillating (open symbols) and nonoscillating components (from Wiesinger et al., 1994).

Zero-field μSR measurements on CeCu$_5$ were undertaken in the framework of a study of the gradual loss of magnetism in Ce(Cu$_{1-x}$Al$_x$)$_5$ and Ce(Cu$_{1-x}$Ga$_x$)$_5$ (Wiesinger et al., 1994). In CeCu$_5$ above T_N the μ^+ depolarization function is well described by a Kubo-Toyabe function [see Eq. (26)] with a depolarization rate $\Delta = 0.16(1)\ \mu s^{-1}$. This value is consistent with a μ^+ stopping site in the vicinity of $(00\frac{1}{2})$ (b, k, or m site, see Sec. III.C). Upon lowering the temperature below $T_N \simeq 4.1$ K, a spontaneous precession signal is detected, the amplitude of which increases, at the expense of the nonoscillating one, but never accounts for more than $\sim 30\%$ of the total μSR signal amplitude (see Fig. 52). The μ^+ frequency of $\nu_0 \simeq 6.6$ MHz obtained for the lowest investigated temperature corresponds to an internal field at the μ^+ site of $B_\mu \simeq 500$ G.

Several conclusions can be obtained from the μSR data. If the μ^+ stopping site is assumed to be the axial b site, a primitive magnetic order, as deduced by neutron-scattering studies, can be excluded since the internal field at the μ^+ site would cancel. Consequently, based on the μSR data, Wiesinger et al. (1994) proposed an antiferromagnetic structure constituted by a "2 up-2 down" ordering of the moments parallel to the c axis, along with a ferromagnetic ordering within the basal plane. Under this assumption the cancellation of the internal field on every second μ^+ site could explain, together with the usual nonoscillating $\frac{1}{3}$ term in polycrystalline samples, the large nonoscillating component below T_N.

On the other hand, by considering that the muons stop either at the k site or at the m site, the observed value of $B_\mu \simeq 500$ G appears compatible with the magnetic structure and the static moment proposed by neutron scattering. However, all the k and m sites are magnetically equivalent, implying that, contrary to what is observed, the nonoscillating component of the μSR signal should be limited to the usual $\frac{1}{3}$ term. In order to

reconcile the μSR and neutron-scattering data, one should therefore either consider that the muons stop not only at the k or m site, but also at the b site, where $B_\mu = 0$, or alternatively that part of the sample volume remains paramagnetic for $T \to 0$, as, for example, observed in CeAl$_3$ (see Sec. IV.A.1).

In any case, the μSR data reveal that the magnetic order does not immediately involve the total volume of the sample, but rather the magnetic volume grows gradually as the temperature is lowered below T_N. Whether this peculiar behavior is related, as in CeAl$_3$, to the particular metallurgy of CeCu$_5$ remains to be seen. In particular, this observation appears to demonstrate that the condensation energy of the magnetic state is not large and the magnetic and paramagnetic ground states are almost degenerate.

4. CeCu$_5$Au

This system is closely related to the well-known CeCu$_6$ system, possessing the same complex orthorhombic structure (space group $Pnma$). The CeCu$_{6-x}$Au$_x$ systems were investigated as an example of the occurrence of magnetism induced by atomic substitution (Amato *et al.*, 1995; see also, Secs. V.A and VI.A.2). The Au ions substituting the Cu ions exclusively occupy the Cu(2) site (Ruck *et al.*, 1993), classifying the system CeCu$_5$Au as a real compound.

Zero-field μSR data reveal that at high temperature the μ^+ depolarization function is best described by a Kubo-Toyabe function [see Eq. (26)] that is characteristic of a paramagnetic state, where the μ^+ depolarization is solely due to the dipolar fields from the nuclear moments (mainly ^{63}Cu and ^{65}Cu). Below $T_N \simeq 2.3$ K an antiferromagnetic transition is clearly detected by the occurrence of spontaneous μ^+ Larmor frequencies. In the magnetic phase the time evolution of the μ^+ polarization can be well described by a damped J_0 Bessel function (see Fig. 53), which, as we saw in Sec. III.C, is theoretically expected for an incommensurate magnetic structure described by one **q** wave vector. The occurrence of an incommensurate structure was determined by neutron diffraction for a CeCu$_{5.5}$Au$_{0.5}$ sample, with propagation wave vector **q**$=(\pm 0.59,0,0)$ and moments aligned along the c axis (Schröder, Lynn *et al.*, 1994). Assuming the same magnetic structure for CeCu$_5$Au, a value of $\mu_s \simeq 0.8\,\mu_B$/Ce for the static magnetic moment can be extracted from the μSR data. Such a value is in fairly good agreement with the rough estimations of 0.5–1 μ_B/Ce obtained by neutron studies on CeCu$_{5.5}$Au$_{0.5}$ (Chattopadhyay *et al.*, 1990; Schröder, Lynn *et al.*, 1994).

Finally, we remark that for CeCu$_5$Au, which has a simple congruent melting, the μSR data show that the whole sample is involved in the magnetic state below T_N, as is usually observed in traditional magnetic systems. This could be interpreted as an additional indication that the observation of inhomogeneous forms of magnetism in heavy-fermion local-moment magnets is limited to systems with complicated melting behavior
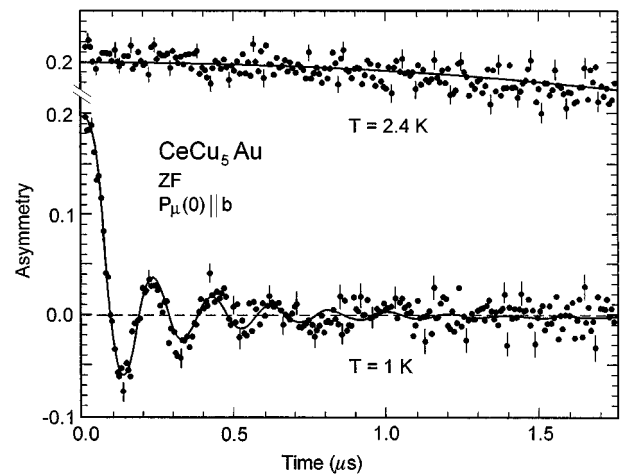

FIG. 53. Zero-field μSR spectra obtained above and below the Néel temperature in CeCu$_5$Au. The initial polarization was along the orthorhombic b axis. For $T=1$ K, the line represents a fit of an exponentially damped J_0 Bessel function (from Amato *et al.*, 1995).

susceptible to producing a distribution of internal strains, which, in view of the low condensation energy of the magnetic phase, could lead to inhomogeneous magnetic features.

5. CeTSn (T=Pd,Pt)

These systems crystallize in a complex orthorhombic structure (space group $Pn2_1a$) that is closely related to the structure of $\mathcal{E}$-TiNiSi (Higashi *et al.*, 1993). Whereas the parent system CeNiSn is a Kondo insulator with a narrow gap of only a few Kelvins (see Sec. VI.C), the increase of the unit-cell volume for CePdSn and CePtSn reduces the hybridization of the $4f$ electrons with the conduction electrons, which allows the RKKY interaction to overcome the Kondo effect. Hence complex antiferromagnetic order is observed for the two latter systems with $T_N \simeq 7$–8 K.

a. CePtSn

Neutron-diffraction studies show a rather complex structure below $T_N \simeq 7.5$ K. The moments lie in the (a,c) plane and are incommensurably modulated along the b axis [**q**$=(0,0.418,0)$] (Kadowaki *et al.*, 1993). Near 5 K, one observes the occurrence of a second magnetic transition, where the static Ce moments possess components in the three principal directions but are still modulated along the b axis [**q**$=(0,0.466,0)$]. Although the static moments for both phases ($\mu_s \simeq 0.6$ and $0.8\,\mu_B$) are considerably reduced compared to the effective moment deduced from high-temperature susceptibility data, they are well in line with the reduction of μ_s observed in other heavy-fermion local-moment magnets, owing to the Kondo effect. For CePtSn, T^* is estimated to be of the order 10 K.

Zero-field μSR studies on this system revealed unexpected features for the region around the magnetic transitions (see Fig. 54; Kalvius *et al.*, 1994). Down to 8.8 K,
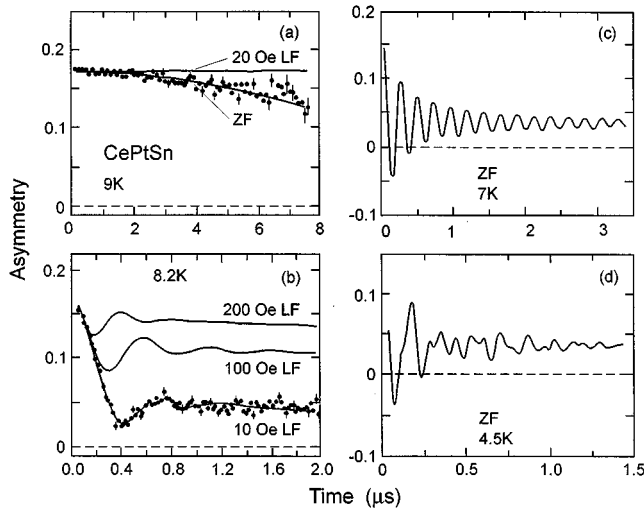
FIG. 54. Zero-field μSR spectra in CePtSn at various temperature below 9 K: (a) paramagnetic state; (b) static random order just above T_N; (c) and (d) coherent long-range order. As shown in (a) and (b), the static character of the field distribution at 8.2 K and 9 K is verified by decoupling experiments in longitudinal fields (from Kalvius et al., 1994).

the zero-field spectra are characterized by a fairly small depolarization rate, which can mostly be suppressed in a weak longitudinal field of 20 Oe. The static nuclear moments of ^{195}Pt prove to be the dominant contribution leading to μ^+ depolarization. The very weak remaining depolarization in longitudinal-field studies has to be traced back to fluctuating electronic moments on Ce^{3+} with $\nu_{4f} \gtrsim 10^{13}$ Hz. When lowering the temperature by a few tenths of a Kelvin, the zero-field signal shows a clear Kubo-Toyabe behavior, characterized by a rapid depolarization corresponding to a width of the field distribution of $\sqrt{\langle \Delta B^2 \rangle} \simeq 45$ G, which is two orders of magnitude larger than the field spread created by the ^{195}Pt nuclei above 8.8 K and therefore must arise from electronic moments. The static nature of the field distribution was demonstrated by the decoupling observed in longitudinal fields (Fig. 54). These results indicate that the long-range magnetic order is preceded just above T_N by a precursor state, where tiny electronic moments ($\mu_s \simeq 0.05\,\mu_B$) appear randomly oriented and static within the μSR time window.

When further lowering the temperature, the Kubo-Toyabe component decreases in intensity and is replaced by a spontaneous precession signal, characterized by a narrowly peaked frequency distribution that is fully developed around 7 K and reflects the long-range magnetic order. The interesting point revealed by the μSR data is that the magnetic transition is not sharply defined in temperature and different types of spectra can exist simultaneously. Furthermore, the static spin state just above T_N, characterized by the Kubo-Toyabe function, can be reached both by cooling and warming the sample. In view of these μSR results, Kalvius et al. (1994) questioned the classification of the magnetic transition as being of conventional second order. Moreover, following the observations in $CeAl_3$, $CeAl_2$, $CeCu_5$, and $CeCu_2Si_2$

(see above), the observation of a rather large spread of the magnetic transition temperature is an additional indication that inhomogeneous features are rather common among the heavy-fermion compounds.

The magnetic behavior observed by zero-field μSR just above T_N offers a simple explanation for the broad peak seen in the specific heat (Takabatake et al., 1993). The rise in C/T below 9 K could be ascribed to the random-spin freezing detected by μSR, whereas the step increase of C/T below 7.7 K reflects the onset of long-range order as observed by the concomitant occurrence of spontaneous μ^+ frequencies in the μSR signal.

The occurrence of a narrowly peaked frequency distribution in the μSR spectra for the upper magnetic phase appears incompatible with the claim of an incommensurate magnetic structure reported by neutron studies. On the other hand, the μSR data exhibit a drastic change of the coherent precession pattern below ~5 K (which contains at least three frequencies), in agreement with the occurrence of a second magnetic state suggested by the neutron-scattering results. However, the different components show again a small depolarization, in apparent contradiction with the complex incommensurate structure observed for the lower magnetic phase by neutron-scattering studies. In order to reconcile μSR and neutron-scattering data, and in analogy with the situation observed in Holmium and Erbium, Kalvius et al. (1994) suggested that magnetically ordered state of CePtSn is locally commensurate, but is interrupted by spin-slip defects that make the larger-scale structure incommensurate. A similar problem is observed for our next example, CePdSn.

b. CePdSn

The spin-glass precursor state above T_N observed in CePtSn does not have a counterpart in the parent system CePdSn (Kalvius et al., 1994). In CePdSn the transverse-field μ^+ depolarization rate shows a clear increase when lowering the temperature just above T_N, which was ascribed to the usual slowing down of the dynamical $4f$ fluctuations present down to T_N. Below $T_N \simeq 7.5$ K, zero-field studies indicate the presence of a spontaneous spin-precession signal. The beat structure of the μSR signal reveals the presence of two well-resolved frequencies associated with small depolarization rates (see Fig. 55). Again, this sharply defined field distribution is unexpected in view of the proposed incommensurate structure with propagation vector $\mathbf{q} = (0, 0.473, 0)$ deduced from neutron-scattering measurements (Kohgi et al., 1992). As for the upper magnetic phase of CePtSn (see above), this discrepancy has been tentatively explained in terms of spin-slip defects (Kalvius et al., 1994).

6. U_2Zn_{17}

This rhombohedral system (Th_2Zn_{17}-type structure; space group $R\bar{3}m$) undergoes an antiferromagnetic transition below 9.7 K, as shown by neutron-diffraction studies (Cox et al., 1986). The magnetic structure is consti-
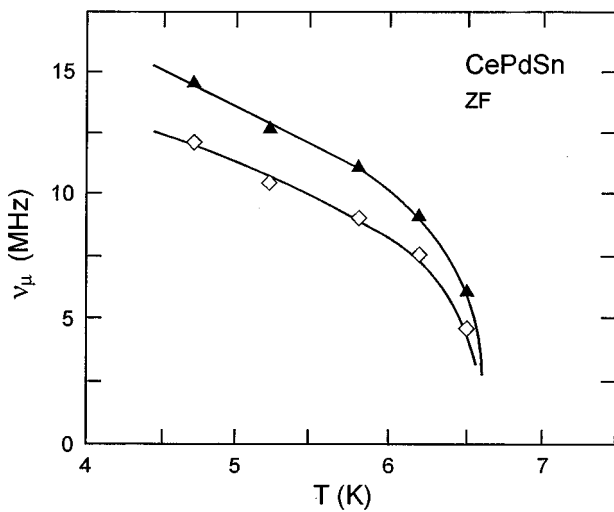
FIG. 55. Temperature dependence of the two spontaneous μ^+ frequencies observed below T_N in the zero-field μSR spectra of CePdSn (from Kalvius *et al.*, 1994).

tuted by ferromagnetic (110) planes coupled antiferromagnetically along the c axis, and with the U moments ($\mu_s \simeq 0.8\mu_B$) aligned in the (111) plane. In contrast to this rather simple picture, the μSR data obtained on this system have raised a number of questions that remain unsolved.

Zero-field μSR data show that the majority of the implanted muons stop at μ^+ sites where the dipole fields arising from the magnetic structure cancel below T_N (Barth *et al.*, 1986). From the observed temperature and angular dependence of the high temperature μ^+ Knight shift for the principal components of the transverse-field μSR signal, one deduces that indeed the c site (with $x = \frac{1}{3}$ and $x = \frac{1}{6}$), for which the dipole fields cancel is occupied (Barth, 1988). However, zero-field and transverse-field μSR measurements also show that about 25% of the amplitude of the μSR signal is lost when cooling the sample below T_N. This loss of amplitude is ascribed to the occurrence of a huge static-field spread below T_N in part of the sample, or at a particular μ^+ site, which leads to a rapid depolarization occurring within the deadtime of the μSR spectrometer ($\sim 2 \times 10^{-8}$ s). Longitudinal-field measurements yield a value of about 1000 G (for $T \rightarrow 0$) for the width of the internal-field distribution responsible for this rapid μ^+ depolarization, which is fully unexpected on the basis of the simple antiferromagnetic structure determined by neutron scattering. Since very similar results are obtained in polycrystalline and monocrystalline samples, as well as for measurements utilizing low- and high-energy muons probing different regions of the samples, it is believed that the observed effect reflects intrinsic properties of the system. This suggests the formation of a rather complex magnetic structure unlike that deduced from neutron studies.

More puzzling is the observation that the same fraction of the muon ensemble, which undergoes the fast depolarization below T_N, exhibits a highly peculiar behavior above T_N, as observed in transverse-field measurements (Schenck *et al.*, 1992). This fraction is associated with at least three components exhibiting a highly unusual angular dependence of the μ^+ Knight shift, involving direction cosines up to the eighth order. Such angular dependence cannot be generated by dipole fields from the field-induced U moments [see Eq. (18)], which do not involve direction cosines higher than the second order. It is therefore suggested that the peculiar angular dependence of this fraction results from a competition between the Zeeman and some additional interaction. In this context, the questions to be solved are why such competition is only observed by a restricted portion of the muons, and in which way this competition is connected to the complex magnetism seen by this particular fraction of the muon ensemble.

Obviously the properties of U_2Zn_{17}, as evidenced by the μSR data, reveal complex subtleties that are at present not understood at all. It is to be hoped that additional experimental and theoretical studies will provide a deeper insight into this peculiar heavy-fermion system.

7. UNiB$_4$

This hexagonal system crystallizes in the hexagonal $CeCo_4B$-type structure (space group $P6/mmm$) and undergoes an antiferromagnetic transition at $T_N \simeq 20$ K. The magnetic structure is quite unique, exhibiting the ordering of only $\frac{2}{3}$ of the spins with wave vector $\mathbf{q} = (\frac{1}{3}, \frac{1}{3}, 0)$ and moment direction in the basal plane (Mentink *et al.*, 1994). These spins align in hexagonal structures in the basal plane that are ferromagnetically coupled along the c axis. The spins in these hexagonal structures have orientation $150°$, $90°$, $30°$, $-30°$, $-90°$, and $-150°$. The remaining $\frac{1}{3}$ of the spins are fully frustrated and are located in the center of and in between the hexagonal structures.

Zero-field μSR studies confirmed the presence of a magnetic state below $T_N = 20$ K by detecting the occurrence of a rapid depolarization [$\Delta(T \rightarrow 0) \simeq 27$ μs^{-1}], with the initial μ^+ polarization aligned either along the c axis or in the basal plane (Nieuwenhuys *et al.*, 1995). This rapid depolarization, which reflects static magnetism, as proven by longitudinal-field experiments, has to be traced back to the highly complicated magnetic structure producing a large field spread at the μ^+ stopping sites. When the initial μ^+ polarization is directed along the c axis, in addition to the component showing rapid depolarization, a second component with reduced amplitude, representing a spontaneous precession behavior is detected. This latter component was tentatively attributed to muons stopping at the f sites ($\frac{1}{2}00$) surrounding a frustrated U moment inside one of the hexagonal structures. Indeed, such a site was found to be occupied, together with the n site, by hydrogen ions in the isostructural compound $LaNi_4B$ (Spada *et al.*, 1984).

Figure 56 exhibits the temperature dependence of the normalized results for the observed spontaneous μ^+ frequency and depolarization rate, together with the ordered moment deduced from neutron diffraction. No anomaly is detected around 10 K, where the magnetic
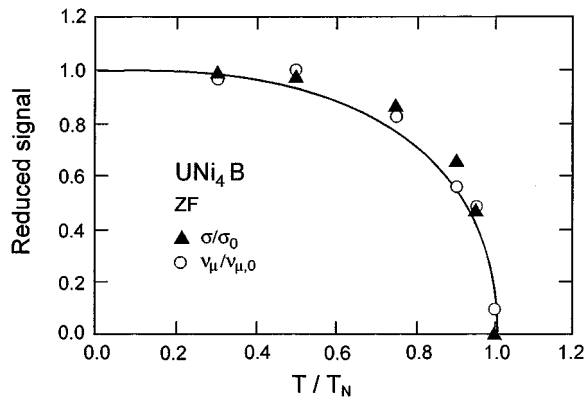
FIG. 56. Plot as a function of T/T_N of the reduced values of the spontaneous μ^+ frequency and depolarization rate measured on a monocrystalline UNi$_4$B sample with the initial μ^+ polarization along the c axis. The line represents the ordered moment as deduced by neutron diffraction (from Nieunwenhuys et al., 1995).

susceptibility and specific heat show a maximum, which supports the conclusions that no additional magnetic phase or reorientation of the U moments arises below T_N. Accordingly, the peculiar temperature dependence of the macroscopic properties below T_N were explained by Mentink et al. (1994) to result from the summation of one-dimensional ferromagnetic spin waves ($\frac{1}{3}$ of the moments) and those of a three-dimensionally ordering antiferromagnet (the remaining $\frac{2}{3}$ of the moments).

8. UCd$_{11}$

UCd$_{11}$ crystallizes in the cubic BaHg$_{11}$ structure (space group $Pm\overline{3}m$) and exhibits a magnetic order at $T_N\simeq5$ K but with a still unknown magnetic structure.

Zero-field and transverse-field μSR measurements (Barth et al., 1986) showed a loss of the μSR signal below T_N, which was ascribed to the development of a huge internal-field spread (several 100 G) seen by the muons. As in the case of U$_2$Zn$_{17}$ (see Sec. IV.B.6), this huge field spread leads to a very rapid μ^+ depolarization within the deadtime of the μSR spectrometer. Such a large field distribution could reflect either a complicated magnetic structure, or, alternatively, a high number of magnetically inequivalent μ^+ stopping sites in the magnetic unit cell. This latter hypothesis is quite reasonable in view of the rather complex crystallographic structure, which provides a large number of possible interstitial μ^+ sites. Regardless of the exact magnetic structure, the huge field spread indicates that the ordered U moments must be of the order of ~1 μ_B.

Unlike the situation of the other heavy-fermion compounds, the $5f$ spin fluctuations could be observed above T_N in longitudinal-field experiments (see Fig. 57). The μ^+ depolarization rate λ_{LF}, which reflects the spin-lattice relaxation $1/T_1$, follows a power law

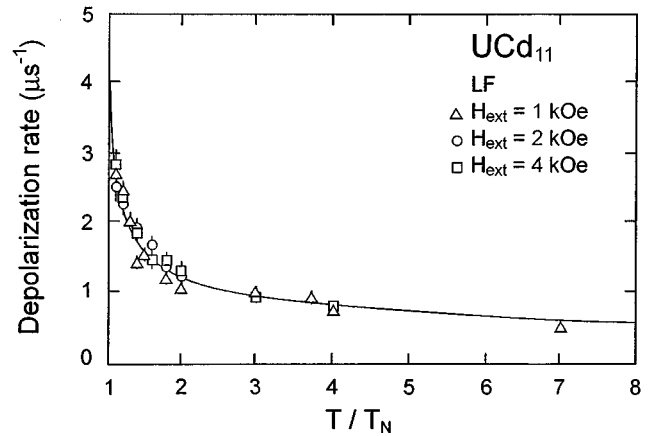$$\lambda_{LF,T>T_N} = \frac{1}{T_1} \propto (T-T_N)^{-(0.4\pm0.1)}, \tag{48}$$

FIG. 57. Temperature dependence of the spin-lattice relaxation rate $1/T_1 = \lambda_{LF}$ in UCd$_{11}$. Note that λ_{LF} is independent of the longitudinally applied magnetic field. The solid line represents a fit of Eq. (48) to the data (from Barth et al., 1986).

which implies that for $T \gg T_N$ the $5f$ spin-fluctuation rate varies as $\nu_{5f} \propto \sqrt{T}$, with an estimation of $\nu_{5f} \simeq 10^{10}$ Hz for $T = 2/T_N$. As already noticed by Schenck (1993), this dependence, which is consistent with the theory of Cox et al. (1985), is typical for Kondo lattices and is observed by NMR and inelastic neutron scattering in numerous systems (see, for example, Qachaou et al., 1987). It is believed that in the particular case of UCd$_{11}$, the relative closeness between the μ^+ and the nearest U neighbors provides a strong enough hyperfine coupling constant to render possible the observation of the $5f$ spin dynamics within the μSR time window.

9. Other U-based heavy-fermion local-moment magnets

As we saw in Sec. III.C, the antiferromagnetic transition observed in UPd$_2$Al$_3$ involves a rather large value of the static U moment ($\mu_s \simeq 0.85$ μ_B) and a transition temperature $T_N \lesssim T^*$. These observations indicate that the magnetic state involves localized f moments. The same conclusion can be drawn regarding the high-temperature magnetic phase of UCu$_5$ (see Sec. IV.A.4). However, for both systems the local-moment magnetism is found by μSR to microscopically coexist with a more itinerant subset of heavy quasiparticles, which present an additional instability at lower temperature (superconductivity for UPd$_2$Al$_3$ and heavy-fermion band magnetism (HFBM) for UCu$_5$). This strongly suggests that, whereas part of the f moment is frozen out below T_N by the static magnetic intersite correlations, another part continues to present on-site fluctuations characteristic of the Kondo effect, which results in the formation of the heavy quasiparticles, which, in turn, are involved in the low-temperature phase transitions.

V. FERMI-LIQUID PARAMAGNETS

The detection by μSR of weak static magnetism in such heavy-fermion systems as CeAl$_3$ or CeRu$_2$Si$_2$, which were long considered to be examples of a para-

magnetic Fermi liquid, has considerably modified the phenomenological classification of the heavy-fermion compounds. Hence the paramagnetic Fermi-liquid ground state once considered to be predominant suddenly appeared to be only an exception at best. It was therefore considered of some importance to investigate by microscopic techniques the few remaining heavy-fermion compounds still classified as paramagnetic and to search for the possible occurrence of heavy-fermion band magnetism with reduced ordered moments, which could appear as a common feature among the heavy-fermion compounds.

A. CeCu$_6$

Since its classification as a heavy-fermion compound (Ō nuki *et al.*, 1984; Stewart *et al.*, 1984), CeCu$_6$ has attracted considerable experimental attention. The key role played by this orthorhombic system (space group *Pnma*) was generated by the possibility of growing large single crystals. Furthermore, since the discovery of a magnetic transition in CeAl$_3$, and in an increasing number of other heavy-fermion systems (see Sec. IV), CeCu$_6$ has been considered the archetypical example of a heavy-fermion system with normal ground state. Nevertheless, CeCu$_6$ seems on the verge of magnetic ordering, as it exhibits, for example, dynamical short-range magnetic correlations below 10 K (Regnault *et al.*, 1987). Moreover, some properties point to the occurrence of some kind of magnetic anomaly. The magnetoresistivity shows a maximum for $T<0.5$ K (Ō nuki *et al.*, 1985), as observed also in magnetic heavy-fermion systems such as CeAl$_3$, and a sudden change in slope occurs in the thermoelectric power near 250 mK (Amato *et al.*, 1987).

The μ^+ stopping site was determined by measuring the angular dependence of the μ^+ frequency ν_μ, as well as its temperature dependence, in an external transverse field of $H_{ext}=5$ kOe. Figure 58 shows the angular dependence of ν_μ for $\mathbf{H}_{ext}$ rotated in the (101) plane. The presence of two symmetrical signals of identical amplitude is indicative of crystallographically equivalent but magnetically inequivalent μ^+ sites. Figure 59 shows the μ^+ Knight shift as a function of the macroscopic magnetic susceptibility for the principal directions. From the observed scaling, which indicates that the atomic susceptibility probed by the muon is identical to the macroscopic susceptibility, one can extract the dipolar and contact hyperfine coupling constants ($A_{dip}^{xx}=0.89$ kG/μ_B, $A_{dip}^{yy}=-0.10$ kG/μ_B, $A_{dip}^{zz}=-0.79$ kG/μ_B, and $A_{cont}=0.17$ kG/μ_B). Among all the possible interstitial sites, only the site $(00\frac{1}{2})$ (*b* site, multiplicity 4) has a compatible theoretical value for $\vec{A}_{dip}$ ($A_{dip,theor}^{xx}=0.97$ kG/μ_B, $A_{dip,theor}^{yy}=-0.11$ kG/μ_B, and $A_{dip,theor}^{zz}=-0.86$ kG/μ_B) and splits into two subsets of magnetically inequivalent sites when $\mathbf{H}_{ext}$ is rotated in the (101) plane.

μSR zero-field measurements down to 40 mK show no sign of a magnetic transition, such as a spontaneous μ^+ frequency and/or additional depolarization arising from a change in the dynamics of the 4f moments (Amato, Feyerherm, Gygax, Jaccard *et al.*, 1993). Figure
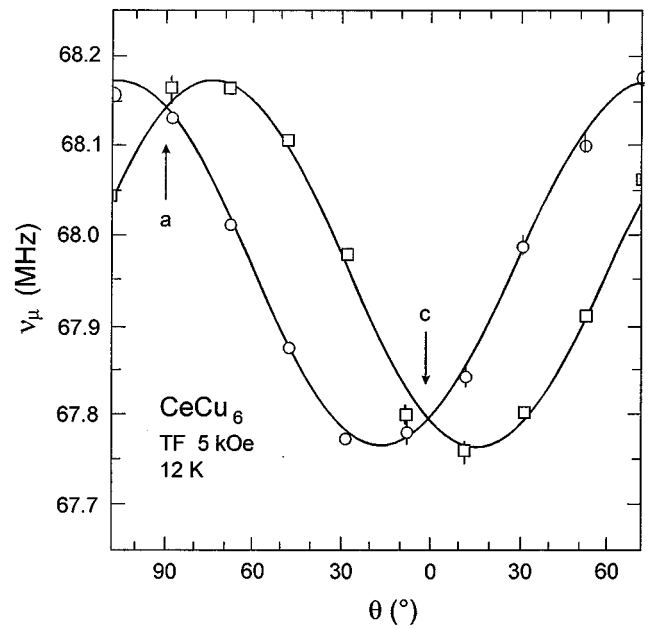

FIG. 58. Measurement at 12 K of the angular dependence of the μ^+ frequency ν_μ with the external field rotated in the (101) plane ($H_{ext}=5$ kOe). Two components of similar amplitude are detected in the μSR signal.

60 exhibits an example of a μSR spectrum recorded at 2.2 K together with a fit to a Kubo-Toyabe function. Measurements in longitudinal fields did not reveal any μ^+ depolarization, indicating that the linewidth of the zero-field signal is exclusively quasistatic in origin with fluctuation rates, if present, smaller than 1 MHz. The value of the zero-field μ^+ depolarization rate ($\Delta\simeq0.23$ μs^{-1}) is, moreover, compatible with the calculated linewidth only due to dipolar fields from ^{63}Cu and ^{65}Cu nuclear moments at the *b* site and is temperature independent down to at least 40 mK (see Fig. 61). The ob-
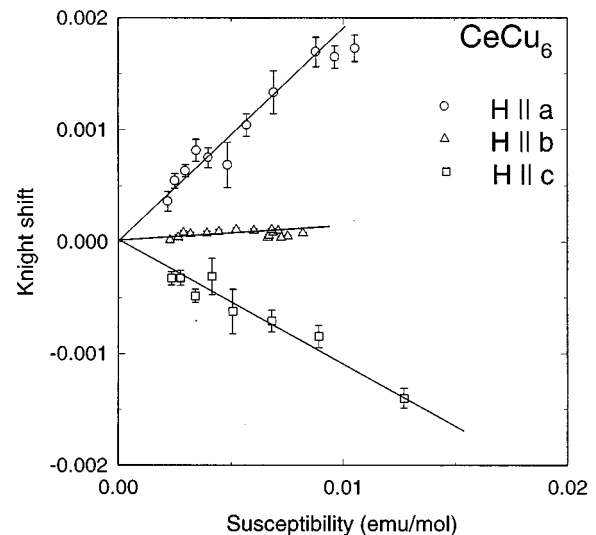

FIG. 59. Plot of the μ^+ Knight shift measured in CeCu$_6$ for the principal directions as a function of the bulk susceptibility. The temperature is an implicit parameter.
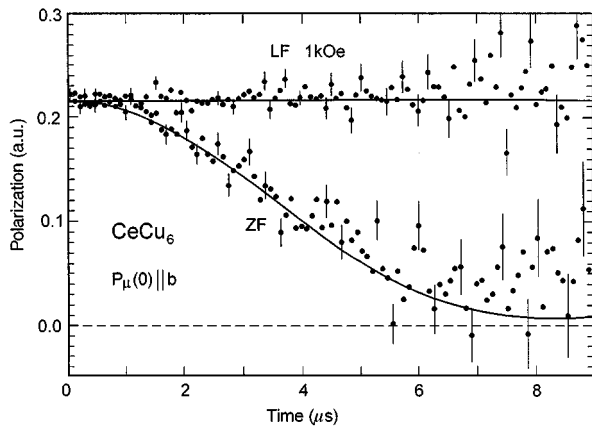
FIG. 60. Time evolution of the μ^+ polarization in CeCu$_6$ at 2.2 K with $\mathbf{P}_\mu(0)\|\mathbf{b}$. Lower curve: Zero-field data with a Kubo-Toyabe fit; upper curve: longitudinal-field data with $H_{\text{ext}}=1$ kOe (from Amato, Feyerherm, Gygax, Jaccard *et al.*, 1993).

servation of a constant depolarization rate for the whole temperature range sets an upper limit of $\Delta_{4f}\simeq 0.10\ \mu s^{-1}$ for an additional depolarization due to a hypothetical magnetic ordering of the Ce $4f$ moments. Considering for the hypothetical magnetic ordering the incommensurate magnetic structure observed for CeCu$_{5.5}$Au$_{0.5}$ (see Sec. VI.A.2), the upper limit of Δ_{4f} represents an upper limit of $3\times 10^{-3}\ \mu_B$/Ce for a static $4f$ moment. Assuming, on the other hand, a dense-spin-glass picture where the static moments are randomly oriented, an upper limit of $1.5\times 10^{-3}\ \mu_B$/Ce is obtained.

Therefore the μSR data virtually exclude the presence of magnetic order and confirm that CeCu$_6$ plays quite a unique role among the heavy-fermion compounds by possessing a paramagnetic ground state and clear Fermi-liquid properties at low temperature.
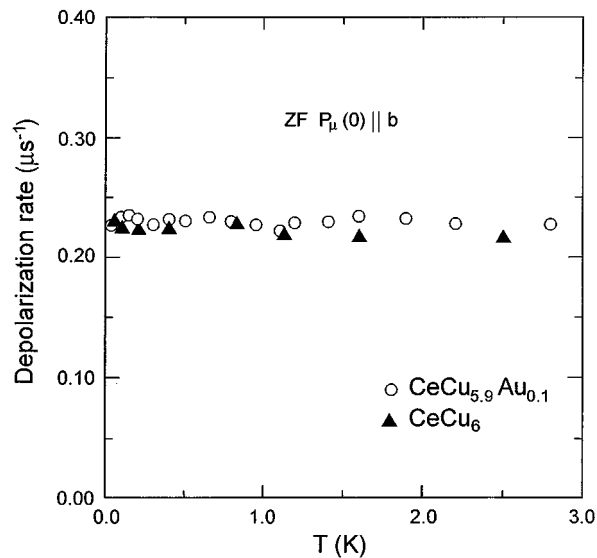

FIG. 61. Temperature dependence of the zero-field depolarization rate in pure CeCu$_6$ and CeCu$_{5.9}$Au$_{0.1}$ (see Sec. VI.A.2). The error bars are smaller than the data-point size (from Amato *et al.*, 1995).

B. CePt$_2$Sn$_2$

As stated above, the class of heavy-fermion compounds with paramagnetic ground state is quite limited, and until recently CeCu$_6$ was still the only heavy-fermion compound for which the paramagnetic ground state was confirmed by μSR technique. Recent μSR measurements in the system CePt$_2$Sn$_2$ (Luke *et al.*, 1995) seem nevertheless to reveal that CeCu$_6$ does not constitute an accident of nature and that other systems could present a similar ground state. However, the situation of CePt$_2$Sn$_2$ is still controversial, and conflicting results were reported.

Beyermann, Hundley, Canfield, Thompson, Latroche *et al.* (1991) and Beyermann, Hundley, Canfield, Thompson, Fisk *et al.* (1991) reported specific-heat, magnetic-susceptibility, and resistivity measurements of CePt$_2$Sn$_2$ and inferred antiferromagnetic order below $T_N=0.88$ K from a peak in the specific heat. For the investigated polycrystalline sample, the nominally tetragonal crystal structure (space group $P4/nmm$) has undergone a monoclinic distortion. The value of the linear coefficient of the electronic specific heat $\gamma \simeq 3.5$ J/(K^2 mol) measured above the reported magnetic transition is one of the largest ever observed and is consistent with the value of $T^*\simeq 1$ K reported from quasielastic neutron-scattering studies (Mignot *et al.*, 1993).

This rather clear picture was challenged by specific-heat results obtained on a single crystal in which the monoclinic distortion was absent (Shigeoka *et al.*, 1993). No evidence for magnetic order could be detected, suggesting that the lattice distortion may promote magnetic order.

To obtain additional information, μSR studies were recently undertaken on a monocrystalline sample without monoclinic distortion (Luke *et al.*, 1995). Zero-field studies indicate that at high temperature the Gaussian μ^+ depolarization rate is solely due to the static, randomly oriented ^{195}Pt nuclear dipole moments. By lowering the temperature, an additional exponential depolarization is detected, which is only weakly affected by applied longitudinal fields less than 1 kOe. This therefore indicates that fluctuating moments of electronic origin are responsible for this depolarization. Figure 62 shows the longitudinal-field depolarization rate λ_{LF}. Upon cooling the first increase of λ_{LF} corresponds to the narrowing of the quasielastic linewidth seen in neutron-scattering experiments [see also Eq. (48)] and reflects the Kondo spin fluctuations. The first saturation of λ_{LF}, corresponding to the temperature where the fluctuation rate of the f spin saturates, was taken as an estimation of T^* ($\simeq 20$ K), which is considerably larger than the value extracted from neutron scattering. Alternatively, the occurrence of a temperature-independent μ^+ depolarization rate could indicate that another mechanism for the f-spin fluctuations becomes dominant at lower temperatures. Since the overall f spin-fluctuation rate ν_f mainly reflects the faster fluctuation-rate mechanism according to $\nu_f=\Sigma\nu_i$, the slow Kondo fluctuations at low temperature could therefore be dominated by a faster and
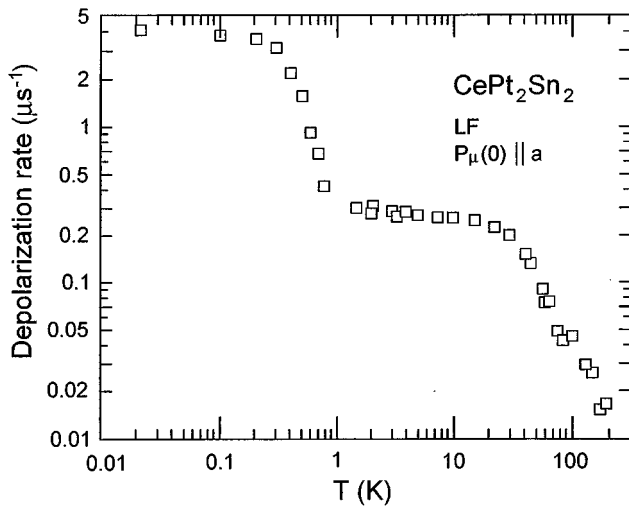
FIG. 62. Temperature of the longitudinal-field μ^+ depolarization rate (H_{ext}=100 Oe) measured in $CePt_2Sn_2$ with the initial μ^+ polarization along the a axis (from Luke et $al.$, 1995).

temperature-independent mechanism. The RKKY interaction between the f spins leads effectively to a temperature-independent spin-fluctuation rate given by

$$\nu_{RKKY} = \frac{1}{\tau_{RKKY}} = \frac{1}{9\hbar} \left(\frac{\pi}{6} (g_J - 1)^2 J(J+1) \right)^{1/2} N(E_F) \mathcal{J}^2 \tag{49}$$

(Kumagai et $al.$, 1981), where g_J is the Landé factor. Hence the $CePt_2Sn_2$ results could represent an example of the possibility of detecting by μSR the crossover between two different mechanisms responsible for the f-spin fluctuations.

Below 1 K (i.e., at a similar temperature as T_N observed by specific heat, see above), the further increase of λ_{LF} indicates a slowing down of the f moments. The fact that the depolarization rate is only weakly affected by a longitudinal field of 1 kOe demonstrates that the origin of the depolarization still has a dynamical character at low temperature. However, and in contrast to the high-temperature situation, decoupling experiments in high fields showed that the moments are fluctuating rather slowly. It therefore appears that below 1 K there is a tendency for the moments to try to order, but spin freezing is somehow prevented and slow fluctuations continue down to millikelvin temperatures.

In view of the μSR results, the observation via the specific heat of static magnetism in a $CePt_2Sn_2$ sample with monoclinic distortion suggests that the distortion may promote magnetic order, perhaps by removing a geometrical frustration of the spins. Without distortions, the presence of geometrical frustrations leads to slow fluctuations persisting for $T \to 0$.

It is worth mentioning that $CePt_2Sn_2$ samples without an indication of static magnetism show a rapid increase of the ratio C/T at low temperature. The concomitant presence of a large C/T ratio and the proximity of magnetic order is strongly reminiscent of the situation observed for heavy-fermion compounds showing non-Fermi-liquid behavior (see Sec. VI.A), where an

invoked explanation for the large specific heat at low temperature is based on the potential presence of low-lying collective spin excitations connected with a zero-temperature phase transition. It is therefore suggested that additional investigations should be undertaken on $CePt_2Sn_2$ with the specific goal to test for the presence of a ground state with non-Fermi-liquid behavior.

Although μSR results show that $CePt_2Sn_2$ and $CeCu_6$ possess a paramagnetic ground state, the origins for the absence of magnetism in both compounds are probably conceptually very different, involving possibly frustrations for $CePt_2Sn_2$ and the presence of a paramagnetic Fermi-liquid state for $CeCu_6$.

The confirmation by μSR, of the existence of heavy-fermion systems possessing a purely paramagnetic ground-state represents more than simple measurements with anecdotal character. Thus such an observation appears to support the simple model, described in Sec. I, for which the properties of the majority of the heavy-fermion systems are explained within a Landau Fermi-liquid framework, where a one-to-one correspondence between the excitations of the complex metallic systems and those of a free-electron gas with strongly renormalized parameters is assumed to exist.

VI. "EXOTIC" HEAVY-FERMION CLASSES

A. Non-Fermi-liquid behavior

As discussed in Sec. I, the observations of a large linear coefficient of the electronic specific heat, a large Pauli-like susceptibility, and a T^2-dependent electrical resistivity are usually considered as characteristic features of the heavy-fermion compounds. A recently discovered class of heavy-fermion compounds with unconventional low-temperature properties is attracting increasing interest. For the systems belonging to this class, opposite of what was discussed at the end of the previous section, transport and thermodynamic measurements indicate that the Fermi-liquid description does not apply. One observes, for example, a logarithmic divergence of the specific heat [i.e., $C/T \propto -\ln(T/T_0)$] and a linear dependence of the electrical resistivity, which are both taken as signatures of non-Fermi-liquid behavior. Considerable discussion has taken place about the source of such behavior, and conceptually different origins have been invoked.

A two-channel quadrupolar Kondo effect has been considered, where the quadrupolar moment of the f ion interacts with the conduction electrons and the spin of the conduction electrons provides the two available channels (D. L. Cox, 1987). This single-impurity effect has been shown to be possibly present in systems where the U ions are in a $5f^2$ configuration and also in Ce-based systems with hexagonal and cubic symmetry (Cox, 1993). Another possible origin of the non-Fermi-liquid behavior is based on the suggestion that a paramagnetic and a magnetically ordered ground state are practically degenerate, leading to a quantum phase transition at zero temperature (Löhneysen et $al.$, 1994). Finally, it

was also proposed that a non-Fermi-liquid behavior might arise, in a single-impurity model, from a distribution of Kondo temperatures in disordered systems (Dobrosavljevic *et al.*, 1992).

In the following we present the main conclusions obtained by μSR, where this method has been mainly utilized to check for the complete absence of static magnetism in the non-Fermi-liquid regime.

1. $Y_{1-x}U_xPd_3$

The cubic system $Y_{1-x}U_xPd_3$ (space group $Pm3m$) displays a variety of magnetic behaviors ranging from localized f moments characteristic of $x=1$ (note that UPd_3 has a dhcp hexagonal structure with space group $P6_3/mmc$), to spin-glass behavior for $0.5 \gtrsim x \gtrsim 0.3$ (Seaman *et al.*, 1992). On the other hand, the alloy $Y_{0.8}U_{0.2}Pd_3$ was the first system for which the magnetic susceptibility and specific-heat data have been interpreted in terms of a non-Fermi-liquid behavior arising from a two-channel quadrupolar Kondo effect (Seaman *et al.*, 1991). μSR experiments were undertaken to study the crossover, and possible connection, between spinglass order and the non-Fermi-liquid state (Wu *et al.*, 1994).

Zero-field experiments at low temperature on alloys with $x=0.4$ and 0.75 show a sharp decrease of the μ^+ polarization at early time, followed by a minimum and a $\frac{1}{3}$ recovery.[5] This recovery is a clear signature of a spinglass order.

In canonical spin-glass systems, such as $\underline{Au}Fe$ or $\underline{Cu}Mn$, the μ^+ depolarization, below the freezing temperature T_g and for short times, assumes an exponential form arising from the fact that the total distribution of the local fields has a Lorentzian character. This Lorentzian distribution is obtained by assuming a Gaussian distribution (with a width Δ/γ_μ) at each muon site and a Gaussian distribution $\rho(\Delta)$ of the values of Δ to account for different ranges of magnetic fields at different muon sites. On the other hand, for dense spin-glass systems, the total distribution of the local fields can be represented by a Gaussian distribution, since all the μ^+ stopping sites have similar magnetic environments. A Kubo-Toyabe μ^+ depolarization function [Eq. (26)] is therefore expected for dense spin glasses below T_g.

The U concentrations in the $Y_{0.6}U_{0.4}Pd_3$ and UPd_4 alloys lie between the above described two limiting cases, so a modified probability function $\rho(\Delta)$ had to be adopted (for more details, see Wu *et al.*, 1994). Figure 63 shows the half width at half maximum (HWHM) of the thus obtained internal-field distribution, together with the freezing temperature, as a function of the U concentration. For the U concentrations $x=0.1$ and $x=0.2$ only a reduced portion of the samples (~10% and ~40%, respectively) show the occurrence of static magnetism.
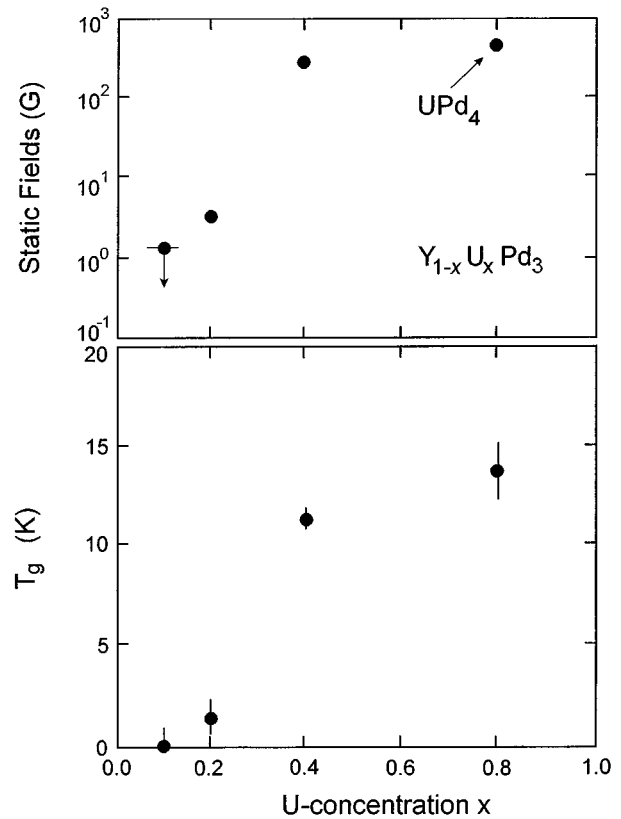

FIG. 63. Zero-field μSR measurements on UPd_4 and $Y_{1-x}U_xPd_3$. *Upper part:* Low-temperature width of the static random fields as a function of the U concentration x. *Lower part:* Magnetic phase diagram (freezing temperature) determined by μSR (from Wu *et al.*, 1994).

The sharp decrease of the HWHM of the static-field distribution and of the freezing temperature, when lowering the U concentration, indicates the disappearance of spin-glass order around the threshold concentration of $x=0.2$. The large nonmagnetic fractions for $x \lesssim 0.2$ can be taken as evidence for the existence of a nonmagnetic Γ_3 ground state, which is confirmed by neutronscattering data (Mook *et al.*, 1993). As stated above, such a nonmagnetic ground state is required for a twochannel quadrupolar Kondo effect, which could explain the non-Fermi-liquid behavior in these systems. On the other hand, the μSR data confirm that the systems exhibiting non-Fermi-liquid behavior are close to a magnetic instability, which in this case is spin-glass freezing. In accordance with the approximate scaling functions shown by the specific heat and the magnetization in magnetic field, this proximity indicates that a single-ion quadrupolar Kondo effect is not the source of the nonFermi-liquid behavior in $Y_{1-x}U_xPd_3$. Hence no definitive conclusions can be drawn at the moment. Nevertheless, Löhneysen (1995) noted that the presence of nonFermi-liquid behavior for a variety of samples (i.e., for $x \lesssim 0.3$), regardless of their proximity to magnetic order or not, is a strong indication that the quadrupolar Kondo effect must be the cause of this effect. However, it remains to be seen whether the occurrence of non-

---

[5]The 0.75 concentration is obtained with a UPd_4 sample possessing the same cubic structure with stoichiometry $\bigcirc_{0.25}U_{0.75}Pd_3$, where $\bigcirc$ represents a vacancy.

Fermi-liquid behavior for different U concentrations is an intrinsic characteristic or might be related to small distributions of local U concentration. In this vein, Süllow (1994) has demonstrated, via detailed metallurgical analysis, that compounds with $x \lesssim 0.2$ are intrinsically inhomogeneous.

2. CeCu$_{6-x}$Au$_x$

This alloy has been extensively investigated, since, according to symmetry-based selection rules (Cox, 1993), a two-channel Kondo effect should be absent.

As stated in Sec. V.A, CeCu$_6$ has a paramagnetic ground state, but the substitution of Cu by atoms of larger atomic radius (e.g., Au) expands the lattice and therefore weakens the exchange interaction, leading to the stabilization of the local f magnetic moment against the formation of local Kondo singlets (see, for example, Germann *et al.*, 1988). For $x = 0.1$ (CeCu$_{5.9}$Au$_{0.1}$), the magnetic order is suppressed to zero temperature, and the nonmagnetic and magnetic ground states are degenerate (i.e., $g = g_c$, see Fig. 2; Löhneysen *et al.*, 1994). The observation of non-Fermi-liquid features in CeCu$_{5.9}$Au$_{0.1}$ seems therefore to arise from the proximity of the magnetic ordering occurring for $x > x_c \simeq 0.1$ and points to a quantum phase transition between magnetic and nonmagnetic ground states at zero temperature.

Zero-field μSR measurements were undertaken to check, by microscopic technique, for the complete absence of static magnetism for $x \rightarrow x_c$. Measurements performed down to 20 mK fail to detect any clear magnetic transition. For all the investigated temperatures, the time evolution of the μ^+ polarization is best described by a Kubo-Toyabe function [Eq. (26)], which is characteristic of a paramagnetic ground state, where the μ^+ depolarization is solely due to the dipolar fields from the nuclear moments (mainly ^{63}Cu and ^{65}Cu).

Although the Au ions substituting the Cu ions expand the lattice and possess a strongly reduced nuclear moment, the measured values of the μ^+ depolarization rate Δ of the Kubo-Toyabe function are identical in CeCu$_{5.9}$Au$_{0.1}$ and in CeCu$_6$ (see Fig. 61). This similarity results from the fact that for $x \leqslant 1$ the Au atoms exclusively occupy the Cu(2) sites (Ruck *et al.*, 1993), which are not located in the vicinity of the μ^+ site $(00\frac{1}{2})$ and therefore only marginally contribute to the field distribution at the μ^+ site. The main components of this field distribution arise firstly from the Cu atoms located at the Cu(5) sites and secondly from those located at the Cu(1) sites. Assuming a small, local-lattice relaxation around the μ^+ deduced from the Knight-shift data, one calculates for pure CeCu$_6$ (see Sec. V.A) a theoretical value of $\Delta = 0.246$ μs^{-1} for the μ^+ depolarization rate at the b site, which is in fairly good agreement with the measured value. With the observed linear variation of the lattice parameters between $x = 0$ and $x = 1$ (Schröder, Lynn *et al.*, 1994), one calculates for $x = 0.1$ an almost negligible decrease of 0.4% for the second moment of the local-field distribution at the μ^+ site, which corre-

sponds to a change of the μ^+ depolarization rate smaller than the experimental resolution.

Regardless of the subtle contributions to the depolarization rate, the complete absence of spontaneous Larmor frequencies in the first place and/or of a clear change of behavior of the depolarization rate in the μSR signal of CeCu$_{5.9}$Au$_{0.1}$ strongly supports a nonmagnetic ground state for this alloy. Since, as stated above, a two-channel quadrupolar Kondo effect is very unlikely for this orthorhombic structure, and keeping in mind that for $x > x_c$ clear signs of static magnetism are observed by macroscopic techniques, the μSR data appear compatible with the suggestion that the non-Fermi-liquid behavior reported in CeCu$_{5.9}$Au$_{0.1}$ occurs in the proximity of magnetic order.

Although more systematic μSR experiments should be undertaken on other systems exhibiting non-Fermi-liquid behavior, the μSR studies described above for CeCu$_{5.9}$Au$_{0.1}$ and Y$_{1-x}$U$_x$Pd$_3$ are compatible with a picture where the magnetic transition is suppressed to zero temperature. Within this picture, the $T \ln T$ dependence of the specific heat and T dependence of the electrical resistivity would arise from the presence of low-lying collective-spin excitations near the zero-temperature phase transition. Although phenomenological models of non-Fermi-liquid behavior resulting from a critical point at $T = 0$ have been proposed recently (see, for example, Tsvelik and Reizer, 1993), more theoretical work lies ahead to understand the collective effect arising from a zero-temperature phase transition.

B. Rare-earth heavy-fermion compounds with low carrier density

This class of heavy-fermion compounds is attracting a growing interest particularly in connection with the high-T_c CuO$_2$ layered systems which, in many respects, appear to possess similar properties (see, for example, Kasuya *et al.*, 1993).

For this class of heavy-fermion systems, the non-f reference compounds are usually either semimetals or narrow-gap semiconductors, and, as a consequence, the f systems exhibit extremely low carrier concentrations $[n_e \lesssim 10^{-2}/(f \text{ atom})]$. Although the number of conduction electrons available to interact with the localized f moments is strongly reduced, some of these systems present close similarities with the more traditional, metallic heavy-fermion systems. Gigantic C/T ratios are, for example, observed, and this raises the basic problem of the nature of the degree of freedom giving rise to the low-energy excitations underlying the large linear contribution to the specific heat. These observations have led to speculations about the presence of a many-body Kondo resonance within the band gap or the occurrence of magnetic transitions at very low temperature. Hence, for this class of compounds, μSR was specifically utilized as a check on such speculations, due to its high sensitivity to static magnetism.
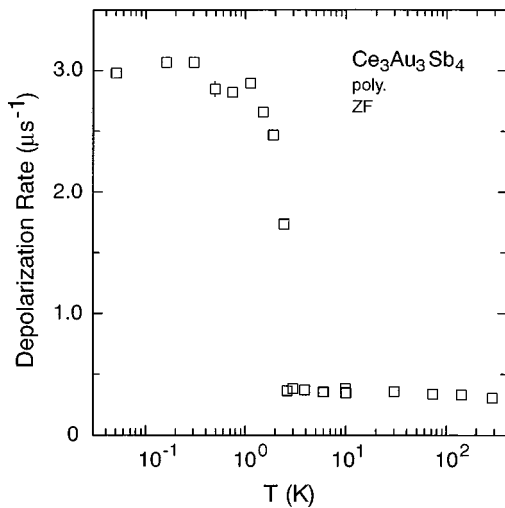
FIG. 64. Temperature dependence of the zero-field μ^+ depolarization in polycrystalline $Ce_3Au_3Sb_4$. The depolarization function is represented at all the temperatures by a Gaussian relaxing function (see text; from Amato, 1995b).

1. $Ce_3Au_3Sb_4$

The cubic system $Ce_3Au_3Sb_4$ ($Y_3Au_3Sb_4$ structure, space group $I\bar{4}3d$) is a narrow-gap semiconductor with the Ce atoms in a well-defined $4f^1$ state (Kasaya et al., 1991). Specific-heat data at low temperature exhibit the presence of a clear peak for $T \lesssim 3$ K [leading to a ratio $C/T(T \to 0) \simeq 2.5$ J/(K^2 mol)], attributed to the occurrence of a Kondo resonance within the band gap (Kasaya et al., 1994).

Zero-field μSR measurements have recently been undertaken to gain more insight into the nature of such specific-heat anomalies (Amato, 1995b). The μ^+ depolarization function is represented at all temperatures by a Gaussian function $G(t) = \exp(-\sigma^2 t^2/2)$, for which the temperature dependence of the depolarization parameter σ is reported in Fig. 64. Above 2.5 K the depolarization function is due to the dipolar fields of the ^{121,123}Sb nuclei. (For these temperatures the Gaussian function represents the short-time behavior of the expected Kubo-Toyabe function [see Eq. (26)] with the correspondence $\sigma = \Delta \cdot \sqrt{2}$.) Below about 2.5 K the dramatic increase of the depolarization rate (which reaches ~ 3 μs^{-1} for $T \to 0$) represents the development of quasistatic magnetic moments of electronic origin supposedly randomly oriented, which creates a field distribution with zero average at the μ^+ site. The depolarization caused by such a distribution should be best described by a Kubo-Toyabe function with the typical $\frac{1}{3}$ recovery of the μ^+ polarization (Schenck, 1985). Consequently, the absence of the $\frac{1}{3}$ recovery in the present data points to a small fluctuation rate of the magnetic moments. In any case, the μSR data reveal that at least part of the entropy release below 2.5 K must arise from some kind of magnetic ordering. On the other hand, specific-heat data in a magnetic field exhibit an *increase* both of the temperature and the amplitude of the low-temperature peak, which appears compatible with an anomaly inferred from the Kondo effect (Hewson, 1993). Therefore one point of view would be to invoke both mechanisms to describe the specific heat at low temperature. An alternative point of view is to consider that the Gaussian decay of the μ^+ polarization arises from a dense spin-glass-type order (see, for example, the discussion in Sec. VI.A.1). On this assumption, the linear term of $C(T)$ could be associated with the almost linear behavior of the specific heat of spin glasses due to magnonlike excitations (see, for example, Maletta and Zinn, 1989). Such huge terms linear in T, have, for example, been observed in insulating spin glasses such as $Eu_{0.25}Sr_{0.75}S$ (Löhneysen et al., 1985). Interestingly, measurements in magnetic fields of the specific heat of spin glasses indicate a shift of the low-T anomaly toward higher T, compatible with what is observed in $Ce_3Au_3Sb_4$ (Kasaya et al., 1994).

A possible origin of the presence of a spin-glass-like short-range ordering is the large deficiency on the Sb and Ce sites (Adroja et al., 1995), which breaks the translational symmetry of the Ce lattice and could hamper the development of long-range ordering. In the same vein, Adroja et al. (1995) have detected an unusual sample dependence of the transport properties in $Ce_3Au_3Sb_4$ with, for example, the electrical resistivity exhibiting either Kondo-lattice or semiconducting behavior.

An alternative explanation for the short-range ordering has been invoked by Katoh (1994) based on the idea of a magnetic polaron formulated by Kasuya et al. (1993). In the low-carrier limit, impurity states can form magnetic polarons with localized Ce $4f$ electrons. It was speculated that such magnetic polarons, heterogeneously located in the crystal, could disturb a potential long-range magnetic ordering due to the exchange interaction between the Ce^{3+} ions.

2. Sm_3Se_4

A description in terms of the Kondo effect and magnetic ordering had to be utilized for another low-charge-carrier-density heavy-fermion system: Sm_3Se_4 (Frass et al., 1992). This system crystallizes in the cubic Th_3P_4 structure, which is closely related to the $Y_3Au_3Sb_4$ structure with the same space group $I\bar{4}3d$.

This compound shows a semiconducting behavior, with, for example, an electrical resistivity revealing an activation energy of $E_a \simeq 0.13$ eV, but here again low-T specific-heat measurements have shown the presence of a huge linear term of $\gamma \simeq 0.79$ J/(K^2 mol Sm^{3+}).

μSR data recorded in zero field above about 20 K (Takagi et al., 1993) indicate the presence of an exponential depolarization rate $\lambda_{ZF} \simeq 0.4$ μs^{-1} (see Fig. 65), which cannot be ascribed to the linewidth, due to dipolar fields from ^{77}Se, ^{147}Sm, and ^{149}Sm for reasonable μ^+ stopping sites. The presence of a nonzero depolarization in longitudinal-field data (with λ_{LF} only slightly smaller than λ_{ZF}) strongly suggest the presence of slow Sm spin fluctuations. The slowing down of the spin fluctuations is indicated by the increase of λ_{ZF} and λ_{LF} with decreasing
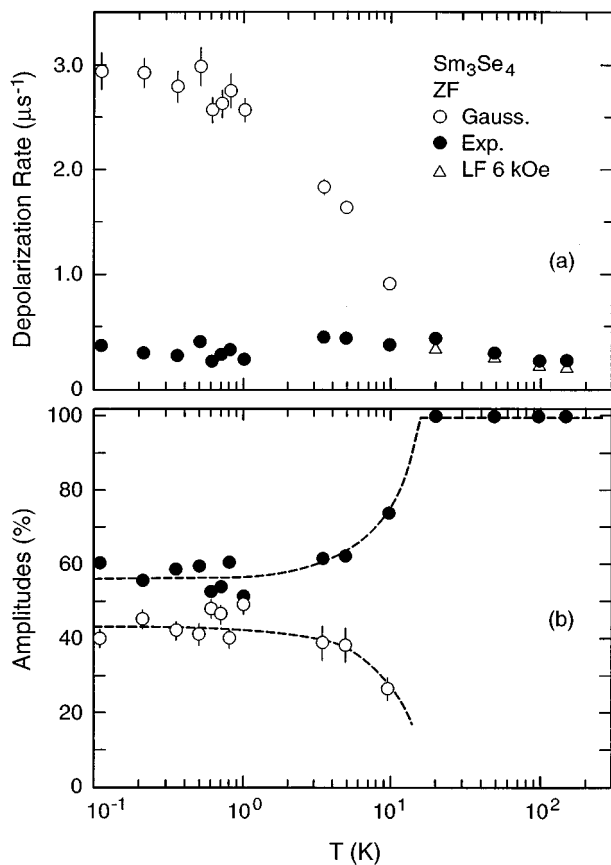
FIG. 65. Zero-field μSR measurements on a polycrystalline Sm$_3$Se$_4$ sample. *Upper part*: Temperature dependence of the zero-field (ZF) depolarization rates for the exponential and Gaussian components. Longitudinal-field (LF) results at high temperature are also reported. *Lower part*: Temperature dependence of the amplitudes of the two components of the zero-field signal.

temperature. Below about 10 K, the zero-field μSR signal starts to develop a clear two-component function with the presence of an additional fast Gaussian component, the amplitude of which reaches ~45% at very low temperature (see Fig. 65). Its Gaussian character indicates the onset of static or quasistatic spin correlations in the form of spatially disordered magnetism, at least in part of the sample, and the linewidth reflects local fields of the order of 25 G, which correspond to static Sm moments of ~0.04 μ_B. In addition, at about 10 K the specific heat (Frass *et al.*, 1992) starts to develop a broad peak, which culminates at about 1 K, precisely the temperature where the depolarization rate of the fast Gaussian component has reached a constant value. Therefore, if, on one hand, the μSR data strongly suggest that the observed specific-heat anomaly at low temperature is due to the removal of local spin degrees of freedom from the Sm^{3+} ions, they are, on the other hand, not compatible with a simple description of the specific-heat anomaly by a simple-impurity Kondo model.

The absence of a clear transition in the μSR data as well as the broadness of the specific-heat contribution

have to be traced back to the absence of charge ordering in superlattices of the Sm^{2+} and Sm^{3+} (present in a 1:2 ratio), which is, for example, observed in the related compound Yb$_4$As$_3$ (Ochiai *et al.*, 1993). For Sm$_3$Se$_4$, the μSR data are again compatible with a dense spin-glass-type behavior, which is also supported by the history-dependent behavior of the magnetization and the behavior of the specific heat in a magnetic field (Frass *et al.*, 1992). Therefore, as for Ce$_3$Au$_3$Sb$_4$, possible magnon-like excitations could be responsible for part of the large term linear in T in the specific heat.

These latter two examples of μSR studies on heavy-fermion compounds without charge carriers illustrate the possibility that low-temperature magnetic transitions and/or magnetic excitations strongly contribute to their specific heat and could mimic the presence of an electronic contribution with a huge linear coefficient. Hence it is advocated that microscopic studies, such as μSR, should be undertaken as a further check of heavy-fermion behavior.

3. Yb$_4$As$_3$

Among the rare-earth pnictides with the anti-Th$_3$P$_4$ cubic crystal structure (which is an inverse structure of the Th$_3$P$_4$-type structure with same space group $I\bar{4}3d$), the compound Yb$_4$As$_3$ exhibits astonishing properties.

From Hall-coefficient (Ochiai *et al.*, 1987) and optical-reflectivity measurements (Kwon *et al.*, 1987), this system has been shown to possess an extremely low carrier concentration of $n_e \simeq 10^{-3}$ per Yb^{3+} ion. Nevertheless, Yb$_4$As$_3$ exhibits a heavy-fermion behavior, which is usually seen as a typical metal phenomenon and is characterized by a large electronic contribution to the specific heat [$\gamma \simeq 0.2$ J/(K^2 mol)] and a quadratic behavior of the electrical resistivity ($\rho - \rho_0 = AT^2$). It has been shown, moreover (Ochiai *et al.*, 1990), that the T^2 coefficient of the resistivity scales with the linear coefficient of the specific heat in the same universal way (Kadowaki and Wood, 1986) as for usual heavy-fermion metals with large carrier concentration.

Preliminary μSR studies were undertaken to test whether low-lying collective-spin excitations could possibly account for part of the large specific heat at low temperature (Takagi, 1994). Zero-field μSR data, down to ~3 K, indicate a constant depolarization rate (see Fig. 66), which could be suppressed in longitudinal fields. This depolarization rate, which is solely due to the nuclear dipolar fields from the Yb and As isotopes, indicates the absence of static $4f$ spin correlations and therefore raises the question of the origin of the large linear term in the specific heat. If no low-lying magnetic excitations can be invoked, the large linear term must arise from a large density of electronic states at the Fermi level, which appears rather surprising in view of the classification of this system as a low-charge-carrier-density heavy-fermion compound. Thus, assuming that the whole linear term in the specific heat is associated with the free charge carriers, and taking into account the
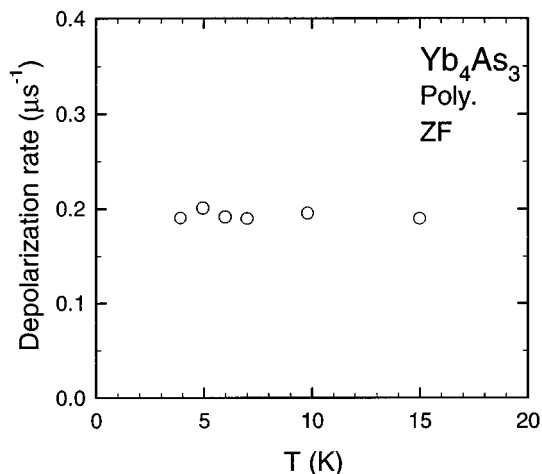
FIG. 66. Temperature dependence of the μ^+ depolarization rate recorded in zero applied field in polycrystalline Yb_4As_3 (from Takagi, 1994).

low carrier concentration, one estimates a mass enhancement over 1000, which would constitute the highest observed value.

To conclude, the origin of the heavy-fermion state in Yb_3As_4 is still a mystery, and the study of the low-energy excitations in this system should provide a fascinating subject for further investigations.

C. Kondo insulators

Early in the study of heavy-fermion compounds, extensive theoretical work was devoted to the comprehension of the Kondo-lattice problem and its dependence on the number n_e of conduction electrons per f site. If the conduction band is half-filled ($n_e = 1$), the solution of the Kondo lattice problem, for a parameter g [see Eq. (4)] sufficiently large and no Coulomb interaction U between f states, is an insulator with a gap. This arises from the fact that, according to Luttinger's theorem (Luttinger, 1960), the volume enclosed by the Fermi surface is not dependent on the presence of interactions. Martin (1982) showed that so long as there is no long-range order, the same result is obtained even for $U \neq 0$. In terms of a simple Kondo model, this situation would correspond to the filling of the Brillouin zone by additional states due to the Abrikosov-Suhl resonance. The occurrence of an insulating gap is indeed observed for a group of mostly cubic rare-earth-based systems labeled as Kondo insulators (for a recent review, see Fisk et al., 1995). These systems behave as disordered metals at high temperatures but become semiconducting below T^*. The isostructural compounds, obtained, for example, by replacing the Ce ions of a Kondo insulator by trivalent non-f ions, are ordinary metals. Conversely, by replacing the Ce ions by tetravalent non-f ions, one obtains band-gap semiconductors, which confirm the theoretical prediction that the particular ground state of the Kondo insulators is based on the hybridization of one occupied f state with exactly one half-filled conduction band.

Examples of Kondo insulators, such as the cubic systems SmB_6, SmS, TmS, and YbB_{12}, have been known for more than two decades. A renewed interest in this field was generated by recent neutron-scattering experiments on SmB_6, which revealed that the gap could be due to the local formation of an excitonic band state between f electrons and d holes, questioning therefore the simple picture of a hybridization gap. Moreover, the discovery of the noncubic Ce-based Kondo semiconductors CeNiSn and CeRhSb has also stimulated theoretical and experimental studies of the Kondo insulators.

The few μSR studies of Kondo insulators were undertaken with the aim to investigate their magnetic properties at low temperature and possibly observe an interplay between gap formation and magnetic interactions, in order to understand the origin of the gapping of the electronic spectrum.

1. CeNiSn

This orthorhombic system (space group $Pn2_1a$) is the first example of a Ce-based Kondo insulator (Takabatake and Fujii, 1993). Above 20 K, CeNiSn behaves like a metallic heavy-fermion compound with a high characteristic temperature $T^* \simeq 100$ K. Susceptibility and resistivity data show signs of the development of coherence in this Kondo lattice below about 20 K. Below 7 K a gap is formed in the heavy quasiparticle band [this latter being characterized by a ratio $C/T \simeq 200$ mJ/(K^2 mole)]. NMR, as well as transport, thermal, and elastic properties indicate the opening of an anisotropic gap. Furthermore, inelastic neutron measurements (Mason et al., 1992) revealed the presence of a spin gap at a particular wave vector that was one order of magnitude larger than the charge gap.

Based on macroscopic studies, possible transitions involving some kind of "weak" magnetism were reported at 12 K (Takabatake et al., 1990) and below 0.5 K (Aliev et al., 1993), but no definitive conclusions could be drawn. Additional information was provided by μSR measurements (Kalvius et al., 1995). Zero-field studies on single crystals established the absence of a magnetic transition down to at least 0.011 K. This was inferred from the absence of a spontaneous μ^+ frequency or a rapidly depolarizing signal. In principle, the absence of a spontaneous μ^+ frequency for an antiferromagnet might reflect the fact that the muon stops at an interstitial site with vanishing internal field. However, this requires a μ^+ stopping site of high local symmetry, which is not available in the orthorhombic structure of CeNiSn.

Since in CeNiSn only scarcely abundant isotopes of Sn carry a nuclear moment, the influence of the $4f$ Ce-spin dynamics on the μ^+ depolarization rate is detectable in zero-field and transverse-field studies. As an example, the orientational dependence of the transverse-field μ^+ depolarization rate is reported in Fig. 67. Additional in-
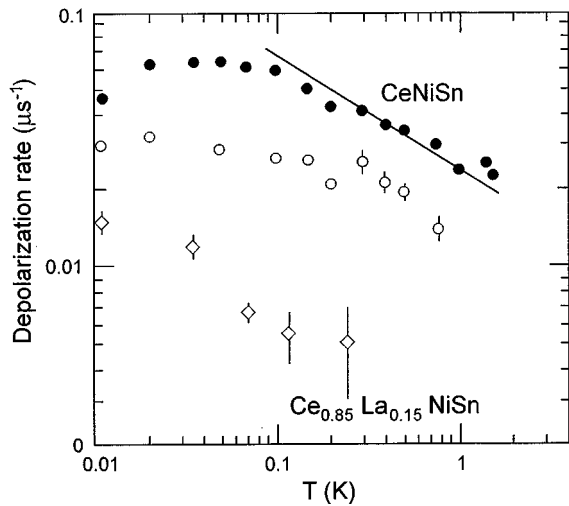
FIG. 67. Temperature dependence of the transverse-field (H_{ext}=1 kOe) μ^+ depolarization rate for single crystalline CeNiSn with the a axis (solid symbols) or the c axis (open symbols) oriented parallel to the external field. The lower set of data points represents similar data for polycrystalline $Ce_{0.85}La_{0.15}NiSn$. The solid line through one set of data points represents a $T^{-1/2}$ dependence of the depolarization rate (from Kalvius *et al.*, 1995).

formation was provided by longitudinal-field measurements that demonstrated the dynamical origin of the μ^+ depolarization rate λ_{LF}. From the field dependence of $\lambda_{LF}(H_{ext})$, a $4f$ spin-fluctuation rate ν_{4f} could be extracted at low temperatures, using the relation (see, for example, Slichter, 1978)

$$\lambda_{LF}(H_{ext}) \propto \frac{\lambda_{ZF}}{1+(\gamma_\mu H_{ext}/\nu_{4f})^2}. \qquad (50)$$

From the values of $\nu_{4f} \simeq 40$ MHz and λ_{ZF}, one obtains an extremely small value for the field width $\Delta/\gamma_\mu = \sqrt{\langle B_\mu^2 \rangle} \simeq 10$ G at the μ^+ stopping site, pointing to an effective Kondo compensation of the $4f$ moments. If all the Ce atoms carry a moment, the obtained field width implies that the Ce-moment size is of the order of $4 \times 10^{-3} \mu_B$. On the other hand, by considering that a reduced fraction of evenly distributed Ce atoms contributes to the linewidth, the involved moment could be much higher (see Fig. 68). However, the consistency of the μSR data obtained from the different samples and the observed spatial anisotropy makes the scenario of a few impurities with large moment an unlikely one.

Interpreting the change of the μ^+ depolarization rate reported in Fig. 67 as a change of ν_{4f}, one observes that $\nu_{4f} \propto \sqrt{T}$, as represented by the solid line through the data points. Similar to the situation observed for UCd_{11} (see Sec. IV.B.8), the $\sqrt{T}$ dependence of ν_{4f} is consistent with the typical NMR and neutron-scattering data observed for Kondo lattices. Whereas for UCd_{11} the observation of dynamical effects by μSR was possible due to the strong hyperfine coupling constant, in CeNiSn dynamical effects in zero-field or transverse-field experiments can be observed, as stated above, due to the absence of a sizable nuclear-moment contribution and to
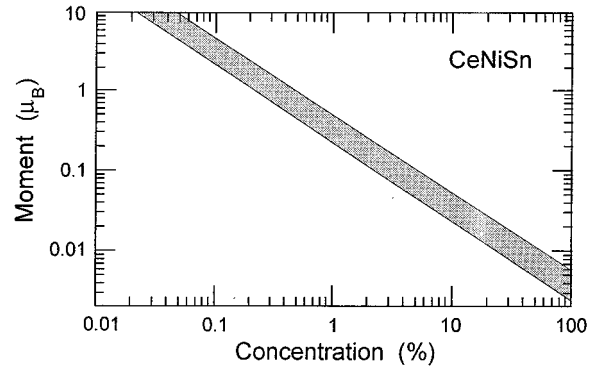

FIG. 68. Range of magnitude versus concentration of magnetic moments, as derived from Monte-Carlo simulations, compatible with the spectral parameters of CeNiSn in zero field (from Kalvius *et al.*, 1995).

the relatively slow fluctuation rate of the $4f$ moments.

2. $Ce_{0.85}La_{0.15}NiSn$

Due to small-gap semiconductor properties, the effects of coherence in heavy-fermion systems are most pronounced in the Kondo insulators. In particular, the Kondo insulators are very sensitive to strains in the crystal and impurities. Adding small amounts of nonmagnetic impurities leads to the formation of Kondo holes (Doniach and Fazekas, 1992). A Kondo hole is a missing f electron at a given site, which is introduced by a large local f-level energy that prevents the occupation of the f state. The presence of Kondo holes in a Kondo lattice breaks the translational invariance and gradually destroys the coherence of the heavy-fermion ground state. When the concentration of Kondo holes is increased, an impurity band forms in the gap of the Kondo insulators and progressively smears the hybridization gap. Hence it was speculated that hole-hole exchange coupling could lead to an antiferromagnetic ground state. In order to test such a hypothesis, μSR studies have been performed on the system $Ce_{0.85}La_{0.15}NiSn$, which corresponds to the La concentration for which the energy gap is destroyed (Kalvius *et al.*, 1995).

The search for a spontaneous μ^+ frequency in zero-field experiments gave a negative result down to 0.011 mK. Interestingly, transverse-field results even indicate a weakening of the magnetic behavior compared to the pure CeNiSn (see Fig. 67). Therefore the μSR data teach us that a transition, driven by a Kondo-hole–Kondo-hole exchange interaction, into a long-range magnetically ordered state can be safely excluded for $Ce_{0.85}La_{0.15}NiSn$.

3. CeRhSb

CeRhSb presents close similarities to CeNiSn. It possesses the same orthorhombic crystal structure, with a roughly 3% larger unit cell, and also belongs to the recently discovered Ce-based Kondo insulators.

Like CeNiSn, zero-field μSR experiments did not indicate any tendency of CeRhSb to enter into a magneti-
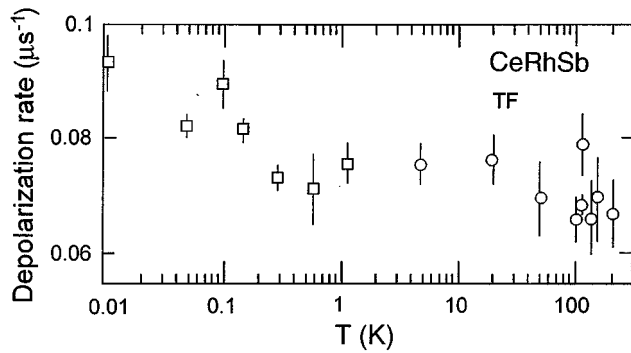
FIG. 69. Temperature dependence of the μ^+ depolarization rate (Gaussian fits) measured in a 100 Oe transverse field in a CeRhSb polycrystalline sample (from Rainford *et al.*, 1995).

cally ordered state (Rainford *et al.*, 1995). In particular, no spontaneous μ^+ frequency or rapidly depolarizing signal could be detected. Down to 0.5 K the time evolution of the μ^+ polarization is well described by a Kubo-Toyabe function arising from the ^{121}Sb and ^{123}Sb nuclear moments. The corresponding depolarization can be totally suppressed in longitudinal-field measurements, indicating that the Ce moments fluctuate rapidly with a rate in the THz regime.

In agreement with the zero-field results, transverse-field data show a temperature-independent μ^+ depolarization rate down to 0.5 K. Figure 69 shows that below 0.5 K the μ^+ depolarization rate exhibits a slight rise, which reflects, in a similar way to CeNiSn, the slowing down of the f-moment fluctuation rate. However, in CeRhSb the onset of this depolarization rate of electronic origin occurs at lower temperatures and has a lower magnitude compared to the signal observed in CeNiSn. Rainford *et al.* (1995) ascribed this difference to the fact that in CeRhSb the f-spin fluctuations remain faster, which is supported by the large linewidth observed in inelastic-scattering studies (Rainford, 1995).

Although the μSR investigations of Kondo insulators are still limited, the few available results appear to indicate a slowing down of the fluctuation of the f moments, which become detectable in the μSR time window. This slowing down seems to be much more pronounced than for the other heavy-fermion classes, for which the f fluctuations were only detected for exceptional cases. This observation is also corroborated by preliminary μSR studies on another cubic Kondo insulator system, $Ce_3Bi_4Pt_3$ (space group $I\bar{4}3d$), for which the zero-field μ^+ depolarization rate shows again a barely detectable increase at low temperature, the origin of which appears connected to rather slow fluctuations of the f moments, as proven by longitudinal-field experiments (Heffner, 1994). Whether the apparently anomalous slowing down of these fluctuations in Kondo insulators is connected to the possible opening of a spin gap concomitant with the opening of the charge gap remains to be seen and will require careful comparisons between μSR and inelastic neutron measurements.

VII. SUMMARY AND OUTLOOK

In this review, I have attempted to give a survey of the μSR studies on heavy-fermion compounds. Due to the unique information obtained for this class of compounds by the implanted muons and the increasing availability and quality of μSR facilities around the world, the number of publications relating μSR studies in heavy-fermion compounds is steadily increasing. A consequence may therefore be that the present review will rapidly become obsolete. However, the results discussed in the preceding sections already demonstrate that a wealth of diverse and unique information can be obtained from μSR investigations on heavy-fermion systems. While it appears impossible to draw a general and consistent picture of the available data to date, some emphasis can be placed on a few novel phenomena, discovered or confirmed by μSR, that have enriched the complexity and, sometimes, the comprehension of heavy-fermion physics.

The occurrence of magnetic phases with extremely small static moments is now a well-established phenomenon. μSR studies have demonstrated that this magnetic behavior, which is formed in the low-temperature Fermi-liquid state and is usually ascribed to the itinerant magnetism of the heavy quasiparticles, is a widespread characteristic among heavy-fermion systems.

The microscopic coexistence of different electronic subsystems in the ground state of some heavy-fermion compounds has been detected by μSR for at least two U-based systems (see Secs. III.C and IV.A.4). Whereas a more localized f-electron subsystem is responsible for the long-range antiferromagnetism, another itinerant subsystem formed by the heavy quasiparticles appears unstable against either a low-moment itinerant magnetic phase (UCu_5) or a superconducting phase (UPd_2Al_3). A similar situation could occur for two other U-based heavy-fermion superconductors (namely, URu_2Si_2 and UNi_2Al_3), for which a microscopic coexistence between magnetism and superconductivity has been established by μSR studies (see Secs. III.D and III.C). On the other hand, for the only known Ce-based heavy-fermion superconductor, $CeCu_2Si_2$, the μSR data have clearly proven that superconductivity and magnetism do not microscopically coexist. This has led to the hypothesis that, for this system, magnetism and superconductivity are two different, mutually exclusive ground states of the same subset of electrons.

A number of μSR data on Ce-based heavy-fermion systems indicate that the segregation of the sample volume in multiple domains is not limited to the superconductivity-magnetism problem, but is also reflected by the occurrence of domains of different magnetic behavior. In addition, some Ce-based magnetic heavy-fermion systems show an apparent absence of clear cooperative phase transitions. Rather, the magnetically ordered domains appear to grow gradually out of the paramagnetic domains over a wide temperature range. On the contrary, but with the still unclear exception of U_2Zn_{17} (see Sec. IV.B.6), U-based heavy-fermion

systems appear microscopically homogeneous. Such an observation could be related to the extremely large values of the heavy-fermion Grüneisen parameter Γ_{hf}, which leads to an extreme sensitivity to internal strains. Considering that U- and Ce-based heavy-fermion systems exhibit equally large Γ_{hf} values (de Visser *et al.*, 1990), this would imply that strains are more generally present in Ce-based specimens. Whether such an observation has a fortuitous character (CeAl$_3$ and CeCu$_5$, for example, which exhibit multidomain structures are both formed through a complicated solid reaction, see Sec. IV.A.1 and IV.B.3), or whether it is a result of a more fundamental difference between 5f and 4f heavy-fermion systems (Yb- and Sm-based heavy-fermion systems such as Yb$_{1-x}$Y$_x$BiPt and Sm$_3$Se$_4$ also exhibit multidomain features, see Secs. IV.A.6 and VI.B.2) still needs to be investigated by systematic microscopic studies on high-quality single crystals.

Numerous μSR studies of the magnetic properties of heavy-fermion systems have revealed features similar to those of spin glasses, notably random magnetic order. In particular, such a behavior was observed for several heavy-fermion compounds classified as systems with low charge-carrier density (see Sec. VI.B), and for which the origin of the gigantic ratio C/T at low temperature appears unclear. Consequently, these μSR data suggest that at least part of the huge term linear in T of $C(T)$ in these systems could be associated with the almost linear behavior of the specific heat of spin glasses, due to magnonlike excitations. An important lesson to be learned from such studies concerns the absolute necessity of performing microscopic studies prior to classifying a system as a heavy-fermion compound.

Finally, μSR has provided evidence for the unconventional character of the superconducting state of some heavy-fermion systems. In this respect, the results obtained on U$_{1-x}$Th$_x$Be$_{13}$, and possibly on UPt$_3$, may set severe constraints on any further theoretical considerations.

In conclusion, μSR has provided an impressive amount of new information on different facets of the heavy-fermion problem. Although a complete understanding of a significant part of the present data is still missing and will require additional and systematic experiments, it appears reasonable to say that μSR has already significantly enhanced our level of comprehension of the microscopic aspects of heavy-fermion systems.

REFERENCES

Aarts, J., A. P. Volodin, A. A. Menovsky, G. J. Nieuwenhuys, and J. A. Mydosh, 1994, Europhys. Lett. **26**, 203.

Abragam, A., 1970, *The Principles of Nuclear Magnetism* (Clarenden, Oxford).

Adroja, D. T., B. D. Rainford, Z. Hossain, E. A. Goremychkin, R. Nagarajan, L. C. Gupta, and C. Godart, 1995, Physica B **206&207**, 216.

Aeppli, G., D. Bishop, C. Broholm, E. Bucher, K. Siemensmeyer, M. Steiner, and N. Stüsser, 1989, Phys. Rev. Lett. **63**, 676.

Alekseev, P. A., V. N. Lazukov, I. P. Sadikov, M. N. Khlopkin, G. A. Takzei, Y. P. Grebenyuk, and I. I. Sych, 1992, J. Magn. Magn. Mater. **110**, 119.

Aliev, F. G., R. Villar, S. Vieira, M. A. Lopez de la Torre, R. V. Scolozdra, and M. B. Maple, 1993, Phys. Rev. B **47,** 769.

Amato, A., 1994, Physica B **199&200**, 91.

Amato, A., 1995a, unpublished.

Amato, A., 1995b, Physica B **206&207**, 49.

Amato, A., C. Baines, R. Feyerherm, J. Flouquet, F. N. Gygax, P. Lejay, A. Schenck, and U. Zimmermann, 1993, Physica B **186-188**, 276.

Amato, A., P. C. Canfield, R. Feyerherm, Z. Fisk, F. N. Gygax, R. H. Heffner, E. A. Knetsch, D. E. MacLaughlin, H. R. Ott, A. Schenck, J. D. Thompson, and U. Zimmermann, 1993, Physica B **186-188**, 615.

Amato, A., P. C. Canfield, R. Feyerherm, Z. Fisk, F. N. Gygax, R. H. Heffner, D. E. MacLaughlin, H. R. Ott, A. Schenck, and J. D. Thompson, 1992, Phys. Rev. B **46,** 3151.

Amato, A., R. Feyerherm, B. Gaulin, F. N. Gygax, and A. Schenck, 1994, *Nuclear and Particle Physics Newsletter* (Paul Scherrer Institut, Villigen, Switzerland), p. 66.

Amato, A., R. Feyerherm, C. Geibel, F. N. Gygax, T. Komatsubara, N. Sato, A. Schenck, M. Sigrist, F. Steglich, and K. Ueda, 1992, *Nuclear and Particle Physics Newsletter* (Paul Scherrer Institut, Villigen, Switzerland), p. 77.

Amato, A., R. Feyerherm, F. N. Gygax, D. Jaccard, A. Schenck, J. Sierro, E. Walker, and U. Zimmermann, 1993, Physica B **186-188**, 273.

Amato, A., R. Feyerherm, F. N. Gygax, Y. Ō nuki, H. R. Ott, N. Sato, A. Schenck, and U. Zimmermann, 1993, *Nuclear and Particle Physics Newsletter* (Paul Scherrer Institut, Villigen, Switzerland), p. 85.

Amato, A., R. Feyerherm, F. N. Gygax, A. Schenck, J. Flouquet, and P. Lejay, 1994, Phys. Rev. B **50,** 619.

Amato, A., R. Feyerherm, F. N. Gygax, A. Schenck, and D. Jaccard, 1994, Hyperfine Interact. **85**, 369.

Amato, A., R. Feyerherm, F. N. Gygax, A. Schenck, H.v. Löhneysen, and H. G. Schlager, 1995, Phys. Rev. B **52,** 54.

Amato, A., R. Feyerherm, F. N. Gygax, A. Schenck, M. Weber, R. Caspary, P. Hellmann, C. Schank, C. Geibel, F. Steglich, D. E. MacLaughlin, and R. H. Heffner, 1992, Europhys. Lett. **19,** 127.

Amato, A., C. Geibel, F. N. Gygax, R. H. Heffner, E. Knetsch, D. E. MacLaughlin, C. Schank, A. Schenck, F. Steglich, and M. Weber, 1992, Z. Phys. B **86,** 159.

Amato, A., D. Jaccard, J. Flouquet, F. Lapierre, J. L. Tholence, R. A. Fisher, S. E. Lacy, J. A. Olsen, and N. E. Phillips, 1987, J. Low Temp. Phys. **68**, 371.

Amato, A., A. Schenck, F. Gygax, and S. H. Kilcoyne, 1996, *The ISIS Facility Annual Report 1995–96* (CLRC Rutherford Appleton Laboratory, Chilton, U.K.), A124.

Anderson, P. W., 1961, Phys. Rev. **124**, 41.

Arrot, A., S. A. Werner, and H. Kendrick, 1965, Phys. Rev. Lett. **14**, 1022.

Barbara, B., M. F. Rossignol, J. X. Boucherle, and C. Vettier, 1980, Phys. Rev. Lett. **45,** 938.

Barford, W., and J. M. F. Gunn, 1988, Physica C **156,** 515.

Barth, S., 1988, Ph.D. thesis (ETH-Zürich, Switzerland).

Barth, S., H. R. Ott, F. N. Gygax, B. Hitti, E. Lippelt, A. Schenck, and C. Baines, 1987, Phys. Rev. Lett. **59**, 2991.

Barth, S., H. R. Ott, F. N. Gygax, A. Schenck, T. M. Rice, and Z. Fisk, 1986, Hyperfine Interact. **31,** 397.

Batlogg, B., D. Bishop, B. Golding, C. M. Varma, Z. Fisk, J. L. Smith, and H. R. Ott, 1985, Phys. Rev. Lett. **55**, 1319.

Bauer, E., M. Rotter, L. Keller, P. Fischer, M. Ellerby, and K. A. McEwen, 1994, J. Phys.: Condens. Matter **6**, 5533.

Beyerman, W. P., R. H. Heffner, J. L. Smith, M. F. Hundley, P. C. Canfield, and J. D. Thompson, 1995, Phys. Rev. B **51,** 404.

Beyerman, W. P., M. F. Hundley, P. C. Canfield, J. D. Thompson, Z. Fisk, J. L. Smith, M. Selsane, C. Godart, and M. Latroche, 1991, Phys. Rev. Lett. **66**, 3289.

Beyerman, W. P., M. F. Hundley, P. C. Canfield, J. D. Thompson, M. Latroche, C. Godart, M. Selsane, Z. Fisk, and J. L. Smith, 1991, Phys. Rev. B **43**, 13130.

Blount, E. I., C. M. Varma, and G. Aeppli, 1990, Phys. Rev. Lett. **64**, 3074.

Brandt, E. H., 1988, Phys. Rev. B **37**, 2349.

Brewer, J. H., 1994, in *Encyclopedia of Applied Physics*, edited by G. L. Trigg (VCH Publishers, New York), Vol. 11, p. 23.

Brison, J. P., P. Lejay, A. Bazdin, and J. Flouquet, 1994, Physica C **229,** 79.

Brodale, G. E., R. A. Fisher, N. E. Phillips, and J. Flouquet, 1985, Phys. Rev. Lett. **56**, 390.

Broholm, C., G. Aeppli, R. N. Kleinmann, D. R. Harshmann, D. J. Bishop, E. Bucher, D. L. Williams, E. J. Ansaldo, and R. H. Heffner, 1990, Phys. Rev. Lett. **65**, 2062.

Broholm, C., J. K. Kjems, W. J. L. Buyers, P. Matthews, T. T. M. Palstra, A. A. Menovsky, and J. A. Mydosh, 1987, Phys. Rev. Lett. **58**, 1467.

Bruls, G., D. Weber, B. Wolf, P. Thalmeier, B. Lüthi, A. de Visser, and A. Menovsky, 1990, Phys. Rev. Lett. **65**, 2294.

Bruls, G., B. Wolf, D. Finsterbusch, P. Thalmeier, I. Kouroudis, W. Sun, W. Assmus, B. Lüthi, K. Gloos, F. Steglich, and R. Modler, 1994, Phys. Rev. Lett. **72**, 1754.

Camani, M., F. N. Gygax, W. Rüegg, A. Schenck, and H. Schilling, 1977, Phys. Rev. Lett. **39**, 836.

Caspary, R., P. Hellmann, M. Keller, G. Sparn, C. Wassilew, R. Köhler, C. Geibel, C. Schank, F. Steglich, and N. E. Phillips, 1993, Phys. Rev. Lett. **71**, 2146.

Chattopadhyay, T., H.v. Löhneysen, T. Trappmann, and M. Loewenhaupt, 1990, Z. Phys. B **80,** 159.

Cooke, D. V., R. H. Heffner, R. L. Hutson, M. E. Schillaci, J. L. Smith, J. O. Willis, D. E. MacLaughlin, C. Boekema, R. L. Lichti, A. B. Denison, and J. Oostens, 1986, Hyperfine Interact. **31**, 425.

Cox, D. L., 1987, Phys. Rev. Lett. **59**, 1240.

Cox, D. L., 1993, Physica B **186-188**, 312.

Cox, D. L., N. E. Bichers, and J. W. Wilkins, 1985, J. Appl. Phys. **57**, 3166.

Cox, D. L., G. Shirane, S. M. Shapiro, G. Aeppli, Z. Fisk, J. L. Smith, J. K. Kjems, and H. R. Ott, 1986, Phys. Rev. B **33,** 3614.

Cox, S. F. J., 1987, J. Phys. C **20**, 3107.

Dalmas de Réotier, P., A. Huxley, A. Yaouanc, J. Flouquet, P. Bonville, P. Imbert, P. Pari, P. C. M. Gubbens, and A. M. Mulders, 1995, Phys. Lett. A **205**, 239.

de Visser, A., J. J. M. Franse, A. Lacerda, P. Haen, and J. Flouquet, 1990, Physica B **163**, 49.

Dobrosavljevic, V., T. R. Kirkpatrick, and G. Kotliar, 1992, Phys. Rev. Lett. **69**, 1113.

Doniach, S., 1977, Physica B **91**, 231.

Doniach, S., and P. Fazekas, 1992, Philos. Mag. B **65,** 1171.

Effantin, J. M., J. Rossat-Mignod, P. Burlet, H. Bartholin, S. Kunii, and T. Kasuya, 1985, J. Magn. Magn. Mater. **47&48**, 145.

Einzel, D., P. J. Hirschfield, F. Gross, B. S. Chandrasekhar, K. Andres, H. R. Ott, J. Beuers, Z. Fisk, and J. L. Smith, 1986, Phys. Rev. Lett. **56**, 2513.

Endstra, T., G. J. Nieuwenhuys, and J. A. Mydosh, 1993, Phys. Rev. B **48**, 9595.

Erkelens, W. A. C., L. P. Regnault, P. Burlet, J. Rossat-Mignod, S. Kunii, and T. Kasuya, 1987, J. Magn. Magn. Mater **63&64**, 61,

Fåk, B., C. Vettier, J. Flouquet, P. Lejay, and J. M. Mignot, 1995, Physica B **206&207**, 415.

Felder, E., A. Bernasconi, H. R. Ott, Z. Fisk, and J. L. Smith, 1989, Physica C **162-164**, 429.

Feyerherm, R., 1995, Ph.D. thesis (ETH-Zürich, Switzerland).

Feyerherm, R., A. Amato, C. Geibel, F. N. Gygax, P. Hellmann, R. H. Heffner, D. E. MacLaughlin, R. Müller-Reisener, G. J. Nieuwenhuys, A. Schenck, and F. Steglich, 1995, Physica B **206&207,** 596.

Feyerherm, R., A. Amato, F. N. Gygax, A. Schenck, C. Geibel, F. Steglich, N. Sato, and T. Komatsubara, 1994, Phys. Rev. Lett. **73**, 1849.

Feyerherm, R., A. Amato, F. N. Gygax, A. Schenck, Y. Ō nuki, and N. Sato, 1994, Physica B **194-196,** 357.

Feyerherm, R., A. Amato, F. N. Gygax, A. Schenck, U. Zimmermann, A. Grayevsky, and N. Kaplan, 1994, Hyperfine Interact. **85**, 329.

Fisch, G. E. J. J. Rhyne, S. G. Sonkar, and W. E. Wallace, 1979, J. Appl. Phys. **50,** 2003.

Fischer, Ø, 1978, Appl. Phys. **16**, 1.

Fisher, R. A., S. Kim, B. F. Woodfield, N. E. Phillips, L. Taillefer, K. Hasselbach, J. Flouquet, A. L. Giorgi, and J. L. Smith, 1989, Phys. Rev. Lett. **62**, 1411.

Fisher, R. A., C. Marcenat, N. E. Phillips, P. Haen, F. Lapierre, P. Lejay, J. Flouquet, and J. Voiron, 1991, J. Low Temp. Phys. **84**, 49.

Fisk, Z., P. C. Canfield, W. P. Beyermann, J. D. Thompson, M. F. Hundley, H. R. Ott, E. Felder, M. B. Maple, M. A. Lopez de la Torre, P. Visani, and C. L. Seaman, 1991, Phys. Rev. Lett. **67**, 3310.

Fisk, Z., D. W. Hess, C. J. Pethick, D. Pines, J. L. Smith, J. D. Thompson, and J. O. Willis, 1988, Science **239**, 33.

Fisk, Z., J. L. Sarrao, J. D. Thompson, D. Mandrus, M. F. Hundley, A. Miglory, B. Bucher, Z. Schlesinger, G. Aeppli, E. Burcher, J. F. DiTusa, C. S. Oglesby, H. R. Ott, P. C. Canfield, and S. E. Brown, 1995, Physica B **206&207**, 798.

Flouquet, J., J. C. Lasjaunias, J. Peyrard, and M. Ribault, 1982, J. Appl. Phys. **53**, 2117.

Frass, K., U. Ahlheim, P. H. P. Reinders, C. Schank, R. Caspary, F. Steglich, A. Ochiai, T. Suzuki, and T. Kasuya, 1992, J. Magn. Magn. Mater. **108**, 220.

Friedel, J., 1952, Philos. Mag. **43**, 153.

Frings, P., B. Renker, and C. Vettier, 1987, J. Magn. Magn. Mater. **63&64**, 202.

Garg, A., and D. C. Chen, 1994, Physica B **199&200,** 204.

Gavilano, J. L., J. Hunziker, O. Hudak, T. Sleater, F. Hulliger, and H. R. Ott, 1993, Phys. Rev. B **47**, 3438.

Geibel, C., 1995, private communication.

Geibel, C., A. Böhm, R. Caspary, K. Gloos, A. Grauel, P. Hellmann, R. Modler, C. Schank, G. Weber, and F. Steglich, 1993, Physica B **186-188,** 188.

Geibel, C., C. Schank, S. Thies, H. Kitazawa, C. D. Bredl, A. Böhm, M. Rau, A. Grauel, R. Caspary, R. Helfrich, U. Ahlheim, G. Weber, and F. Steglich, 1991, Z. Phys. B **84**, 1.

Geibel, C., S. Thies, D. Kaczorowski, A. Mehner, A. Grauel, B. Seidel, U. Ahlheim, R. Helfrich, K. Petersen, C. D. Bredl, and F. Steglich, 1991, Z. Phys. B **83**, 305.

Germann, A., A. K. Nigam, J. Dutzi, A. Schröder, and H.v. Löhneysen 1988, J. Phys. Colloq. **49**, C-8, 755.

Golding, B., D. J. Bishop, B. Batlogg, W. H. Haemmerle, Z. Fisk, J. L. Smith, and H. R. Ott, 1985, Phys. Rev. Lett. **55**, 2479.

Goldman, A. I., G. Shivan, G. Aeppli, B. Batlogg, and E. Bucher, 1986, Phys. Rev. B **34**, 6564.

Goremychkin, E. A., I. Natkanie, E. Mühle, H. Müller, and P. Froch, 1987, Solid State Commun. **64**, 1437.

Gor'kov, L. P., 1987, Sov. Sci. Rev. A 9, 1.

Grewe, N., 1988, Solid State Commun. **66**, 1053.

Grewe N., and F. Steglich, 1991, in *Handbook on the Physics and Chemistry of Rare Earths*, edited by K. A. Gschneidner, Jr., and L. Eyring (North Holland, Amsterdam), Vol. 14, p. 343.

Grewe, N., and B. Welslau, 1988, Solid State Commun. **65**, 437.

Gross, F., K. Andres, and B. S. Chandrasekhar, 1989, Physica C **162-164**, 419.

Gulásci, M., and Zs. Gulásci, 1989, Phys. Rev. B **39**, 12352.

Haiden, S. M., L. Taillefer, C. Vettier, and J. Flouquet, 1992, Phys. Rev. B **46,** 8675.

Han, S., K. W. Ng, E. L. Wolf, A. Millis, J. L. Smith, and Z. Fisk, 1986, Phys. Rev. Lett. **57,** 238.

Harrison, W. A., 1983, Phys. Rev. B **28**, 550.

Hartmann, O., R. Wäppling, A. Yaouanc, P. Dalmas de Réotier, B. Barbara, K. Aggarwal, L. Asch, A. Kratzer, G. M. Kalvius, F. J. Litterst, F. N. Gygax, B. Hitti, E. Lippelt, and A. Schenck, 1989, Hyperfine Interact. **51**, 955.

Hayano, R. S., Y. J. Uemura, J. Imazato, N. Nishida, T. Yamazaki, and R. Kubo, 1979, Phys. Rev. B **20**, 850.

Heal, T. J., and G. I. Williams, 1955, Acta Crystallogr. **8**, 494.

Heffner, R. H., 1990, Hyperfine Interact. **64**, 497.

Heffner, R. H., 1994, unpublished.

Heffner, R. H., A. Amato, P. C. Canfield, R. Feyerherm, Z. Fisk, F. N. Gygax, D. E. MacLaughlin, A. Schenck, J. D. Thompson, and H. R. Ott, 1994, Physica B **199-200,** 113.

Heffner, R. H., W. P. Beyerman, M. F. Hundley, J. D. Thompson, J. L. Smith, Z. Fisk, K. Bedell, P. Birrer, C. Baines, F. N. Gygax, B. Hitti, E. Lippelt, H. R. Ott, A. Schenck, and D. E. MacLaughlin 1991, J. Appl. Phys. **69**, 5481.

Heffner, R. H., D. W. Cooke, A. L. Giorgi, R. L. Hutson, M. E. Schillaci, H. D. Rempp, J. L. Smith, J. O. Willis, D. E. MacLaughlin, C. Boekema, R. L. Lichti, J. Oostens, and A. B. Denison, 1989, Phys. Rev. B **39**, 11345.

Heffner, R. H., J. L. Smith, J. O. Willis, P. Birrer, C. Baines, F. N. Gygax, B. Hitti, E. Lippelt, H. R. Ott, A. Schenck, E. A. Knetsch, J. Mydosh, and D. E. MacLaughlin, 1990, Phys. Rev. Lett. **65**, 2819.

Hewson, A. C., 1993, *The Kondo Problem to Heavy Fermions* (Cambridge University, New York).

Higashi, I., K. Kobayashi, T. Takabatake, and M. Kasaya, 1993, J. Alloys Compd. **193**, 300.

Jaccard, D., R. Cibin, and J. Sierro, 1988, Helv. Phys. Acta **61**, 530.

Jaccard, D., J. M. Mignot, B. Bellarbi, A. Benoit, H. F. Braun, and J. Sierro, 1985, J. Magn. Magn. Mater. **47&48**, 23.

Joynt, R., 1988, Supercond. Sci. Technol. **1**, 210.

Kadowaki, H., T. Ekino, H. Iwasaki, T. Takabatake, H. Fujii, and J. Sakurai, 1993, J. Phys. Soc. Jpn. **62**, 4426.

Kadowaki, K, and S. B. Wood, 1986, Solid State Commun. **58,** 507.

Kalvius, G. M., A. Kratzer, K. H. Münch, T. Takabatake, G. Nakamoto, H. Fujii, R. Wäppling, H. H. Klauss, R. Kiefl, S. Kreitzman, and D. R. Noakes, 1994, Hyperfine Interact. **85**, 411.

Kalvius, G. M., A. Kratzer, R. Wäppling, T. Takabatake, G. Nakamoto, H. Fujii, R. F. Kiefl, and S. R. Kreitzmann, 1995, Physica B **206&207**, 807.

Kasuya, T., H. Haga, Y. S. Kwon, and T. Suzuki, 1993, Physica B **186-188,** 9.

Kasaya, M., K. Katoh, M. Kohgi, T. Osakabe, and N. Sato, 1994, Physica B **199&200**, 534.

Kasaya, M., K. Katoh, and T. Takegahara, 1991, Solid State Commun. **78**, 797.

Katoh, K., 1994, Ph.D. thesis (Tohoku University, Sendai, Japan).

Kiefl, R. F., D. A. Bonn, J. H. Brewer, J. F. Carolan, K. H. Chow, P. Dosanojh, W. N. Hardy, R. Liang, W. A. MacForlane, P. Mendels, G. D. Morris, T. M. Riseman, and J. W. Schneider, 1994, Hyperfine Interact. **86**, 537.

Kitazawa, H., C. Schank, S. Thies, B. Seidel, C. Geibel, and F. Steglich, 1992, J. Phys. Soc. Jpn. **61**, 1461.

Kleinman, R.N., D. J. Bishop, H. R. Ott, Z. Fisk, and J. L. Smith, 1990, Phys. Rev. Lett. **64**, 1975.

Knetsch, E. A., 1993a, unpublished.

Knetsch, E. A., 1993b, Ph.D. thesis (Leiden University, The Netherlands).

Knetsch, E. A., A. A. Menovsky, G. J. Nieuwenhuys, J. A. Mydosh, A. Amato, R. Feyerherm, F. N. Gygax, A. Schenck, R. H. Heffner, and D. E. MacLaughlin, 1993, Physica B **186-188**, 300.

Knetsch, E. A., A. A. Menovsky, J. J. Petersen, G. J. Nieuwenhuys, J. A. Mydosh, P. J. C. Signore, S. E. Brown, and M. W. Meisel, 1992, J. Magn. Magn. Mater. **108**, 71.

Knetsch, E. A., G. J. Nieuwenhuys, J. A. Mydosh, R. H. Heffner, and J. L. Smith, 1993, Physica B **186-188**, 251.

Kohara, T., Y. Kohori, K. Asayama, Y. Kitaoka, M. B. Maple, and M. S. Torikachvili, 1986, Solid State Commun. **59**, 603.

Kohgi, M., K. Ohoyama, T. Osakaba, and K. Kasaya, 1992, J. Magn. Magn. Mater. **108**, 187.

Komatsubara, T., N. Sato, S. Kunii, I. Oguro, Y. Fuukawa, Y. Ōnuki, and T. Kasuya, 1983, J. Magn. Magn. Mater. **31-34**, 368.

Krimmel, A., P. Fischer, B. Roessli, H. Maletta, C. Geibel, C. Schank, A. Grauel, A. Loidl, and F. Steglich, 1992, Z. Phys. B **86**, 161.

Kubo, R., and T. Toyabe, 1967, in *Magnetic Resonance and Relaxation*, edited by R. Blinc (North-Holland, Amsterdam), p. 810.

Kumagai, K., Y. Inoue, Y. Kohori, and K. Asayama, 1981, in *Ternary Superconductors*, edited by G. K. Shenoy, B. D. Dunlap, and F. Y. Fradin (North-Holland, Amsterdam), p. 185.

Kuramoto, Y., and K. Miyake, 1990, J. Phys. Soc. Jpn. **59**, 2831.

Kwon, Y. S., A. Ochiai, H. Kitazawa, N. Sato, H. Abe, N. Nanba, M. Ikezawa, K. Takegahara, O. Sakai, T. Suzuki, and T. Kasuya, 1987, J. Magn. Magn. Mater. **70**, 397.

Kyogaku, M., Y. Kitaoka, K. Asayama, C. Geibel, C. Schank, and F. Steglich, 1993, J. Phys. Soc. Jpn. **62**, 4016.

Lapertot, G., R. Calemczuck, C. Marcenat, J. Y. Henry, J. X. Boucherle, J. Flouquet, J. Hamman, R. Cibin, J. Cors, D. Jaccard, and J. Sierro, 1993, Physica B **186-188**, 454.

Le, L. P., G. M. Luke, B. J. Sternlieb, W. D. Wu, Y. J. Uemura, J. H. Brewer, R. V. Upasani, L. Y. Chiang, and P. M. Chaikin, 1991, Europhys. Lett. **15**, 547.

Löhneysen, H.v., 1995, Physica B **206&207**, 101.

Löhneysen, H.v., T. Pietrus, G. Portisch, H. G. Schlager, A. Schröder, M. Sieck, and T. Trappmann, 1994, Phys. Rev. Lett. **72**, 3262.

Löhneysen, H.v., T. Trappmann, and L. Taillefer, 1992, J. Magn. Magn. Mater. **108**, 49.

Löhneysen, H.v., R. van den Berg, G. V. Lecomte, and W. Zinn, 1985, Phys. Rev. B **31**, 2920.

Luke, G. M., A. Keren, K. Kojima, L. P. Le, W. D. Wu, Y. J. Uemura, G. M. Kalvius, A. Kratzer, G. Makamoto, T. Takabatake, and M. Ishikawa, 1995, Physica B **206&207**, 222.

Luke, G. M., A. Keren, L. P. Le, B. J. Sternlieb, W. D. Wu, and Y. J. Uemura, 1994, Phys. Rev. Lett. **73**, 1853.

Luke, G. M., A. Keren, L. P. Le, Y.J. Uemura, W. D. Wu, D. A. Bonn, L. Taillefer, J. D. Garret, and Y. Ōnuki, 1994, Hyperfine Interact. **85**, 397.

Luke, G. M., A. Keren, L. P. Le, W. D. Wu, Y. J. Uemura, D. A. Bonn, L. Taillefer, and J. D. Garret, 1993a, Physica B **186-188**, 264.

Luke, G. M., A. Keren, L. P. Le, W. D. Wu, Y. J. Uemura, D. A. Bonn, L. Taillefer, and J. D. Garret, 1993b, Phys. Rev. Lett. **71**, 1466.

Luke, G. M., L. P. Le, B. J. Sternlieb, Y. J. Uemura, J. H. Brewer, R. Kadono, R. F. Kiefl, S. R. Kreitzman, T. M. Riseman, C. L. Seaman, Y. Dalichaouch, M. B. Maple, and J. D. Garret, 1990, Hyperfine Interact. **64**, 517.

Luke, G. M., L. P. Le, B. J. Sternlieb, W. D. Wu, Y. J. Uemura, J. H. Brewer, R. Kadono, R. F. Kiefl, S. R. Kreitzman, T. M. Riseman, Y. Dalichaouch, B. W. Lee, M. B. Maple, C. L. Seaman, P. E. Amstrong, R. W. Ellis, Z. Fisk, and J. L. Smith, 1991, Phys. Lett. A **157**, 173.

Luttinger, J. M., 1960, Phys. Rev. **119**, 1153.

Machida, K., and M. Kato, 1988, Phys. Rev. Lett. **58**, 1986.

Machida, K., and M. Ozuki, 1989, J. Phys. Soc. Jpn. **58**, 2244.

Machida, K., and M. Ozuki, 1991, Phys. Rev. Lett. **66**, 3293.

MacLaughlin, D. E., D. W. Cooke, R. H. Heffner, R. L. Hutson, M. W. Elfresh, M. E. Schillaci, H. D. Rempp, J. L. Smith, J. O. Willis, E. Zirngiebl, C. Boekema, R. L. Lichti, and J. Oostens, 1988, Phys. Rev. B **37**, 3153.

MacLaughlin, D. E., C. Tien, W. G. Clark, M. D. Lan, Z. Fisk, J. L. Smith, and H. R. Ott, 1984, Phys. Rev. Lett. **53**, 1833.

MacLaughlin, D. E. *et al.*, 1993, private communication.

Major, J., J. Mundy, M. Schmolz, A. Seeger, K. P. Döring, K. Fürderer, M. Gladisch, D. Herlach, and G. Majer, 1986, Hyperfine Interact. **31**, 259.

Maletta, H., and W. Zinn, 1989, in *Handbook on the Physics and Chemistry of Rare Earths*, edited by K. A. Gschneidner, Jr. and L. Eyring (North-Holland, Amsterdam), Vol. 12, p. 213.

Maple, M. B., J. W. Chen, Y. Dalichaouch, T. Kohara, C. Rossel, M. S. Torikachvili, M. W. Elfresh, and J. D. Thompson, 1986, Phys. Rev. Lett. **56**, 185.

Martin, R. M., 1982, Phys. Rev. Lett. **48**, 362.

Mason, T. E., G. Aeppli, A. P. Ramirez, K. N. Clausen, C. Broholm, N. Stuchele, E. Bucher, and T. T. M. Palstra, 1992, Phys. Rev. Lett. **69**, 490.

Mentink, S. A. M., 1994, Ph.D. thesis (Leiden University, The Netherlands).

Mentink, S. A. M., A. Drost, G. J. Nieunwenhuys, E. Frikkee, A. A. Menovsky, and J. A. Mydosh, 1994, Phys. Rev. Lett. **73**, 1031.

Mignot, J. M., R. Kahn, M.-J. Besnus, J.-P. Kappeler, and C. Godart, 1993, Physica B **186-188**, 475.

Mineev, V. P., 1989, Pis'ma Zh. Eksp. Teor. Fiz. **49**, 624 [JETP Lett. **49**, 719 (1989)].

Modler, R., M. Lang, C. Geibel, C. Schank, R. Müller-Reisener, P. Hellmann, A. Link, G. Sparn, W. Assmus, and F. Steglich, 1995, Physica B **206&207**, 586.

Mook, H. A., C. L. Seaman, M. B. Maple, M. A. Lopez de la Torre, D. L. Cox, and M. Makivic, 1993, Physica B **186-188**, 341.

Moshchalkov, V. V., 1987, Pis'ma. Zh. Eksp. Teor. Fiz. **54**, 181 [JETP Lett. **45**, 224 (1987)].

Murani, A. P., K. Knorr, K. H. J. Buschow, A. Benoit, and J. Flouquet, 1980, Solid State Commun. **36**, 523.

Murasik, A., S. Ligenza, and A. Zygmunt, 1974, Phys. Status Solidi A **23**, K163.

Nakamura, H., Y. Kitaoka, K. Asayama, and J. Flouquet, 1988, J. Phys. Soc. Jpn. **57**, 2644.

Nakamura, H., Y. Kitaoka, M. Inoue, K. Asayama, and Y. Ōnuki, 1990, J. Magn. Magn. Mater. **90&91**, 459.

Nakamura, H., Y. Kitaoka, H. Yamada, and K. Asayama, 1988, J. Magn. Magn. Mater. **76&77**, 517.

Narath, A., 1973, in *Magnetism* (Academic, New York), Vol. V, p. 149.

Nieuwenhuys, G. J., S. A. M. Mentink, A. A. Menovsky, A. Amato, R. Feyerherm, F. N. Gygax, R. H. Heffner, L. P. Le, D. E. MacLaughlin, and A. Schenck, 1995, Physica B **206&207**, 470.

Nozières, P., 1974, J. Low Temp. Phys. **17**, 31.

Ochiai, A., D. X. Li, Y. Haga, O. Nakamura, and T. Suzuki, 1993, Physica B **186-188**, 437.

Ochiai, A., T. Suzuki, and T. Kasuya, 1990, J. Phys. Soc. Jpn. **59**, 4129.

Ochiai, A., K. Takeuchi, N. Niitsuma, T. Suzuki, and T. Kasuya, 1987, J. Magn. Magn. Mater. **63-64**, 618.

Ohmi, T., and K. Machida, 1993, Phys. Rev. Lett. **71**, 625.

Ō nuki, Y., Y. Shimizu, and T. Komatsubara, 1984, J. Phys. Soc. Jpn. **53**, 1210.

Ō nuki, Y., Y. Shimizu, and T. Komatsubara, 1985, J. Phys. Soc. Jpn. **54**, 304.

Ott, H. R., H. Rudigier, E. Felder, Z. Fisk, and B. Batlogg, 1985, Phys. Rev. Lett. **55**, 1595.

Ott, H. R., H. Rudigier, Z. Fisk, and J. L. Smith, 1983, Phys. Rev. Lett. **50,** 1595.

Ott, H. R., H. Rudigier, Z. Fisk, and J. L. Smith, 1985, Phys. Rev. B **31,** 1651.

Palstra, T. T. M., A. A. Menovsky, and J. A. Mydosh, 1986, Phys. Rev. B **33**, 6527.

Palstra, T. T. M., A. A. Menovsky, J. van den Berg, A. J. Dirkmaat, P. H. Kes, G. J. Nieuwenhuys, and J. A. Mydosh, 1985, Phys. Rev. Lett. **55**, 2727.

Paolasini, L., J. A. Paixão, G. H. Landel, A. Delapalme, N. Sato, and T. Komatsubara, 1993, J. Phys.: Condens. Matter **5**, 8905.

Pfifer, A. E., T. Bowen, and K. R. Kendall, 1976, Nucl. Instrum. Methods **135**, 39.

Qachaou, A., E. Beaurepaire, M. Benakki, B. Lemius, J. P. Kappler, A. J. P. Meyer, and P. Panissod, 1987, J. Magn. Magn. Mater. **63&64**, 635.

Rainer, D., 1988, Phys. Scr. **T23**, 106.

Rainford, B. D., 1995, unpublished.

Rainford, B. D., D. T. Adroja, R. Wäppling, G. M. Kalvius, and A. Kratzer, 1995, Physica B **206&207**, 202.

Ramirez, A. P., P. Coleman, P. Chandra, E. Brück, A. A. Menovsky, Z. Fisk, and E. Bucher, 1992, Phys. Rev. Lett. **68**, 2680.

Ramirez, A. P., T. Siegrist, T. T. M. Palstra, J. D. Garret, E. Brück, A. A. Menovsky, and J. A. Mydosh, 1991, Phys. Rev. B **44**, 5392.

Rauchschwalbe, U., 1987, Physica B & C **147**, 1.

Regnault, L. P., W. A. C. Erkelens, J. Rossat-Mignod, J. Flouquet, E. Walker, D. Jaccard, A. Amato, and B. Hennion, 1987, J. Magn. Magn. Mater. **63&64**, 289.

Robinson, R. A., A. Purwanto, M. Kohgi, P. C. Canfield, T. Kamiyama, T. Ishigaki, J. W. Lynn, R. Erwin, E. Peterson, and R. Movshovich, 1994, Phys. Rev. Lett. **50**, 9595.

Ruck, M., G. Portisch, H. G. Schlager, and H.v. Löhneysen, 1993, Acta Crystallogr. Sect. B **49**, 936.

Santini, P., and G. Amoretti, 1994, Phys. Rev. Lett. **73**, 1027.

Schefzyk, R., W. Lieke, and F. Steglich, 1985, Solid State Commun. **54**, 525.

Schenck, A., 1985, *Muon Spin Spectroscopy: Principles and Applications in Solid State Physics* (Adam Hilger, Bristol, England).

Schenck, A., 1993, in *Selected Topics in Magnetism*, edited by L. C. Gupta and M. S. Murani (World Scientific, Singapore), *Frontiers in Solid State Sciences*, Vol. 2, p. 269.

Schenck, A., A. Amato, P. Birrer, F. N. Gygax, B. Hitti, E. Lippelt, S. Barth, H. R. Ott, and Z. Fisk, 1992, J. Magn. Magn. Mater. **108**, 97.

Schenck, A., P. Birrer, F. N. Gygax, B. Hitti, E. Lippelt, M. Weber, P. Böni, P. Fischer, and H. R. Ott, 1990, Phys. Rev. Lett. **65**, 2454.

Schenck, A. and F. N. Gygax, 1995, in *Handbook of Magnetic Materials*, edited by K. H. J. Buschow (North-Holland, Amsterdam), Vol. 9, p. 57.

Schlabitz, W., J. Baumann, J. Diesing, W. Krause, G. Neumann, C. D. Bredl, U. Ahlheim, H. M. Mayer, and U. Rauch-schwalbe, 1984, Poster presented at the *Fourth International Conference on Valence Fluctuations, ICVF*, Cologne, Germany.

Schlabitz, W., J. Baumann, B. Pollit, U. Rauchschwalbe, H. M. Mayer, U. Ahlheim, and C. D. Bredl, 1986, Z. Phys. B **62**, 171.

Schrieffer, J. R., and P. A. Wolff, 1966, Phys. Rev. **149,** 491.

Schröder, A. , J. G. Lussier, B. D. Gaulin, J. D. Garret, W. J. L. Buyers, L. Rebelsky, and S. M. Shapiro, 1994, Phys. Rev. Lett. **72**, 136.

Schröder, A. , J. W. Lynn, R. E. Ewin, M. Loewenhaupt, and H. v. Löhneysen 1994, Physica B **199&200**, 47.

Seaman, C. L., M. B. Maple, B. W. Lee, S. Ghamaty, M. S. Torokachvili, J. S. Kang, L. Z. Liu, J. W. Allen, and D. L. Cox, 1991, Phys. Rev. Lett. **67**, 2882.

Seaman, C. L., M. B. Maple, B. W. Lee, S. Ghamaty, M. S. Torokachvili, J. S. Kang, L. Z. Liu, J. W. Allen, and D. L. Cox, 1992, J. Alloys Compd. **181**, 327.

Shigeoka, T., K. Hirota, M. Ishikawa, T. Takabatake, and H. Fujii, 1993, Physica B **186-188**, 469.

Signore, J. P. C., J. P. Koster, E. A. Knetsch, C. M. van Woerkens, M. W. Meisel, S. E. Brown, and Z. Fisk, 1992, Phys. Rev. B **45**, 10145.

Sigrist, M., and T. M. Rice, 1989, Phys. Rev. B **39,** 2200.

Sigrist, M., and K. Ueda, 1991, Rev. Mod. Phys. **63,** 239.

Slichter, C. P., 1978, *Principles of Magnetic Resonance* (Springer, Berlin).

Smith, J. L., Z. Fisk, J. O. Willis, B. Batlogg, and H. R. Ott, 1984, J. Appl. Phys. **55**, 1996.

Spada, F. E., H. Oesterreicher, R. C. Bowman Jr., and M. P. Guse, 1984, Phys. Rev. B **30**, 4909.

Sparn, G., W. Lieke, U. Gottwick, F. Steglich, and N. Grewe, 1985, J. Magn. Magn. Mater. **47&48**, 521.

Stassis, C., J. Arthur, C. F. Majkrzak, J. D. Axe, B. Batlogg, J. Remeika, Z. Fisk, J. L. Smith, and A. S. Edelstein, 1986, Phys. Rev. B **34**, 4382.

Steglich, F., J. Aarts, C. D. Bredl, W. Lieke, D. Meschede, W. Franz, and H. Schäfer, 1979, Phys. Rev. Lett. **43**, 1892.

Steglich, F., U. Ahlheim, C. D. Bredl, C. Geibel, M. Lang, A. Loil, and G. Sparn, 1992, in *Selected Topics in Superconductivity*, edited by L. C. Gupta and M. S. Murani (World Scientific, Singapore), *Frontiers in Solid State Sciences*, Vol. 1, p. 527.

Steglich, F., C. Geibel, K. Gloos, G. Olesch, C. Schank, C. Wassilev, A. Loidl, A. Krimmel, and G. R. Stewart, 1994, J. Low Temp. Phys. **95**, 3.

Steglich, F., U. Rauchschwalbe, U. Gottwick, H. M. Meyer, G. Sparn, N. Grewe, U. Poppe, and J. J. M. Franse, 1985, J. Appl. Phys. **57,** 3054.

Stewart, G. R., Z. Fisk, and M. S. Wire, 1984, Phys. Rev. B **30**, 482.

Süllow, S., 1994, unpublished.

Szytula, A., and J. Leciejewicz, 1989, in *Handbook on the Physics and Chemistry of Rare Earths*, edited by K. A. Gschneidner, Jr., and L. Eyring (North-Holland, Amsterdam), Vol. 12, p. 133.

Takabatake, T., and H. Fujii, 1993, J. Appl. Phys. **8,** 254.

Takabatake, T., H. Iwasaki, G. Nakamoto, H. Fujii, H. Nakotte, F. R. de Boer, and V. Sechovsky, 1993, Physica B **183**, 108.

Takabatake, T., F. Teshima, H. Fujii, S. Nishigori, T. Suzuki, T. Fujita, Y. Yamagushi, J. Sakurai, and D. Jaccard, 1990, Phys. Rev. B **41**, 9607.

Takagi, S., 1994, unpublished.

Takagi, S., H. Suzuki, A. Ochiai, T. Suzuki, A. Amato, R. Feyerherm, F. N. Gygax, and A. Schenck, 1993, Physica B **186-188,** 422.

Takigawa, M., H. Yasuoka, T. Tanaka, and Y. Ishizawa, 1983, J. Phys. Soc. Jpn. **52**, 728.

Telling, M. T. F., S. Kilcoyne, and R. Cywinski, 1994, Hyperfine Interact. **85**, 209.

Thomas, F., J. Thomasson, C. Ayache, C. Geibel, and F. Steglich, 1993, Physica B **186-188**, 303.

Thompson, J. D., P. C. Canfield, A. Lacerda, M. F. Hundley, Z. Fisk, H. R. Ott, E. Felder, M. Chernikov, M. B. Maple, P. Visani, C. L. Seaman, M. A. Lopez de la Torre, and G. Aeppli, 1993, Physica B **186-188**, 355.

Tokuyasu, T. A., D. W. Hess, and J. A. Sauls, 1990, Phys. Rev. B **41**, 8891.

Tsvelik, A., and M. Reizer, 1993, Phys. Rev. B **48,** 4887.

Uemura, Y. L., W. J. Kossler, X. H. Yu, H. E. Schone, J. R. Kempton, C. E. Stronach, S. Barth, F. N. Gygax, B. Hitti, A. Schenck, C. Baines, W. F. Lankford, Y. Ō nuki, and T. Komatsubara, 1988, Physica C **153-155**, 455.

Uemura, Y. L. and G. M. Luke, 1993, Physica B **186-188,** 223.

Volovik, G. E., and L. P. Gor'kov, 1985, Zh. Eksp. Teor. Fiz. **88**, 1412 [Sov. Phys. JETP **61**, 843 (1985)].

Wiesinger, G., E. Bauer, A. Amato, R. Feyerherm, F. N. Gygax, and A. Schenck, 1994, Physica B **199&200,** 52.

Wu, W. D., A. Keren, L. P. Le, G. M. Luke, B. J. Sternlieb, Y. J. Uemura, C. L. Seaman, Y. Dalichaouch, and M. B. Maple, 1994, Phys. Rev. Lett. **72**, 3722.

Yaouanc, A., P. Dalmas de Réotier, B. Chevalier, and P. L. L'Héritier, 1990, J. Magn. Magn. Mater. **90&91**, 575.

Yaouanc, A. *et al.*, 1994, unpublished.